Rates of cellular attachment to an established biofilm
by J Cahyono Gunawan

A thesis submitted in partial fulfillment of the requirements for the degree of Master of Science in Chemical Engineering
Montana State University

Abstract:
There is no predictive theory available for predicting the attachment rate of viable cells to an established biofilm [11] . The need for a reliable prediction of attachment rate of viable cells to an established biofilm is imperative to generate an accurate mathematical model of biofilm accumulation on a surface.

An experimental method has been developed to use radiolabelled cells to measure the rate at which cells attach to an existing biofilm. First, a C12 Pseudomonas aeruginosa biofilm was grown in a rotating annular bioreactor (RotoTorque). After an established biofilm was obtained, C14 labelled P. aeruginosa cells were introduced into the RotoTorque. The rate of cellular attachment to an established biofilm and the rate of cellular detachment can be measured by counting the radioactive intensity on the surface of the established biofilm using a liquid scintillation counter.

Gross attachment rates (cellular attachment rates in the absence of simultaneous detachment) ranged from 103 to 105 CFU/(cm2 minute), while net attachment rates (cellular attachment rates measured with simultaneous detachment) ranged from 102 to 104 CFU/ (cm2 minute). The difference between the gross and net rate attachment is the rate of detachment.

Preliminary results indicate the attachment rate of viable cells to an established biofilm is a function of temperature and bulk cell concentration. The effect of shear stress was indeterminate.

A model is proposed, coupling film theory and pseudosteady-state transport theory, describing the attachment rate of viable cells to an established biofilm in -a RotoTorque system.

RATES OF CELLULAR ATTACHMENT TO AN ESTABLISHED BIOFILM

by

J.Cahyono Gunawan

A thesis submitted in partial fulfillment
of the requirements for the degree

of

Master of Science

in

Chemical Engineering

MONTANA STATE UNIVERSITY
Bozeman, Montana

AUGUST 1991

APPROVAL

of a thesis submitted by

J.Cahyono Gunawan

This thesis has been read by each member of the thesis committee and has been found to be satisfactory regarding content, English usage, format, citations, bibliographic style, and consistency, and is ready for submission to the College of Graduate Studies.

June 11, 1991
Date

Ronald W. Larsen
Chairperson, Graduate Committee

Approved for the Major Department

June 12, 1991
Date

John T. Sears
Head, Major Department

Approved for the College of Graduate Studies

August 12, 1991
Date

Henry J. Parsons
Graduate Dean

STATEMENT OF PERMISSION TO USE

In presenting this thesis in partial fulfillment of the requirements for a master's degree at Montana State University, I agree that the Library shall make it available to borrowers under rules of the Library. Brief quotations from this thesis are allowable without special permission, provided that accurate acknowledgment of source is made.

Permission for extensive quotation from or reproduction of this thesis may be granted by my major professor, or in his/her absence, by the Dean of Libraries when, in the opinion of either, the proposed use of the material is for scholarly purposes. Any copying or use of the material in this thesis for financial gain shall not be allowed without my written permission.

Signature J. Cahyono Gunawan

Date August 5, 1991

ACKNOWLEDGEMENTS

I would like to thank the following people without whom this thesis would not be possible:

Dr. Ron W. Larsen for his love, encouragement, discipline, support, patience, and enthusiasm which paced me through my graduate work.

Dr. John Sears for his concern, encouragement, advice, and contributions to my graduate program. Dr. Robert Nickelson for serving on my thesis committee.

Dr. Warren Jones, Anne Camper, and Brent Peyton for their valuable time to clarify the problem in the experimental system and their valuable time to go through the draft.

Dr. Clifford Bond for letting me use the liquid scintillation counter. Lyman Fellows, Gordon Williamson and his crew members for technical assistance.

Jane Curtis and Margaret Jensen for their excellent "paper work" assistance and "doughnuts". All my friends at CIMPE and for their support and motivation.

Chemical Engineering Department/Montana State Engineering Experiment Station and National Science Foundation through C.I.M.P.E. for providing the financial support.

My parents, Mr and Mrs Huang, and my wife, Veronica, for their patient and everlasting support; ..... and my lovely daughter, Cynthia Kartika for keeping me awake in the middle of the night so that I can go to school to type this thesis.

TABLE OF CONTENTS

TABLE OF CONTENTS - continued

LIST OF TABLES

LIST OF TABLES - continued

LIST OF TABLES - continued

LIST OF FIGURES

LIST OF FIGURES - continued

LIST OF FIGURES - continued

LIST OF FIGURES - continued

ABSTRACT

There is no predictive theory available for predicting the attachment rate of viable cells to an established biofilm [11]. The need for a reliable prediction of attachment rate of viable cells to an established biofilm is imperative to generate an accurate mathematical model of biofilm accumulation on a surface.

An experimental method has been developed to use radiolabelled cells to measure the rate at which cells attach to an existing biofilm. First, a C^{12} Pseudomonas aeruginosa biofilm was grown in a rotating annular bioreactor (RotoTorque). After an established biofilm was obtained, C^{14} labelled P. aeruginosa cells were introduced into the RotoTorque. The rate of cellular attachment to an established biofilm and the rate of cellular detachment can be measured by counting the radioactive intensity on the surface of the established biofilm using a liquid scintillation counter.

Gross attachment rates (cellular attachment rates in the absence of simultaneous detachment) ranged from 10^3 to 10^5 CFU/(cm^2 minute), while net attachment rates (cellular attachment rates measured with simultaneous detachment) ranged from 10^2 to 10^4 CFU/(cm^2 minute). The difference between the gross and net rate attachment is the rate of detachment.

Preliminary results indicate the attachment rate of viable cells to an established biofilm is a function of temperature and bulk cell concentration. The effect of shear stress was indeterminate.

A model is proposed, coupling film theory and pseudo-steady-state transport theory, describing the attachment rate of viable cells to an established biofilm in a RotoTorque system.

INTRODUCTION

A biofilm, a surface accumulation of cells, organic and inorganic debris immobilized at a substratum and embedded in an organic polymer matrix of microbial origin, is not necessarily uniform in time and space; that is, it may be spatially non-homogeneous, and change with time. A substratum is a support surface which may be either a solid or a liquid. "Cells" in the biofilm may consist of living, non-viable, and/or decaying cells. Non-viable cells are incapable of growth temporarily, while decayed cells are no longer capable of life processes.

Accumulation of biofilm is encountered in many natural and man-made environments. Natural surface water quality, root surfaces, cooling tower fill, teeth and gums are all affected by adsorbed microorganisms. Biofilms serve beneficial purposes in some natural and man-made environments but in certain cases biofilms are considered a nuisance [11].

Zobell (1943) is probably the research pioneer on the association between microorganisms and solid surfaces. This research continued in a spasmodic fashion until the last decade. Rapid progress in this field in recent times has made it possible to take a more fundamental approach to describe biofilm processes in a system.

Adherence of living and/or non-living particles from the fluid to the surface of biofilm, attachment, is one of the

processes leading to biofilm accumulation. This work concerns with the rate of cellular attachment to an established biofilm, which is defined as the sorption rate of living cells from the bulk liquid to an established biofilm.

Although a kinetic expression of attachment is proposed in this work, the focus of this research is to develop a technique to measure cellular attachment rates from suspended pure culture to single population biofilms.

LITERATURE REVIEW

Biofilm

Biofilm Processes

Biofilm accumulation is the result of chemical, physical and microbial processes occurring in the system. These processes are interrelated. The substrate composition, for example, can affect the growth rate and the ability of cells to attach [26]. Increasing calcium concentration has been shown to increase the cohesiveness of the biofilm as indicated by a lower detachment rate [33].

Viruses and most bacteria are so small that they behave as colloidal particles in aqueous systems. Perhaps they are better considered as "living colloids" [7]. Physicochemical principles, coupled with a model to describe growth and microbiological phenomena can be used to describe the biofilm accumulation in a system.

The surface upon which a biofilm will accumulate, the substratum, is first conditioned by adsorped organic macromolecules and nutrients from the liquid system. It does not usually take a long time (within minutes) to condition the substratum [11]. Concentrating nutrients on the substratum because of adsorption will enhance microbial growth on the substratum. On the other hand, adsorped molecules can inhibit

microbial adsorption [11]. Characklis [11] concludes that the role of the conditioning film in microbial adsorption to a surface is not yet clear.

Microorganisms can be transported from the bulk liquid to the liquid-substratum interface by many means. Physical phenomena such as diffusion, gravity, thermophoresis, and radial fluctuation (convection) in a turbulent flow system and cell motility are important factors. System parameters such as temperature, pH, liquid viscosity, and flow pattern will decide which factors are most significant [7].

Microorganisms which have already been transported to the liquid-substratum interface may be adsorped by the substratum. Variables affecting this adsorption process are the character of microorganism, the character of substratum, and the character of the environment [28]. All these variables will determine how fast the microorganism will be adsorbed and whether the adsorption is going to be permanent or non-permanent. Microorganisms leave the substratum surface by a process called desorption.

After an initial accumulation of microorganisms is established, a different phenomena begins to take place. Microorganisms are now attaching to the initial biofilm. The character of the substratum becomes less important for attachment of a microorganism to an established biofilm. The ability of microorganism to form extracellular polymeric substances (EPS) may be an important factor in determining

whether or not a microorganism will adhere to the surface of biofilm [7].

As mentioned before, some of the microorganisms will not adsorb permanently, but will desorb from the substratum and return to the bulk liquid, a process that is called desorption. If either microorganisms or biomass are lost from an established biofilm, the process is called detachment. Desorption, the loss of cells adsorbed to the substratum, occurs from the moment of initial adsorption, while detachment, the loss of cells or biomass away from the substratum, happens only after the biofilm is established.

Characklis and Marshall [11] describe three types of detachment. The first is erosion, a continuous loss of small portions of biofilm, which is highly dependent on fluid dynamic conditions. Sloughing, the second type, is a rapid, massive loss of biofilm which generally occurs with thicker biofilms. The last type is abrasion, i.e., a loss of biofilm due to repeated collisions between suspended particles and the biofilm, or between multiple substratum particles as in a fluidized bed.

Once living microorganisms are adsorbed, they start using substrate on the surface for growth, replication, maintenance, and for the formation of extracellular products. The living microorganisms may use non-viable cells as nutrient sources as well.

The interaction among those processes: adsorption and desorption followed by attachment and detachment, growth and death, will determine the total accumulation of biofilm on a surface. The accumulation, however, is not necessarily uniform in time and space. For example, sloughing, which generally occurs with thicker biofilms can contribute significantly to the unsteady-state behaviour of biofilms accumulation on a substratum. However, it will usually take a few days before "thicker biofilms" accumulate on a substratum. This means that although a steady-state condition is not necessarily accomplished, one or more processes can be forced to reach a nearly steady-state value for a certain period of time under certain conditions. Under such conditions a "pseudosteady-state" hypothesis may be used to describe the processes mathematically.

Biofilm Properties

Biofilm properties are related to properties of their main components, i.e., water and microorganisms with their EPS. The biological properties of the microorganisms: growth rate, substrate utilization, metabolic path, molecular structure of EPS produced, etc.; are dependent on the particular environment in which the microorganisms are growing.

Biofilm thickness (100 - 1000 μm) and dry mass density (10 - 50 kg m^{-3} in fluid flow systems) [33] are highly

dependent on fluid dynamics of the system, the type of microorganism, nutrient substrate composition and concentration. The physical appearance of the biofilm depends partially on the type of microorganisms. Biofilms composed of pure culture Pseudomonas aeruginosa have a relatively "smooth" surface [11].

The chemical properties of a biofilm are highly dependent upon the type of microorganism and the nature of the substrate. Different microorganisms will have different byproducts and different metabolic pathways. The nature of the substrate will especially affect the metabolic path. Sucrose grown Streptococcus mutans produces more EPS than glucose grown S. mutans. Under electron micrography, sucrose grown S. mutans produces diffuse EPS while glucose grown S. mutans produces relatively highly organized EPS [3].

Pseudomonas aeruginosa

P. aeruginosa is a member of the family pseudomonadaceae. The name was created about seventy years ago [37]. As presently defined, the family of pseudomonadaceae are characterized by the absence of prostheceae, a metabolism typically respiratory, an absence of fermentation and photosynthesis, and a capacity for growth at the expense of a large variety of organic substrates with the exception of the 1-carbon compounds [32].

Pseudomonas is a genus within the family of the pseudomonadaceae. It is a motile, gram negative, oxidase positive rod. Only one species is frequently pathogenic in man; others affect plants, fishes and some animals. The oxidation-fermentation (O/F) reaction is oxidative, distinguishing the genus from aeromonas [27].

Phylogenetically, based on 16s-rRNA sequencing, the various genera of pseudomonads scatter within subdivisions alpha, beta, gamma purple bacteria. The delta group, however, does not have pseudomonads within its group. The 16S-rRNA sequences are used as a tool to classify the pseudomonads phylogenetically, showing an evolutionary relationship determined by differences and similarities 16s-rRNA of the bacteria.

Although pseudomonads are diverse groups, Pseudomonas aeruginosa is quite homogeneous physiologically. All isolates fit into a very narrow range of distribution characteristics [9].

P. aeruginosa produces green-blue pigment (pyocyanine) on cultures and wound pus. Yellow pigment (fluorescein) may also be apparent on agar plate. The species occurs as a pathogen in urine, burns, wounds etc., often with other bacteria. Growing pseudomonas produce an antibiotic substance (pyocyanase) inhibitory to some other bacteria [27].

P. aeruginosa is a polymer forming bacterium. The primary mode of growth is in polymer-enclosed microcolonies [31],

attached to a wide variety of substrata. The polymer capsule may act as a protecting layer. The layer is relatively diffuse and easily dispersed in the liquid phase. The polymer capsule, however, may have an important role in assisting the bacteria to attach on a surface [33].

Table 1. General Characteristics of P. aeruginosa. [31]

Shape	Rod
Breadth (μm)	0.5 - 0.8
Length (μm)	1.5 - 4.0
Motility	Polar flagella
Respiration	Obligate aerobe
Gram stain	Negative
Optimal Temperature (°C)	35 - 37
Optimal pH	6.8

Nutrient Medium

Nutrients or substrates are substances in the environment which are used by organisms for metabolism. Nutrients are usually divided into two classes: 1) essential nutrients, without which cell growth will be hindered; 2) non-essential nutrients which are not essential to cell growth, but which will be used by microorganisms if they are available.

Essential nutrients include: carbon, hydrogen, oxygen, nitrogen, phosphorous, sulfur, potassium, magnesium, calcium,

sodium, and iron. The required nutrients are divided into two groups by the amount required by the organism: macronutrients and micronutrients.

Those nutrients listed above are found in nature or provided in a man-made reactor as organic or inorganic compounds. The form in which these substances are available can affect the metabolic efficiency. If the carbon source, for example, were given in the form of CO_2 instead of glucose, the efficiency of metabolism would be lower [1,8]. Cells will take carbon from the environment and change it into cell constituents. The oxidation state of carbon in cell constituents is zero. Some energy, then, is needed to reduce the oxidation state of carbon in CO_2 to zero.

In a man-made reactor, the way a substrate solution is made also an important factor. Most substrate solution is sterilized before being delivered to the reactor. The common way to sterilize substrate is by autoclaving. At high temperature, glucose (a common carbon source) in the presence of phosphate will form substances which may be poisonous to some organisms [2]. Additionally, caramelization should be considered.

The amount of nutrient given will also affect the rate at which microorganisms grow. In general, the higher the nutrient concentration, the faster the microorganisms will grow. The growth rate, however, will be constant above a certain nutrient concentration. The nutrient concentration which gives

the maximum growth rate varies from one organism to another. Some organisms will reach their maximum growth rate at a low substrate concentration and a higher concentration of substrate may inhibit growth or even stop it. Cell lysis may occur because of the osmotic pressure difference between the inside and outside of the cell wall [8].

The important aspect to be noted, then, is that the substrate composition is an important factor which may alter kinetic parameters significantly. Any modelling effort should consider the changes in kinetic parameter values that might be induced because of substrate composition changes.

Previous Mathematical Models

Mathematical Model of Cells

Biological populations consisting of a single species more than likely differ physiologically, morphologically and possibly genetically too [11]. The individuals combine to form populations in which properties, such as size, age, biological activity, etc. follow different distribution patterns although the cells grow in the same environment. To incorporate all these factors will be impossible because of many restrictions such as time limitation and instrument capability. In order to come up with a manageable model, some simplifications will be used.

If the number of cells per unit volume in a particular system is large enough, average state properties can be used. A model which uses average state properties and neglects the distribution of state properties is called a deterministic model [30]. Such a model is used in this research.

In a multicellular microorganism or a complex system like a biofilm, life is segregated into structurally and functionally discrete units, i.e., cells. These cells may grow under different conditions because of spatial inhomogeneity in the system variables such as nutrient concentration, temperature, pH, etc. As a result, the number of cells is an important parameter to, at least partially, describe the system. A system consisting of "n" cells will have a different

biological characteristic than a system which has "2n" cells. If the number of cells in the system is high enough ($n \rightarrow \infty$), n will be approaching 2n and segregation of cells in the system can be ignored. A model in which segregation is ignored is called a non-segregated or distributed model and assumes that there is a uniform cell mass distribution [30].

Two microorganisms which have the same biomass and environment may, however, have different properties and activities. It is a problem of state. The two organisms may have different states; one organism is younger than the other one with respect to the period of time elapsed since the two organisms were formed by fission of their parents. A model which does not recognize the existence of a distribution of states is called a non-structured model. A non-structured model is used in this research. Such a model assumes the biological structure and the state of the cells as determined by previous history need not be taken into account. This assumption is valid if cell growth is balanced, i.e., if all extensive properties of the growth system are altered in the same way as a function of time. Balanced growth is difficult to achieve in a high growth rate system [30].

In the short term, cells may be considered as small living reactors which behave in the same manner under the same conditions.

Cell death and decay. It has long been recognized that only a portion of the biomass present in biochemical operations is actually alive and contributing to the activity. On the other hand, only recently has the spontaneous death of cells become known [18].

Viability is defined as the mass of living or viable cells present divided by total mass of cells.

$$V_i = \frac{X_V}{X_v + X_d} \qquad (1)$$

where

V_i = viability

X_v = mass of viable cells [M]

X_d = mass of non-viable cells [M]

As currently defined, a viable cell is one that will form a colony on solid growth media, and a non-viable cell is one which has lost that ability.

Model for the rate of spontaneous natural death. McKinney [24] was one of the first engineers to try to model the generation of inactive (non-viable and decayed) cells in biochemical operations. His work was followed by B.L. Goodman and A.J Englande [17]; and also by D.R. Christensen and P.L. McCarty [13]. Nevertheless, none of them was trying to

correlate viable cells to the generation rate of non-viable cells.

The only model available today for bacterial death which has been verified against experimental data is that proposed by Sinclair and Topiwala [16]. Their model says that the death rate of viable cells, r_{Dxv}, is directly proportional to the concentration of viable cells in the medium [16].

$$r_{Dxv} = -\gamma\ X_v \tag{2}$$

$$r_{Gxd} = -r_{Dxv} \tag{3}$$

where

γ = death rate coefficient [T^{-1}]

r_{Gxd} = generation rate of non-viable cells [$M\ T^{-1}$]

Cell decay is a term representing the loss of cell mass. If an exogenous substrate, substrate outside the cell which is available to be converted into energy that can be utilized by the cell, falls below the needs for maintenance, minimum energy necessary for keeping the cell functioning, then a portion of cell mass will be degraded to supply maintenance energy. In heterogenous culture predators may consume other cells, resulting in a loss of cell mass because the growth efficiency of predators using other cells is not 100%. As some

cells die, they begin to leak their internal contents into the medium, a process which is called cell lysis. Only the remaining cell wall is large enough to be measured. This also contributes to the loss of cell mass [16].

Thus it can be seen that decay is actually a composite term, incorporating the effects of many factors. For this reason a first-order model of cell decay is strictly empirical. The justification of the model described below is based on its usefulness and ability to predict the loss of cell mass.

The loss of viable cell mass by decay, r_{dxv}, is modelled as a first-order function of viable cell concentration and the loss of non-viable cell mass, r_{dxd}, as a first-order function of non-viable cell concentration [16].

$$r_{dxv} = - b_v X_v \qquad (4)$$

$$r_{dxd} = - b_d X_d \qquad (5)$$

where b_v and b_d are the specific decay constants for viable and non-viable cells, respectively.

Living cells may lose their cell mass by endogenous metabolism (metabolism which are utilized nutrient stored inside the cell when exogenous substrate is available abundantly), maintenance requirements, and predation, whereas

non-viable cells may lose their cell mass mainly by predation. Consequently, the coefficient b_v is more likely to be greater than b_d [18]. However, because of lack of data, it is assumed that b_v and b_d are equal:

$$b_v = b_d = b \tag{6}$$

Yield. Yield is defined as the amount of biomass formed per unit amount of substrate removed, and is a measure of the relative efficiencies of energy conservation and utilization. The vague term "amount" is used to stress that there is more than one definition which leads to different numerical values of the yield.

There are at least four definitions of yield which have been used. Differences among them are in the way the amount of substrate consumed is defined. The "amount of cells" is defined as the dry mass, generally expressed in grams. The amount of substrate consumed is expressed as: 1) the equivalent amount of ATP which could be formed from it [1]; 2) the equivalent amount of total energy removed from the medium [1]; 3) the number of electrons initially available in the substrate for transfer to the terminal electron acceptor or for incorporation into cell material [1] and; 4) the reduction in the amount of organic matter present, expressed as COD

[16]. In this research, the last definition of yield will be used.

Under conditions of unrestricted growth, rate of energy utilization for maintenance is negligible in comparison to the rate of energy utilization for cell synthesis. Accordingly, the "true yield", Y_g, is defined as the amount of cell material formed per unit of substrate utilized in the absence of maintenance energy requirements. For a detailed treatment see reference 1, pages 135 through 148.

Mathematical model for cell growth. The reaction rate for cell growth can be expressed as:

$$r_{Gxv} = \mu X_v \tag{7}$$

where μ is the specific growth rate. The Monod equation [1,2,11] will be used to model the substrate dependence of the specific growth rate. If only one limiting substrate is considered, then the Monod equation can be written as:

$$\mu = \frac{\mu_m S}{K_s + S} \tag{8}$$

where

μ_m = maximum specific growth [T^{-1}]

S = The concentration of growth limiting substrate [M L^{-3}]

K_s = The half saturation constant [M L^{-3}]

Although there is a similarity between the Monod equation and the Michaelis-Menten equation used to describe enzyme reaction rates [2], the Monod equation is not derived on the same theoretical grounds. While the Michaelis-Menten equation can be derived from a consideration of the rates of chemical reaction catalyzed by enzymes, the Monod equation is strictly empirical [2]. The justification of the Monod equation (equation (8)) is based on its demonstrate ability to describe the specific growth rate as a function of substrate concentration [16]. The Monod equation is used in this research.

Using the definition of the true yield [16], Y_g, and the Monod equation, the rate of substrate utilization, $-r_s$, can be expressed as a function of viable cell concentration, X_v, as follows:

$$-r_s = \frac{\mu}{Y_g} X_v \qquad (9)$$

Mathematical Model for Chemostats

A chemostat is a continuous-flow stirred tank reactor (CFSTR); i.e., the bulk liquid concentration gradient can be neglected. The chemostat consists of a reaction vessel and a stirrer. The surface area per unit volume is considerably less than that of a RotoTorque, so that the biofilm which grows on the inside surface of the chemostat may be ignored.

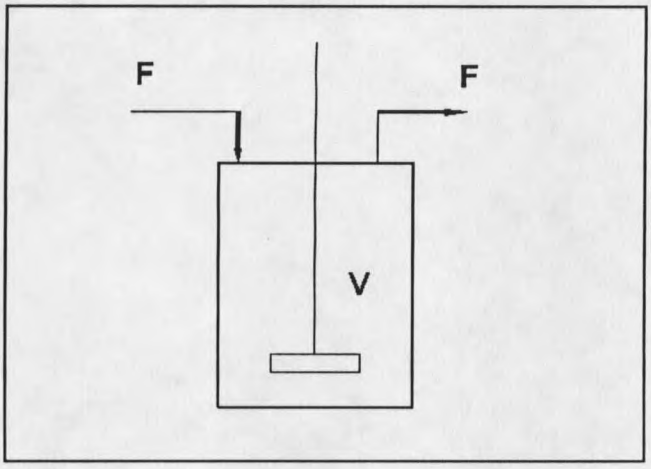

Figure 1. Schematic of a Chemostat

Incorporating the model of cell growth described in the previous section (equation (7)) and, assuming that the only solids in the reactor are cells, suspended solid balance under steady-state conditions [16]:

$$\text{inlet} - \text{outlet} + \text{growth} - \text{death} - \text{decay} = 0$$

$$0 - F X_v + r_{Gxv} V - (-r_{Dxv}) V - (-r_{dxv}) V = 0 \qquad \textbf{(10)}$$

where,

F = inlet and outlet volumetric flow rate [L^3 T^{-1}]

V = volume of the reactor [L^3]

The first term of equation (10), the input term is zero because the total mass of suspended solids, M_0, is zero. M_0 is the sum of inlet inert solids (Z_{i0}), inlet biodegradable solids (Z_{b0}), and inlet cell concentration (X_0) [16].

$$M_o = X_o + Z_{io} + Z_{bo} \tag{11}$$

using equations (2),(4),(5),(6), the Monod equation (equation (8)) and equation (11),

$$\mu = \frac{1}{\tau} + \gamma + b \tag{12}$$

where

$$\tau = \frac{V}{F} \tag{13}$$

Using equations (8) and (12), substrate concentration in the reactor, S, can be expressed as a function of space time, τ, as follows:

$$S = \frac{K_s \left(\frac{1}{\tau} + \gamma + b\right)}{\mu_m - \left(\frac{1}{\tau} + \gamma + b\right)} \tag{14}$$

Equation (14) indicates that the substrate concentration in the chemostat, S, is controlled solely by τ and S does not depend on inlet substrate concentration S_0. C.P.L. Grady, Jr., et al. [16] have demonstrated this for a pure culture growing on a single substrate. For a mixed culture, K_s will be a function of S_0 [16].

If τ becomes large enough, $1/\tau$ will be close to zero and S will reach its minimum value. The minimum value of S, S_{min}, is given by;

$$S_{min} = \frac{K_s\ (\gamma + b)}{\mu_m - (\gamma + b)} \qquad (15)$$

S_{min} is the minimum substrate concentration that can be approached in a CFSTR.

The maximum rate at which a bacteria can grow upon a given substrate depends upon the influent substrate concentration, S_0. The specific growth rate, μ', under this condition is given as follows:

$$\mu' = \frac{\mu_m S_0}{K_s + S_0} \qquad (16)$$

The minimum space time is also known as the point of wash-out because at shorter space times, all cells are washed out of the reactor and no net growth will occur

(provided no cells have adsorbed on the inside surface of the reactor and no cell comes in with the inlet flow). Consequently, the minimum space time, τ_{min}, can be calculated by setting μ in equation (7) equal to μ' in equation (16):

$$\tau_{min} = \frac{K_s + S_o}{S_o\ (\mu_m - \gamma - b) - K_s\ (\gamma + b)} \qquad (17)$$

If there are cells coming in with the influent; the same procedure yields modified expressions for, μ, X_v, S, X_d, X, and V_i which are recorded in reference [16].

Mathematical Model for RotoTorque

A RotoTorque is a continuous-flow stirred tank reactor (CFSTR), i.e., the bulk liquid concentration gradient is negligible. The RotoTorque consists of two concentric cylinders, a stationary outer cylinder and a rotating inner cylinder. The RotoTorque provides a large surface area per unit volume of fluid. In this case, the biofilm which grows on the inner surface of the reactor cannot be ignored.

Fluid kinematics. There are four flow regions to be considered in a RotoTorque: laminar streamline flow, laminar flow with Taylor vortices, turbulent flow, and turbulent flow with vortices [29]. For this study, it is enough to know that the transition between the laminar streamline flow to other

zones flow pattern can be correlated by the transition Reynolds number, Re_{trans}, given by equation (18) [6]. For a detailed treatment see reference 27, pages 525 through 531.

$$R_{e_{trans}} \equiv \left(\frac{\Omega \kappa R^2 \rho}{\mu}\right)_{trans} \approx \frac{41.3}{(1-\kappa)^{\frac{3}{2}}} \qquad (18)$$

where

Ω = angular velocity of the inner cylinder [T^{-1}]

κ = the radius ratio of the inner cylinder to the outer cylinder

R = radius of the outer cylinder [L]

ρ = mass density [M L^{-3}]

μ = viscosity [M L^{-1} T^{-1}]

Some work on the fluid kinematics and mass transfer for laminar and turbulent flow in an annular geometry has been carried out. R.B. Bird and C.F. Curtiss [6] describe the tangential, Newtonian, laminar flow in annuli for unsteady flow conditions. Joseph Kaye and E.C. Elgar [20] describe the mode of fluid motion in an annulus with an inner rotating cylinder. Using a long vertical annulus with the gap to inside diameter ratio of 0.18, they mentioned that the critical rotation rate at which vortexes appeared in the annulus for zero axial velocity is 28.6 rpm; the theoretical value predicted by Taylor's theory is 28.3 rpm [20]. R. Kappesser,

I. Cornet, and R. Greif [19] give a correlation for mass transfer near a rotating cylinder with turbulent flow in terms of the Sherwood number, and as a function of Reynolds number and Schmidt number. They also present a graph which correlates critical Reynolds number to roughness of the wall (Figure 2). A.K. Wang and L.W. Gelhar (1971) give a prediction of the mean velocity profiles for turbulent couette flow. However, one parameter and one constant must be evaluated experimentally in order to apply their prediction to a turbulent annular flow.

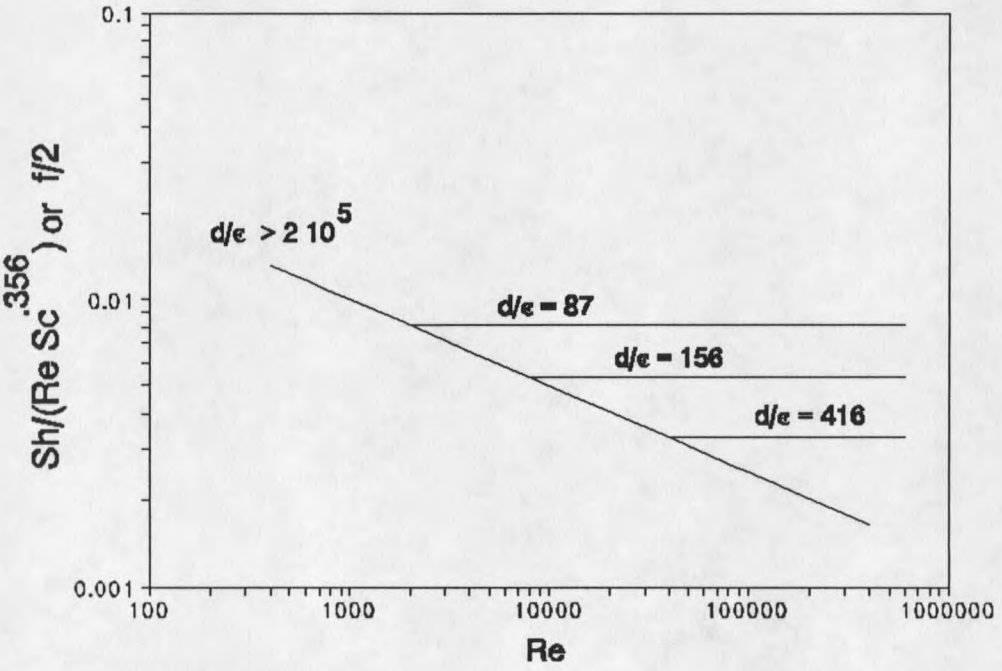

Figure 2. Mass transfer or friction factor vs. Re [19]

Although a lot of work has been done in an attempt to describe the fluid kinematics in an annular geometry, none can be applied directly to describe the fluid kinematics in the RotoTorque used in this experiment unless additional measurements are made. In order to use A.K. Wang and L.W. Gelhart's result, the torque, mixing length, and the velocity at a certain point in the annuli have to be known. To use the mass transfer correlation above; the concentration of substrate at the wall and the roughness of the wall have to be known.

Nevertheless, if the wall surface is assumed very rough ($d/\epsilon = 87$, where ϵ is roughness in cm), which is a reasonable assumption for many biofilm surfaces, then, the correlation for mass transfer and friction factor can be used (Figure 2). Nomenclature for Figure 2 is as follows:

$Sh = (N\ d)/(D\ \Delta C)$

$Re = (w\ d^2)/(2\ \nu)$

Sc = Schmidt number

N = mass flux at wall, g equiv/(cm^2 sec)

d = diameter of the rotor, cm

D = diffusion coefficient, cm^2/sec

C = concentration, g equiv/cm^3

w = angular velocity, radians/sec

ν = kinematic viscosity, cm^2/sec

Using Figure 2, the friction factor can be estimated if the Reynolds number is known.

To estimate the shear stress on the surface of RotoTorque, the circumferential time averaged velocity must be calculated first. Neglecting the curvature, the problem can be simplified into a problem of two parallel plates (couette flow). If the distance between those two parallel plates is 2h, with the lower plate assumed stationery and the upper plate moving with a constant velocity of $2V_w$ in the X direction (Cartesian coordinates are now used and the direction of flow is chosen as the X direction), then, A.K. Wang and L.W. Gelhar have solved the problem using Zagustin's energy balance [34]. The velocity distribution is given as follows:

$$\frac{V - V_w}{V_*} = \frac{1}{k} \ln\left[\frac{\frac{y}{h}}{2 - \frac{y}{h}}\right] \qquad (19)$$

where

$V_* = (\tau_0/\rho)^{-.5}$

τ_0 = shear stress on the wall, (dyne/cm^2)

ρ = fluid density (gram/cm^3)

k = Von Karman constant = 0.4

V_w = fluid velocity at the inner wall (cm/second)

The average velocity over the cross section (A) can be calculated using :

$$V_{av} = \frac{\int_A V \, dA}{\int_A dA} \qquad (20)$$

Using Figure 2 to get the friction factor and equations (30 and 31), shear stress for a given rotor rotation speed can be calculated using the following equation (21):

$$\tau_o = \frac{f}{2} \rho V_{av} \qquad (21)$$

Another method which may be used to calculate shear stress uses Figure 3 [29]. Using this approach, the coefficient of friction is given as a function of Taylor number.

Coefficient of friction is defined as

$$C_m = \frac{M_i}{0.5 \, \pi \, \rho \, V_i^2 \, R_i^2 \, h} \qquad (22)$$

where

M_i = moment induced by the rotor [M L^2 T^{-2}]

ρ_i = density of liquid [M L^{-3}]

V_i = peripheral velocity of the rotor [L t^{-1}]

R_i = radius of the rotor [L]

h = height of the rotor [L]

d = gap between two concentric cylinders [L]

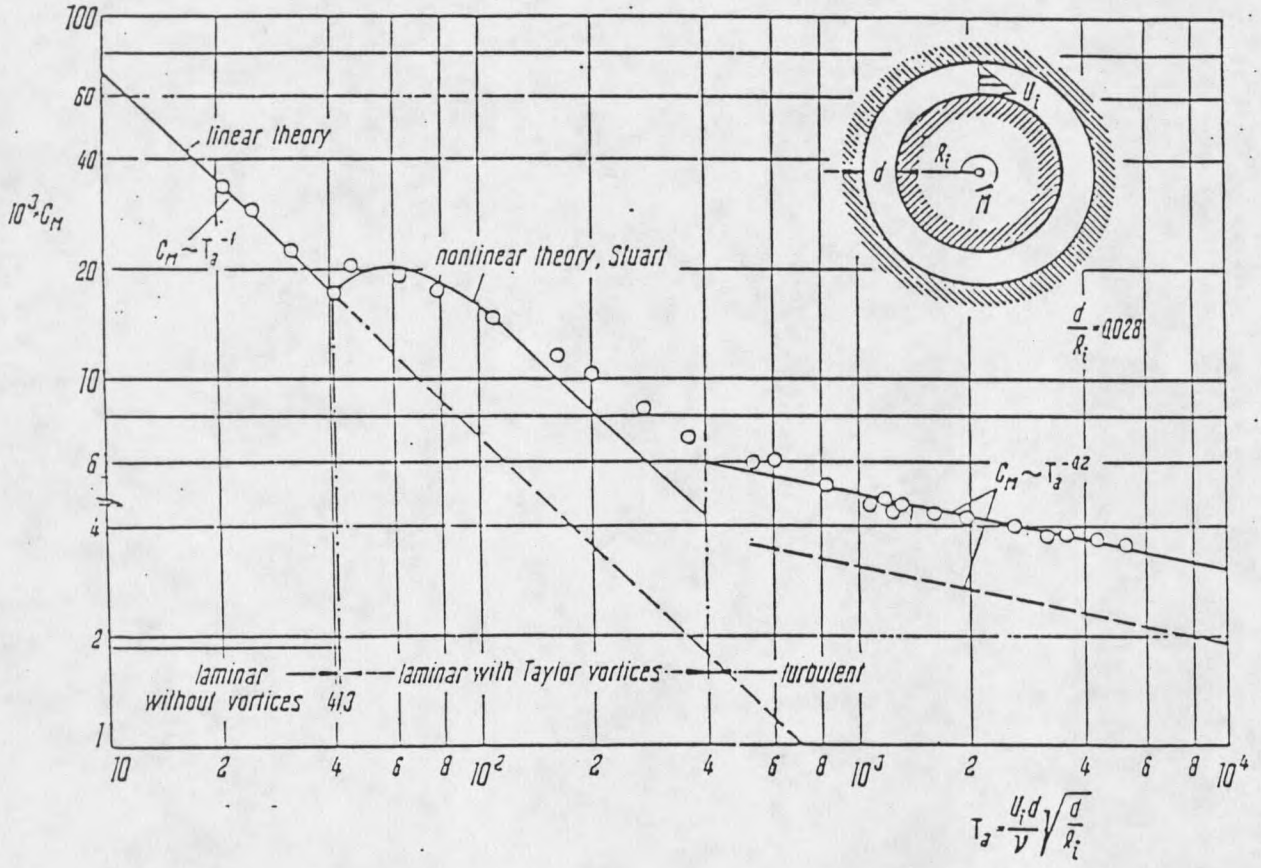

Figure 3. Flow between two concentric cylinders; torque coefficient for inner cylinder in terms of the Taylor number, Ta.[29]

Figure 3 was obtained originally using d/R_i value of 0.028. However the data are reported using Taylor number which has taken the dimension of the system into consideration.

A good approximation of torque coefficient, then, can be obtained for different d/R_i and Reynolds numbers. Figure 3 also indicates that turbulence in the system occurs for Taylor numbers greater than 400, although vortices are apparent for Taylor numbers as low as 41.3.

Substrate balance. A biofilm reactor model can be based on total number of cells or total number of viable cells. From an experimental point of view the choice of variable of cells is determined. For example, if a plate count is utilized, the number of viable cells (actually Colony Forming Units or CFU) is determined. If an optical measurement (e.g. acridine orange analyzer) is used, total number of cells is determined.

A substrate balance on the bulk liquid in a RotoTorque can be written using the same approach as a chemostat, so long as the biofilm is accounted for at steady-state. Grady and Lim [16] have solved the problem as follows:

$$\frac{1}{\tau} = \frac{\mu_m S_b}{K_s + S_b} \left[1 + \frac{X_o}{\frac{Y}{S_o - S_b}}\right] + \frac{q_m S_b \eta_o A_s}{(K_s + S_b)(S_o - S_b) V} \qquad (23)$$

Where,

q_m = maximum substrate consumption [M L^{-2} T^{-1}]

S_b = bulk substrate concentration [M L^3]

A_s = Surface area of the biofilm [L^2]

V = reactor volume [L^3]

η_0 = overall effectiveness factor

The values of the overall effectiveness factor for many different conditions are given in reference 16, page 539. For a detailed treatment see reference 16, pages 523 through 540.

Biofilm accumulation on the inside surface of the reactor is the net result of attachment (r_{att}) and growth in the biofilm (r_{fg}) minus detachment (r_{det}).

$$\frac{dX_f}{dt} = r_{att} + r_{fg} - r_{det} \qquad (24)$$

MODEL DEVELOPMENT

Attachment Model

An expression for the rate of cellular attachment will be developed using a pseudosteady-state hypothesis coupled with a film theory model. A pseudosteady-state hypothesis can be used for a system which changes slowly so that steady-state processes can be assumed.

The rate of cellular attachment to an established biofilm per unit area (R_A) can be described as a two step process. First, cells are transported from the bulk liquid to the liquid-biofilm interface. The rate of cell transport per unit area, N_x, will be developed using the film theory model. The Second is the rate of attachment of cells at the liquid-biofilm interface to the surface of biofilm per unit area, r_a.

The rate of cellular attachment per unit area to an established biofilm, R_A, will be determined by equating the processes above. Assuming pseudosteady-state, the rate of cell transport from the bulk liquid to the liquid-biofilm interface per unit area, N_x, will be equal to the rate at which cells attach (at the liquid-biofilm interface) to the biofilm surface per unit area, r_a.

The film theory model assumes the resistance to mass transport occurs entirely in a thin film adjacent to the surface. Since the flow in the film is primarily laminar,

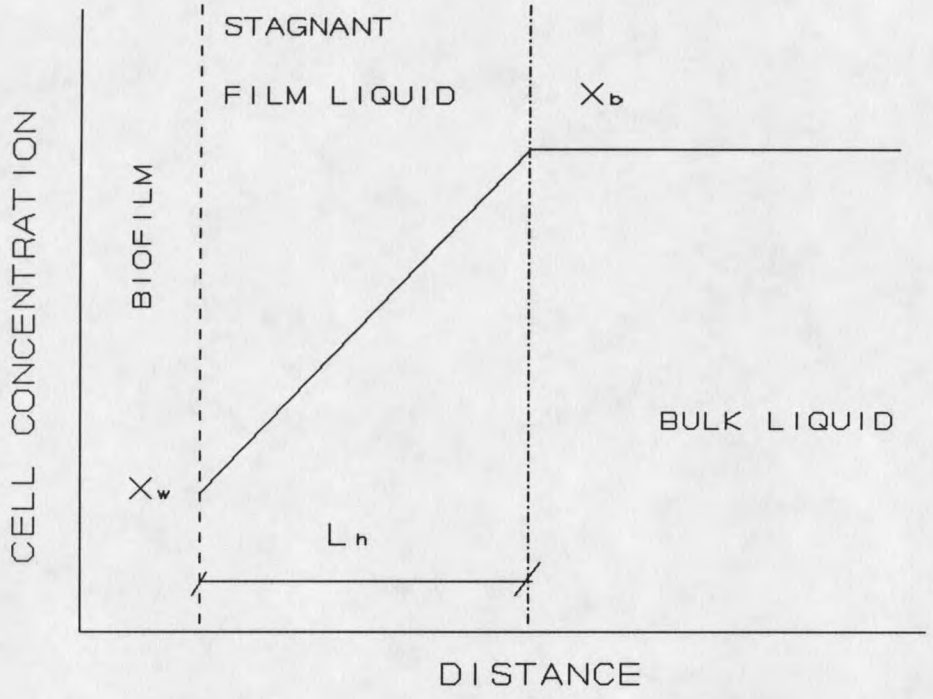

Figure 4. Idealized Film Theory

the suspended cell concentration gradient changes rapidly within the film until the turbulent region is reached. The film theory is usually derived for a flat surface [15].

By hypothesizing a stagnant liquid film of thickness L_h, the cell concentration gradient in the liquid phase is restricted to the stagnant liquid film. The cell concentration throughout the remaining region of liquid, the bulk liquid in Figure 4, is assumed constant. L_h is not the thickness of the

laminar sublayer of fluid flow region but a fictitious film thickness which would be required to account for the entire resistance to transfer of cells from the bulk liquid to the surface if only molecular transport was involved.

Under the idealized model above, the flux of cells from the bulk liquid to the surface is given as follows:

$$N_x = k_x \, (X_b - X_w) \qquad (25)$$

where

N_X = the rate of cell transport per unit area [CFU L^{-2} T^{-1}]

k_X = proportionality constant [L T^{-1}]

X_b = cell concentration in the bulk liquid region [CFU L^{-3}]

X_w = cell concentration on the surface [CFU L^{-3}]

The proportionality constant k_X has dimensions of LT^{-1}, and is a parameter associated with diffusive and convective cell transport. Its value is a function of the properties of the fluid, the diffusion coefficient of cells in the liquid, and Reynolds number [15]. Fortunately, k_X can be obtained by a simple equation derived theoretically for a flat surface as follows [5,15]:

$$k_x = \frac{D_{xb}}{L_h} \tag{26}$$

where

D_{xb} = diffusion coefficient for cells in the liquid [$L^2\ T^{-1}$]

L_h = liquid film thickness [L]

The values for liquid film thickness, L_h, must be found experimentally. This value is independent of the rate of cell transport [15].

Different microorganisms will have quite different values for D_{xb}, as it depends strongly on whether or not the microorganism is motile. Ignoring the motility of cells could underestimate the transport by a factor as much as 20 to 50 times. D_{xb} for motile cells can be predicted using a correlation as follows [11]:

$$D_{xb} = \frac{V_r\ d_r}{3\ (1 - \cos\alpha)} \tag{27}$$

where

V_r = velocity of motility [$L\ T^{-1}$]

d_r = free length of random run [L]

α = angle of turn

The next step in developing the attachment model is obtaining an expression for the attachment of cells on the liquid-biofilm interface to the established biofilm. Many factors, such as ability to form EPS (which is part of the biomass), molecular and physical structure of the biofilm, and others which are not yet fully understood may affect the attachment rate.

The attachment rate of cells from the liquid-biofilm interface to an established biofilm per unit area, r_a, can be modelled as a function of cell concentration at the liquid-biofilm interface as follows:

$$r_a = k_a X_w^n \qquad (28)$$

The attachment of cells, then, is modelled as a two-step process, i.e., transport of cells from the bulk liquid to the surface and the attachment of cells at the liquid-biofilm interface to the established biofilm. An effort to model the rate of attachment has to incorporate these two mechanisms. Mathematically, it is difficult to solve unless a steady-state condition can be assumed.

As mentioned before, biofilm accumulation is not necessarily a steady-state process. In fact, in most cases, it is not a steady-state process. However, if the system conditions such as temperature, pH, substrate concentration, and fluid shear are maintained constant, then, for short

periods of time (at least in the order of the replication time of the cells), the system can be forced to approach steady-state. This argument leads us to use the pseudosteady-state hypothesis to incorporate N_X and r_a into an attachment rate per unit area expression (R_A).

Using the pseudosteady-state hypothesis, then, N_X will be equal to r_a, and R_A will be equal to r_a.

$$R_A = k_x\ (X_b - X_w) = k_a\ X_w^n \tag{29}$$

or,

$$k_a\ X_w^n + k_x\ X_w - k_x\ X_b = 0 \tag{30}$$

and,

$$R_A = k_a X_w^n \tag{31}$$

The problem in obtaining an expression for R_A as a function of bulk cell concentration is, now, to express X_w as a fuction of k_a, k_x, and X_b. Then, the expression for X_w can be subtituted into equation (31) to obtain an expression for R_A.

A numerical value of the power "n" from equation (28) or (31) will be determined by experimental data on the rate of cellular attachment per unit area to an established biofilm, R_A vs. viable cell concentration in the bulk liquid of the

RotoTorque, X_b. If n equals zero, then the rate of cells transport per unit area from the bulk liquid to biofilm-liquid interface, N_x, is the controlling mechanism.

The rate of cellular attachment per unit area to an established biofilm, R_A, in equation (31) is a net rate of attachment per unit area. The net rate of cellular attachment per unit area to an established biofilm can be described with an example. Suppose at a certain period of time, there are 10,000 cells per unit area per unit time attaching to the surface of the biofilm. This is termed a gross rate of cellular attachment per unit area, R_{Ag}. Some of those cells will detach and return to the bulk liquid. Assume that 9,000 cells per unit area per unit time detach, then the net rate of cellular attachment per unit area to an established biofilm, R_A, during that particular period of time will be (1,000 = 10,000 - 9,000) cells per unit area per unit time. The rate of cellular detachment is usually modelled as a function of cell concentration on the surface of the biofilm. This research is concentrated on the rate of cellular attachment so that the rate of cellular detachment will not be explored further.

Hereafter, the term "rate of cellular attachment per unit area" should be understood to refer to the gross rate of cellular attachment per unit area, R_{Ag}. The net rate of cellular attachment per unit area, R_{An}, will be clearly indicated by the subsript "n" when used.

Experimental Approach

Consider a RotoTorque which is being operated with inputs from two sources: 1) a steady input of fresh substrate, e.g., glucose and 2) the effluent of a chemostat operating at steady-state. At time t = 0, the fresh substrate input to the RotoTorque is switched off. The liquid volume inside the RotoTorque is kept constant by maintaining the effluent flow rate equal to the influent flow rate. The condition of the RotoTorque and chemostat at $t = 0^-$ is known. A turbulent flow regime is induced only by the speed of the rotor.

Three balances are required to model the rate of attachment in a RotoTorque. The first is a cell balance on the bulk liquid, and the second is cell balance on the surface. The third is a substrate balance. Ignoring death and decay terms because of their considerably smaller magnitudes compared to the other terms in the balances, the cell balance in the bulk liquid for the unsteady-state condition can be written as follows:

Accumulation of cells in the bulk liquid = input - output

- attachment + detachment + growth (bulk liquid)

Cell balance on the surface (biofilm):

Accumulation of cells on the surface = attachment

-detachment + growth (surface)

Substrate balance over the RotoTorque:

Accumulation of glucose in the bulk liquid = input - output

- substrate uptake (bulk liquid + biofilm)

The Monod equation (equation (8)) is usually used to model growth in the bulk liquid. The same equation can be used to model growth in the biofilm, but mass transfer resistance from the bulk liquid to the biofilm and diffusion of substrate through the biofilm must be taken into account. For a thin biofilm, diffusion within the film is negligible compared to mass transfer resistance in the fluid adjacent to the film [16]. Mass transfer rates for non-living particles are given by reference 2.

A substrate balance is needed because the specific growth rate is a strong function of substrate concentration as given by equation (8).

Accumulation of cells in the bulk liquid, concentration of cells on the surface, and substrate accumulation can be measured experimentally.

The attachment and detachment rate coefficients can then be calculated by simultaneously solving the three equations described above.

Even using first order kinetic model, the procedure to determine attachment and detachment rate coefficients is quite complex.

If the attachment rate coefficient could be obtained independently under steady-state conditions, the effort required to obtain parameters for the system would be simplified. One way to solve the problem is to use radiolabelled cells. This is the approach taken in this work.

First, a biofilm is grown using C^{12} glucose under steady-state conditions (i.e., constant temperature, fluid shear, inlet substrate concentration, and residence time). While a biofilm is being established , the RotoTorque influent is switched to the effluent from a first chemostat which is fed steadily with C^{12} glucose. After a certain period of time ($> 3\tau$) when fluctuations in the RotoTorque are diminished, radiolabelled cells are introduced. At time $t = 0$, the RotoTorque influent is switched to the effluent from a second chemostat which has been operating exactly the same as the first, except for operation on C^{14} glucose.

At time $t = 0^+$, the RotoTorque with a C^{12} cell biofilm and C^{12} cells in the bulk liquid is receiving an effluent of a chemostat operating on C^{14}. Both the chemostat and the RotoTorque are operating at steady-state with respect to the

total cell concentration (C^{12} and C^{14} cells) in the bulk liquid. The fraction of C^{14} cells in the RotoTorque will increase from zero at $t = 0$ to nearly one, at $t \geq t_L$. The concentration of the C^{14} cells in the RotoTorque is not constant over time. The accumulation of radiolabelled cells can be determined by writing a C^{14} cell balance on the RotoTorque (assuming pure CFSTR behavior). The result is as follows:

$$\frac{dX^{14}}{dt} = \frac{F}{V}(X_i^{14} - X^{14}) \qquad (32)$$

where

F = inlet and outlet flow rate of the RotoTorque [$L^3\ T^{-1}$]

V = the liquid volume in the RotoTorque [L^3]

X_i^{14} = inlet C^{14} cell concentration [CFU L^{-3}]

X^{14} = bulk C^{14} cell concentration [CFU L^{-3}]

t = time [T]

The inlet C^{14} cell concentration, X_i^{14}, the volume, V, and the inlet and oulet flow rates, F, are constants. Equation (32) can be integrated easily to give:

$$X^{14} = X_i^{14} (1 - e^{-\frac{t}{\tau}}) \qquad (33)$$

where τ is the space time as given by equation (13).

The total number of cells in the RotoTorque, X^{total}, assuming pure CSFTR behavior, will be equal to the inlet C^{14} cell concentration, X_i^{14}. The assumption is justified since the RotoTorque receives only the effluent from the chemostat, the glucose concentration of the bulk liquid in the RotoTorque is low, and the residence time of the RotoTorque was set considerably lower than the residence time of the chemostat, thus growth is minimized.

The rate of cellular attachment and detachment per unit area are both negligible compared to other terms in equation (32). This will be demonstrated below in the results section.

The ratio of the C^{14} cell concentration to total cell concentration in the RotoTorque, then, can be given as follows:

$$\frac{X^{14}}{X^{total}} = 1 - e^{-\frac{t}{\tau}} \qquad (34)$$

Assuming that the C^{14} cells are behaving the same as the C^{12} cells, the ratio of the gross rate of C^{14} cellular attachment per unit area to an established biofilm, R_{Ag}^{14}, to

the gross rate of total cellular (C^{12} cells + C^{14} cells) attachment per unit area to an established biofilm, will be:

$$R_{Ag}^{14} = (1 - e^{-t/\tau})\, R_{Ag}^{total} \qquad t \geq 0 \qquad (35)$$

Equation (35) holds for any time greater than or equal to zero as indicated above. On the other hand, the ratio of the net rate of C^{14} cellular attachment per unit area to an established biofilm to the net rate of total cellular attachment per unit area to an established biofilm, which will be given below, holds only for a large time as determined by the experiment. This is caused by the fact that the C^{14} cells which just attached to the surface will not detach as fast as the C^{12} cells which have been attached for a longer time and initially cover a larger portion of the surface. Eventually, at time $t \geq t_L$, as indicated by a steady-state rate of C^{14} cellular detachment per unit area, both C^{14} cells and C^{12} cells will behave identical with regard to attachment and detachment, and the ratio of the rate of cellular attachment per unit area of the C^{14} cells to the rate of total cellular attachment per unit area will be:

$$R_{An}^{14} = (1 - e^{-t/\tau})\, R_{An}^{total} \qquad t \geq t_L \qquad (36)$$

Ideally, the time t_L is chosen as the time at which the rate of C^{14} cellular detachment per unit area reaches its steady-state, however, for practical purposes the time t_L could be chosen as the rate of C^{14} cellular detachment per unit area reaches 90% of its steady-state value. Appendix B describes how the time t_L is chosen for this work.

We know that;

$$R_{An}^{14} = R_{Ag}^{14} - R_d^{14} \tag{37}$$

Using equation (35) to substitute for R_{Ag}^{14}.

$$R_{An}^{14} = (1 - e^{-t/\tau})\, R_{Ag}^{total} - R_d^{14} \tag{38}$$

The rate of C^{14} cellular detachment per unit area in equation (37) is zero at time t = 0. Let us assume for a moment that the rate of C^{14} cellular detachment per unit area is zero at any time greater than zero. Integrating equation (38) over time will give the accumulation of C^{14} cells per unit area of biofilm surface, the experimentally measured quantity.

$$acc.\ of\ C^{14} = \int R_{An}^{14}\, dt = \int (1 - e^{t/\tau})\, R_{Ag}^{total}\, dt \tag{39}$$

The (gross) rate of total cellular attachment per unit area to an established biofilm, R_{Ag}, is constant because the

number of total cells (C^{12} + C^{14} cells) in the bulk fluid of the RotoTorque is constant, as are the system parameters such as RPM, temperature, pH, etc. Integrating equation (38) will give:

$$accumulation\ of\ C^{14}\ per\ unit\ area = R_{Ag}^{total}\ [Tm] \qquad (40)$$

where

$$[Tm] = t - \tau\,(1 - e^{-t/\tau}) \qquad (41)$$

t = time [T]

[Tm] = modified time, defined by equation (41) [T]

τ = residence time, F/V [T]

F = inlet and outlet volumetric rate [$L^3\ T^{-1}$]

V = liquid volume of the RotoTorque [L^3]

However, equation (40) is strictly true only for time t = 0 because that is the only time it can be strictly known that the rate of C^{14} cellular detachment per unit area is zero at time t = 0 as assumed during the derivation of equation (39).

For time $t \geq t_L$, equation (36) can be integrated to give:

$$accumulation\ of\ C^{14}\ per\ unit\ area = R_{An}^{total}\ [Tm] \qquad (42)$$

In conclusion, the method described above can theoretically be used to measure the net and gross rates of cellular attachment to an established biofilm, and by difference the rate of cellular detachment for a particular experimental condition. To obtain a model of the rate of attachment as a function of bulk cell concentration many runs with different bulk cell concentrations must be performed.

EXPERIMENTAL

The experiments were carried out under aerobic conditions with a monopopulation system. In order to avoid contamination, substrate and all equipment which was in direct contact with the inside surface of reactors was autoclaved prior to each experiment. Sterile air filters were used to avoid contamination from the surroundings. If one of the reactors had to be opened, direct contact with the inner surface was always avoided and the opening was performed near a bunsen burner to minimize contamination from airborne microorganisms.

Two phases of experiments were performed. First a system which consisted of six small RotoTorques and two chemostats was used. The first chemostat was used to grow C^{12} cells and the other chemostat was used to grow C^{14} cells. At any time, there was only one chemostat connected to the RotoTorques as shown in Figure 5. The attachment data were collected from the rotor surface of each RotoTorque.

The system for the second phase of the experiments consisted of one standard RotoTorque and two chemostats. As above, one RotoTorque was used to grow C^{12} cells while the other one was used to grow C^{14} cells. At any time, there was only one chemostat connected to the RotoTorque (see Figure 6). The attachment data were collected from twelve slides attached to the stationary inside surface of the RotoTorque.

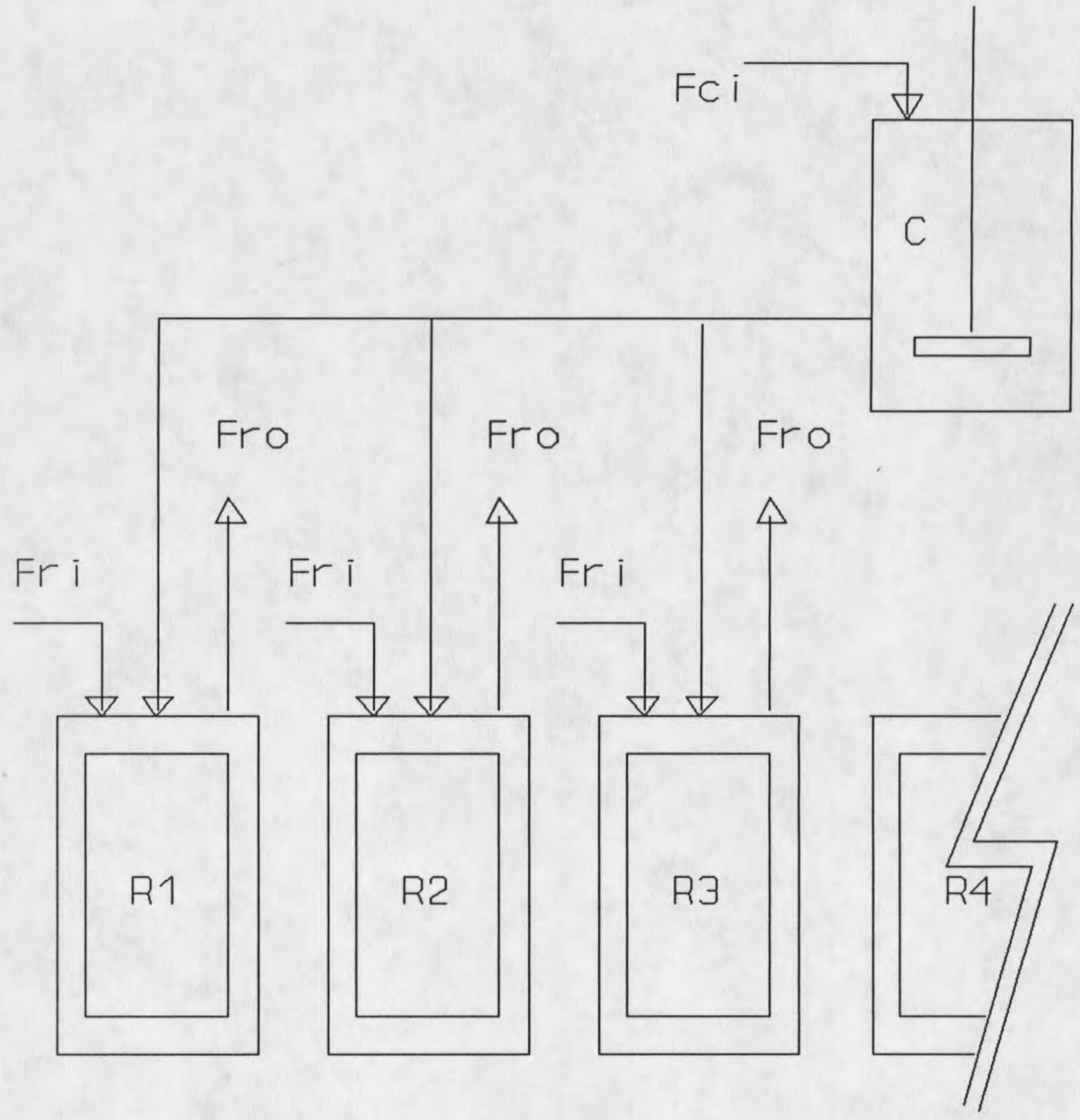

Figure 5. Experimental System of Phase 1, Run 1. Fci - fresh substrate to the chemostat, Fri - fresh substrate to each RotoTorque, Fro - the effluent of the RotoTorques, see Table 3a, 3b, and 3c for numerical value of each flow.

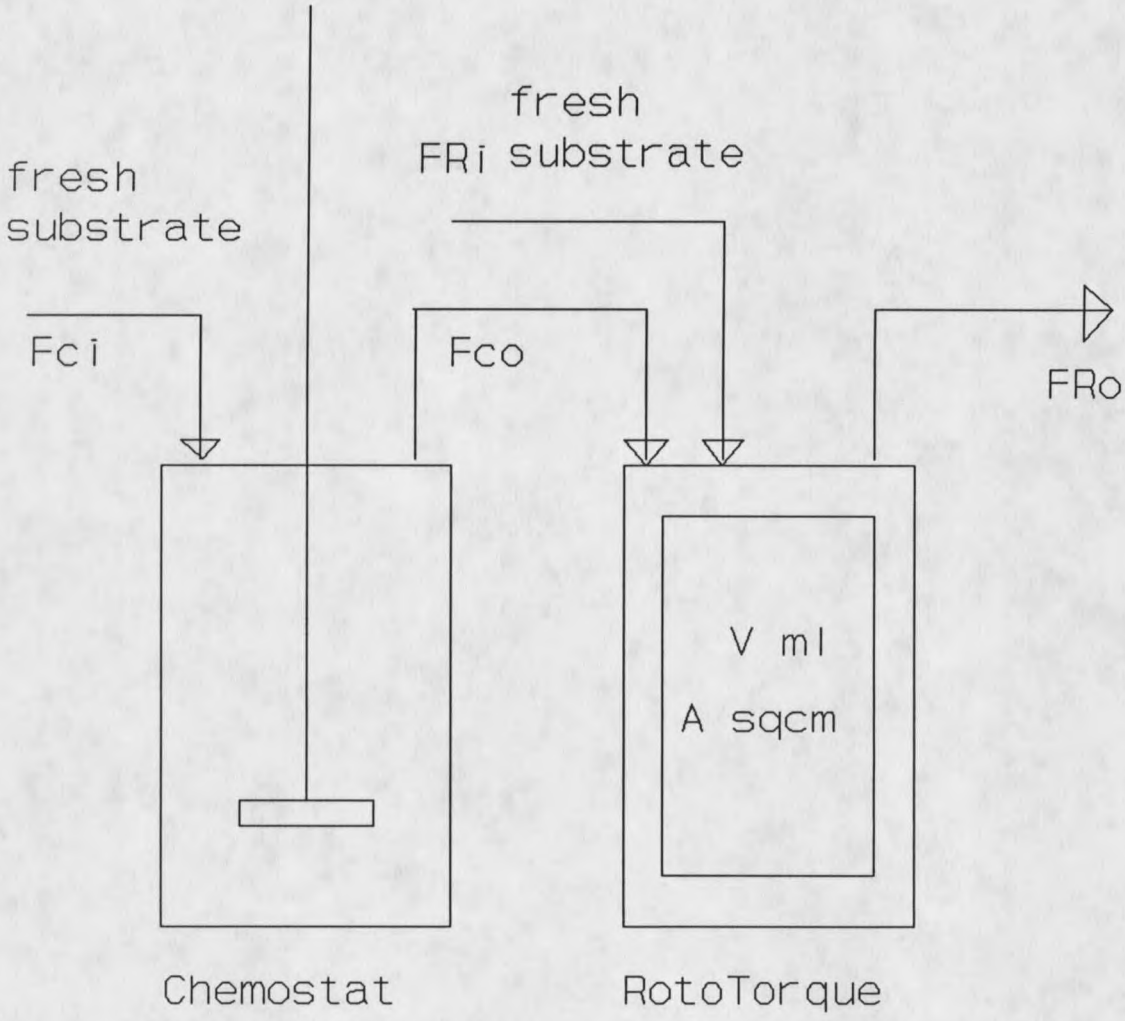

Figure 6. Experimental System of Phase 2 Experiments. Fci - fresh substrate to the chemostat, Fri - fresh substrate to the RotoTorque, Fco - outlet flow of the chemostat, Fro - effluent flow of the RotoTorque, see Table 3a, 3b, and 3c for numerical value of each flow.

Reactors

Chemostat

The characteristics of the chemostats are listed in Table 2.

Table 2. Dimensions of Reactors.

Phase 1		Phase 2	
Chemostat			
Volume	4000 ml	Volume	3840 ml
F_{Ci}	12 ml/min	F_{Ci}	7.11 ml/min
RotoTorque			
Volume	180 ml	volume	640 ml
D 1	5 cm	D 1	10 cm
D 2	6.75 cm	D 2	11.6 cm
L 1	7 cm	SW	1.8 cm
L 2	adjusted	SL	19 cm
A_1	258.5 cm^2	A_2	1289.31 cm^2
F_{ro}	2 ml/min	F_{ro}	7.11 ml/min

where,

D 1 = diameter of the inner cylinder of the RotoTorque

D 2 = diameter of the outer cylinder of the RotoTorque

L 1 = height of the inner cylinder of the RotoTorque

L 2 = liquid height in the phase 1 RotoTorque

SW = slide width

SL = liquid height in the phase 2 RotoTorque

A = surface area for attachment, subscript refers to the experimental phase

F_{Ci} = inlet flow rate into the chemostat

F_{ro} = inlet flow rate into the RotoTorque

RotoTorque

A RotoTorque is an annular reactor consisting of two concentric cylinders, a stationary outer cylinder and a rotating inner cylinder. Draft tubes (two for small RotoTorques (Figure 7) and four for a standard RotoTorque (Figure 8)) were bored at angles in the inner cylinder. The draft tubes cause mixing of the liquid phase in the reactor, by virtue of the rotating cylinder. The inner cylinder is driven by a magnetic stirrer for the small RotoTorque and direct coupling to a motor for the standard version.

The inside wall of the reactor and the peripheral area of the rotor are considered as the only area for attachment. This will give a total area of 258.49 cm^2 (A_1) and 1289.31 cm^2 (A_2) for the small and the standard RotoTorques respectively.

Preparation

General

In preparation for each experiment, all equipment was cleaned. Hydrogen peroxide solution was, then, used to wash all reactor components, followed by rinsing with flowing distilled water for half an hour to wash out all hydrogen peroxide and C^{14} glucose residue. This was followed by drying before the reactors were set up.

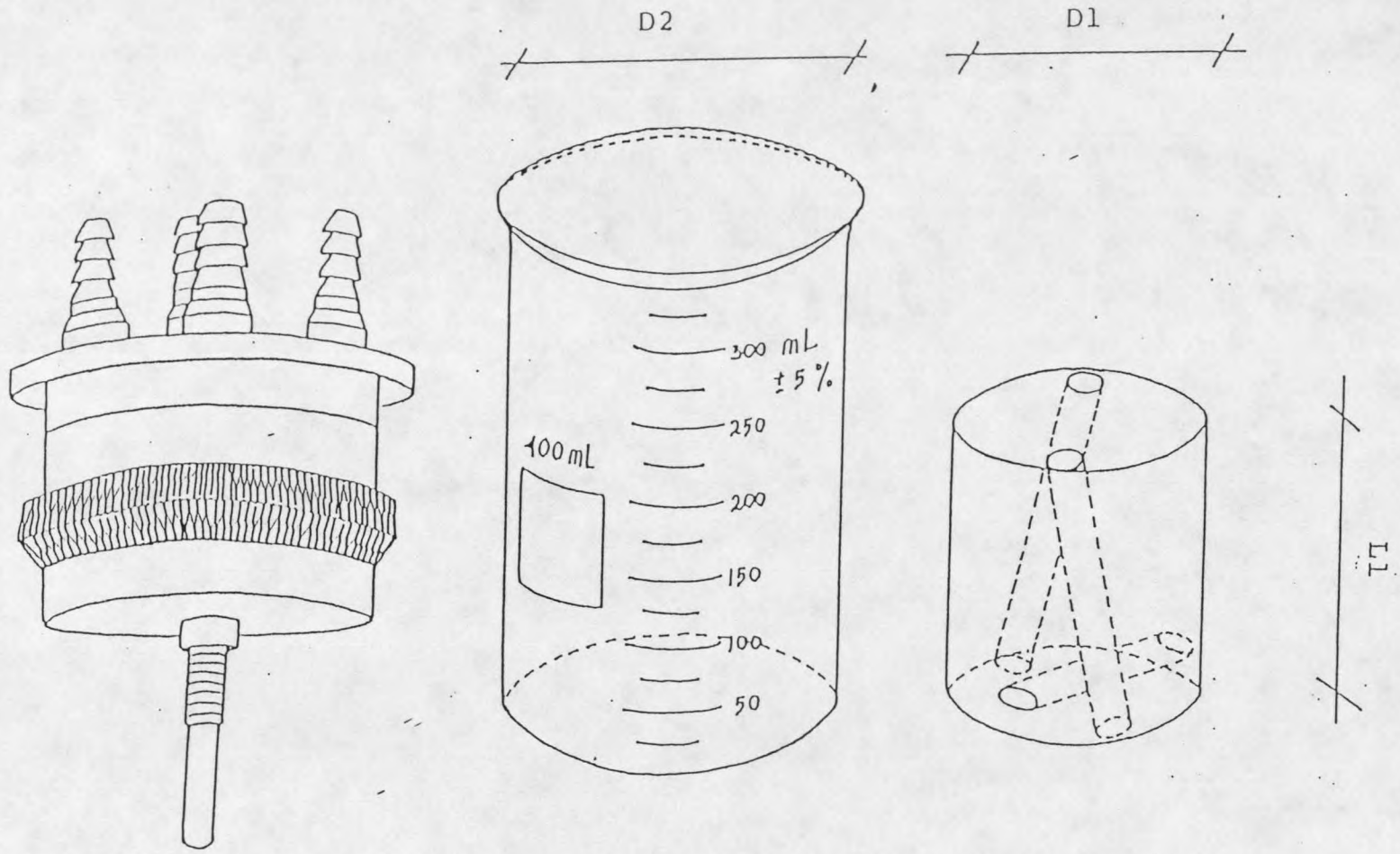

Figure 7. RotoTorque Parts of Phase 1 Experiment.

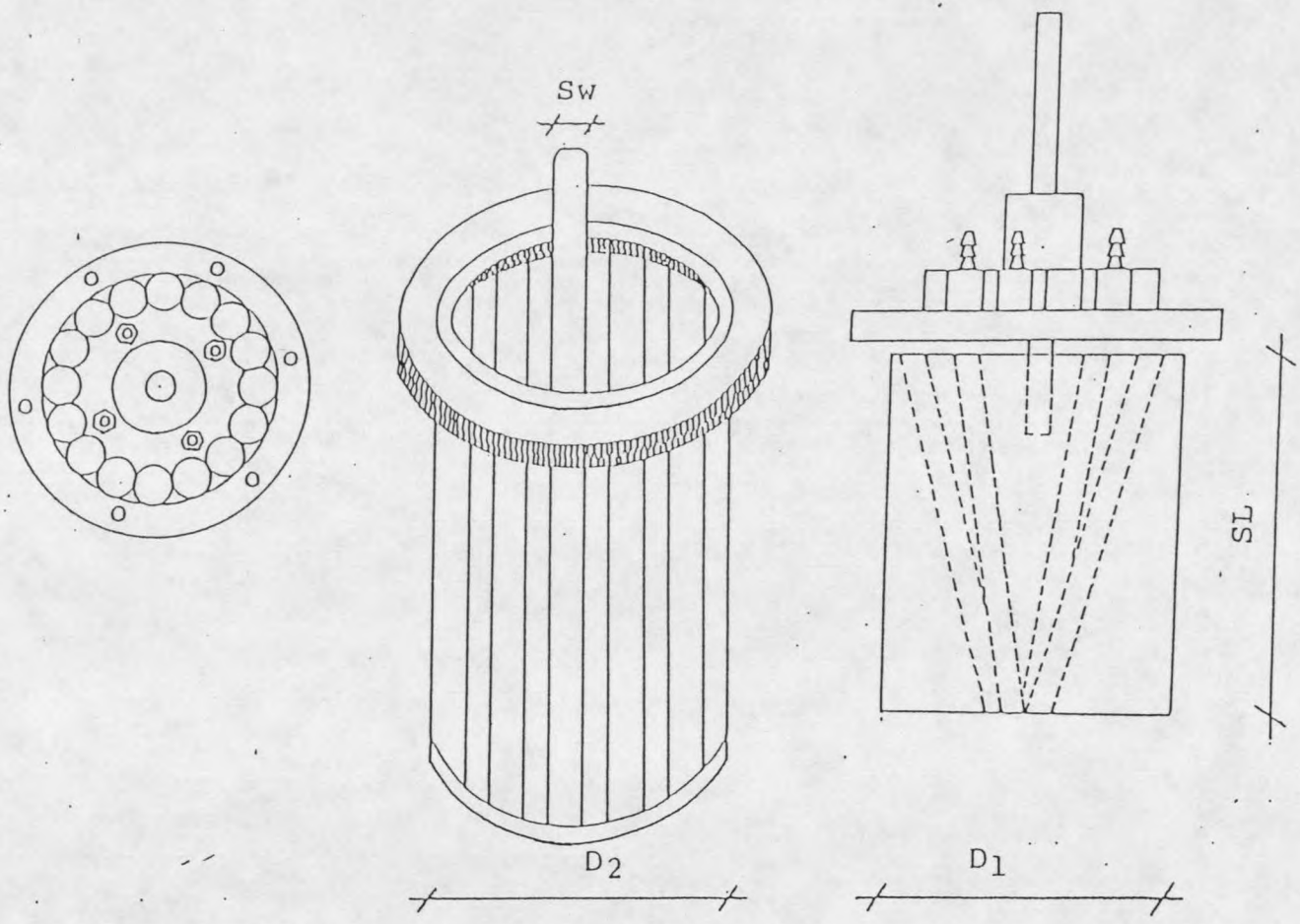

Figure 8. RotoTorque Parts of Phase 2 Experiments.

To minimize contamination during an experiment, any leak on the system was avoided. Before all equipment was autoclaved, the system was operated with water at a flow rate twice as high as the anticipated experimental condition for 24 hours. Any leak found during this period was easily eliminated and contamination during the actual experiment was minimized.

All equipment was autoclaved for fifteen minutes at 121°C prior to use, except for any apparati which were not in direct contact with the growth media. All tube ends were sealed before autoclaving except the air filter inlet.

Nutrient Medium

The composition of the supplied nutrients per liter of solution was as follows:

K_2HPO_4	2800 mg.
KH_2PO_4	1200 mg.
$(NH_4)_2SO_4$	640 mg.
$MgSO_4$	400 mg.

The mineral solution (this term will be used throughout this thesis) was autoclaved first, then, after cooling, the glucose was introduced by filter sterilization. Thirty milligrams of glucose as a carbon source were added and acted as the limiting nutrient.

When an experiment required a different glucose concentration, the concentration of mineral solution was

adjusted accordingly. If 10 mg/l glucose, for example, were used, then, the concentration of mineral solution would be adjusted to one third the original concentration given above. In this way the C/N and N/P ratios were maintained at the same level in all experiments.

Experimental System and Design

The system for the phase one experiment consisted of two chemostats and six small RotoTorques. The chemostat provided a steady supply of planktonic P. aeruginosa along with a low substrate concentration. Biofilms were grown in all six RotoTorques under the same experimental conditions, i.e., the same shear stress (induced by the rotational speed of rotors), identical substrate feeds, and identical dilution rates. Theoretically, the same biofilm in terms of thickness, and physical and morphological properties should be obtained. However, some uncertainties such as human errors, fluctuation of the room temperature, etc. might induce variations in properties of the biofilms obtained from each RotoTorque. Care was taken to minimize these variables.

The same procedure was also followed with the second experimental system, except that, in this system, there was only one standard-sized RotoTorque equipped with slides (there are 12 slides in a RotoTorque), and two chemostats. All experimental conditions are listed in Tables 3, 4, 5, 6.

Original cultures of P. aeruginosa were obtained from Anne Camper, Staff Microbiologist, Engineering Research Center for Interfacial Microbial Process Engineering, Montana State University, Bozeman, Montana.

Each experiment started by growing a pure culture of P. aeruginosa in the chemostat under aerobic conditions. To grow pure culture in the chemostat, the chemostat was inoculated with 1 ml solution of pure stock culture. The outlet of the chemostat went to the RotoTorque(s) (phase one) which were also maintained under aerobic conditions. To maintain aerobic conditions, the chemostat and RotoTorques were purged with filtered air. The rotational speed of each rotor (phase one) was set to the same speed. This speed was changed as a variable in every experiment.

At the beginning of an experiment, fresh substrate was added to each RotoTorque at the rate of 2 ml/min while fresh substrate at the rate of 1 ml/min was fed to the chemostat. During this period, the residence time of the chemostat was 4000 minutes. The system was operated under these conditions for seven days (See Figure 9). The same procedure was followed with the second phase experiment system.

The purpose of the procedure described above was to obtain an established biofilm in each RotoTorque.

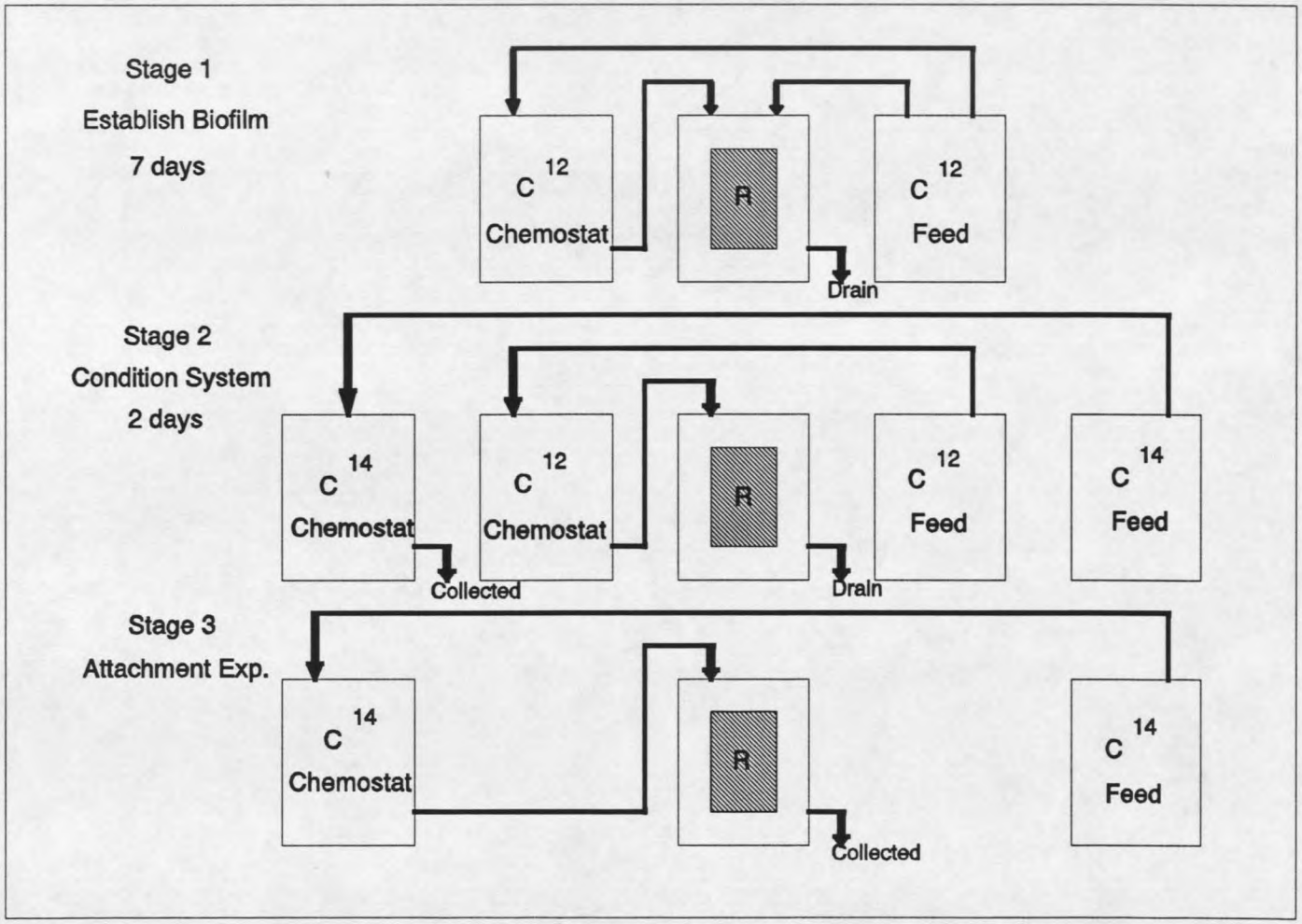

Figure 9. Attachment Experiment.

Table 3. Experimental Conditions - General.

Phase1		Phase 2	
Rotor			
RPM	600	run 1	289
		run 2	20
		run 3	289
		run 4	289
		run 5	289
		run 6	289
		run 7	289
Room Temperature (°C)			
run 1	22	run 1	22
		run 2	22
		run 3	22
		run 4	22
		run 5	22
		run 6	22
		run 7	22
pH			
Fresh Substrate	7.2		7.2
RotoTorque Eff.	6.9		6.9
Concentration of the C^{12} Fresh Substrate glucose (mg/l)			
run 1	30	run 1	30
		run 2	30
		run 3	**
		run 4	30
		run 5	30
		run 6	30
		run 7	30
Concentration of the C^{14} Fresh Substrate Glucose (μCi/l)			
run 1	1.5	run 1	1.5
		run 2 - 7	2.5

**) See Table 4.

Table 4. Experimental Stage 1, Establish Biofilm.

Phase 1		Phase 2	
Duration (days)			
run 1	7	run 1 - 6	7
		run 7	1
Chemostat (ml/min)			
Fc_i	1		7
Fc_o	1		7
RotoTorque (ml/min)			
Fr_i	2		7.1
Fr_o	2.2		14.2

Note: The flow rate of each stream listed in Tables 4, 5, 6 as defined in Figure 5, and Figure 6 are given below. The units are ml/min.

Table 5. Experimental Condition Stage 2, Condition System.

Phase 1		Phase 2	
Duration			
run 1	2	run 2 - 7	2
Chemostat (ml/min)			
Fc_i	12		7
Fc_o	12		7
RotoTorque (ml/min)			
Fr_i	0		0
Fr_o	2.2		7.1

Table 6. Experimental Condition Stage 3, Attachment Experiment.

	Phase 1	Phase 2
Chemostat (ml/min)		
Fc_i	12	7
Fc_o	12	7
RotoTorque (ml/min)		
Fr_i	0	0
Fr_o	2.2	7.1

After seven days, the flow of fresh substrate to each RotoTorque was stopped. At the same time, the flow rate of fresh substrate to the chemostat was changed to 12 ml/min. The effluent of the chemostat went to the RotoTorques so that each RotoTorque received 2 ml/min of fluid from the chemostat. This condition was maintained for 2 days. This procedure conditioned each RotoTorque for the attachment experiment.

Meanwhile, the second chemostat was operated under the same conditions as the first chemostat, except that C^{14} glucose was used instead of C^{12} glucose. In this way, every parameter in both systems was the same except the second chemostat had C^{14} cells and small amounts of C^{14} glucose in the bulk liquid. The specific activity of C^{14} glucose used was 8.1 millicurie per millimole.

The attachment experiment was performed by introducing the second chemostat effluent (with C^{14} cells) to the RotoTorque in place of the first chemostat effluent. All

experimental variables were maintained constant except now, C^{14} cells were entering the RotoTorque system instead of C^{12} cells. The chemostat was still receiving fresh C^{14} substrate. The same procedure was followed for the second, single RotoTorque system.

Data were taken at predetermined intervals. The exact times of data collection were recorded.

In phase 2, run 3 experiment, a lower bulk cell concentration than the bulk cell concentration in the phase 2, run 1 experiment in the RotoTorque was desired. For this experiment, the fresh glucose substrate concentration introduced to the system was changed gradually from 30 mg/l at day 1 to 3 mg/l at day 10 as listed in Table 7. The purpose of the gradual decrease in substrate concentration was to obtain a substantial biofilm growth on the inside surface of the RotoTorque and at the same time to prevent shock in the system.

Phase 2 run 6 (P 2 R 6) was the duplicate experiment of P 2 R 1. P 2 R 7 had the same experiment conditions as P 2 R 1 except the C^{12} biofilm was grown for only 1 day instead of 7 days (i.e.,stage 1 was only one day long).

All liquid contaminated with C^{14} glucose was collected and submitted to the radiological safety officer for proper disposal.

Table 7. Influent Fresh Substrate Glucose Concentration for Phase 2, Run 3 Experiment.

Day	Glucose Concentration	
1	0	mg/l
2	30	mg/l
3	15	mg/l
4	15	mg/l
5	10	mg/l
6	10	mg/l
7	5	mg/l
8	3	mg/l
9	3	mg/l
10	3	mg/l

Detachment Experiment

The rate of total cellular detachment per unit area was measured independently for two sets of experimental conditions, i.e., phase 2 run 4 (P 2 R 4), and phase 2 run 6 (P 2 R 6). For the detachment experiment, the RotoTorque with an established biofilm was flushed with a high flow rate of mineral solution (with a glucose concentration of 2.1 mg/l) so that the RotoTorque would have a shorter residence time than its minimum residence time (the point of washout).

First, a biofilm was grown in the RotoTorque. The experimental condition at this time was the same as the experimental condition at P 2 R 4, and P 2 R 6 (see Table 3).

After one week, the fresh substrate flow rate was increased to 94 ml/min for P 2 R 4, and 67 ml/min for P 2 R 6. The fresh substrate glucose concentration used to flush the RotoTorque was 2.1 mg/l which was the concentration of glucose in the bulk liquid of RotoTorque while the biofilm was being established. One milliliter volumes of bulk liquid RotoTorque effluent were taken at a prescribed times. Plate counts were used to enumerate the viable cells for each sample taken.

Liquid Scintillation Counter

A liquid scintillation counter was used to measure the radioactivity level obtained from biofilm samples. The units of the measured results were counts per minute (CPM).

The following procedure was used to prepare samples for counting. First, each sample was obtained by scraping the surface of a rotor (phase 1) or slide (phase 2). The biofilm then thus obtained was dissolved in 15 ml cocktail solution (Aquasol, Dupont, Massachusetts). Now the sample was ready to be counted in the liquid scintillation machine.

Plate Count

R2A agar was used to make the agar plates. Approximately 20 ml of the agar solution was used for each plate. Two types of samples were taken for plate count. First, samples were taken from the bulk liquid of the RotoTorque. Second, samples were taken from the bulk liquid of the chemostats.

The same plate count procedures were used for both types of liquid samples. One milliliter of sample liquid was transferred to a reaction tube containing 9 ml of mineral solution (the first dilution). The second dilution was performed by transferring 1 ml of solution from the first dilution to a reaction tube containing 9 ml of the solution. Seven serial dilutions were made for each sample.

One-tenth milliliter of each dilution, then, was spread over the surface of an agar plate. A sterile glass spreader was used to spread the solution over the agar surface. After three days of incubation (to minimize contamination) at room temperature, colonies were ready to be counted.

Conversion from CPM to CFU

The number of C^{14} viable cells of experimental run in the bulk liquid of each of chemostat was determined by the plate count method. The unit of the viable cell count was CFU/ml. The intensity of radioactivity level of the bulk liquid, consisted of C^{14} cells and negligible amount of C^{14} glucose, of

the chemostat was measured by a liquid scintillation counter. The unit was CPM/ml.

A correlation was established between the number of viable cells determined by plate count method (the units are CFU) in the chemostat and the CPM of the bulk liquid in the chemostat. This standard was performed for each experiment and was used to convert CPM to CFU for each particular experiment.

RESULTS

Some terms used in this work will be explained again here to avoid confusion. The term "total" means the total number of C^{14} and C^{12} cells. The term "gross", as in the net rate of total cellular attachment per unit area to an established biofilm means the number of cells attaching to the surface per unit area per unit time, i.e. as, if no cells are detaching from the surface. The term "net", as in the net rate of total cellular attachment per unit area to an established biofilm, means the "gross" rate of total cellular attachment per unit area to an established biofilm minus the rate of total cellular detachment per unit area.

The rate of total cellular detachment per unit area, and the gross and net rate of total cellular attachment per unit area to an established biofilm can be determined by measuring slopes of the graph of C^{14} cell concentration on the surface of the biofilm, X_s^{14}, versus [Tm], the modified time defined by equation (51).

As expected, it was observed that the net rate of cellular attachment was very small compared to the number of cells flowing into or out of the RotoTorque. From P 2 R 7 experimental run, the number of cells flowing into the RotoTorque (48 10^6 CFU/ml) x (7.1 ml/minute) = 3.4 10^8 CFU/minute, while the net rate of cellular attachment was (1400 CFU/cm^2 minute) x (1289 cm^2) = 1.8 10^6 CFU/minute (it was

only .5% of the number of cells flowing into the RotoTorque). The profile of bulk C^{14} cell concentration over time could not be used to measure the rates of cellular attachment or detachment. Instead, measurement of the accumulation of the C^{14} cells on the surface over time were used to determine the gross, and net rates of cellular attachment and, by difference, the rate of cellular detachment. Details of this procedure are described in the model development section.

The solid line in Figure 10 is a theoretical prediction of the C^{14} cells concentration profile over time based on the assumption that the RotoTorque is behaving as a CFSTR. The presence of a film is ignored in this calculation. The squares are the actual experimental measurement of the C^{14} cells concentration as a function of time. The difference between these two should be the net rate of attachment per unit area. However, the accuracy of the plate count method limits the ability to determine the rate of cellular attachment and detachment from the X_b^{14} vs. time curve.

Direct measurement of the C^{14} cell accumulation on the surface can be used to determine both the gross and net rates of cellular attachment per unit area, as well as the rate of detachment per unit area. Provided with the graph of X_s^{14}, C^{14} cells on the surface per unit area (CFU/cm^2), vs. [Tm], the modified time (see Figure 11), the slope (slope I) of the graph at the modified time [Tm] = 0 will give the value of the gross rate of total cellular attachment per unit area while

the slope (slope II) of the same graph at time $t \geq t_L$, where t_L is chosen as large as the data allowed, will give the value of the net of C^{14} cellular attachment to an established biofilm.

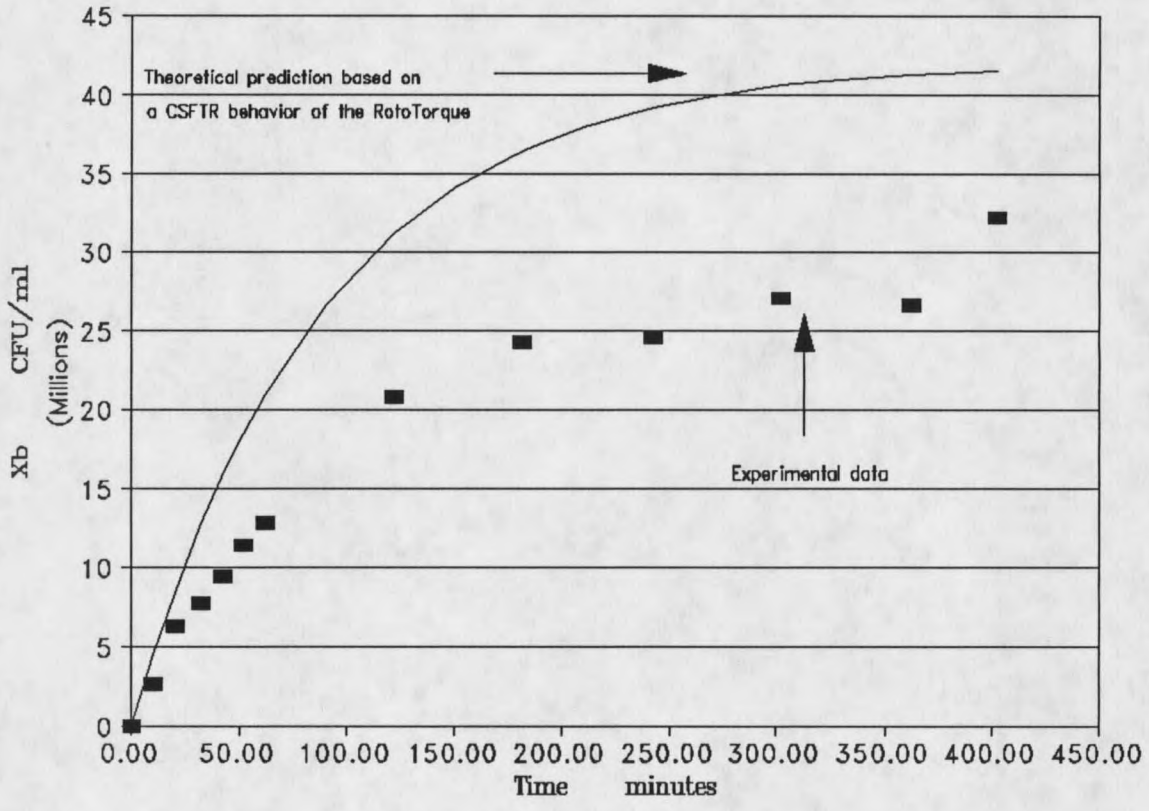

Figure 10. P 2 R 1: C^{14} Viable Cells of The Bulk Liquid in The RotoTorque vs. Time. Inlet flow rate = outlet flow rate = 7.11 ml/min, liquid volume in the RotoTorque = 640 ml.

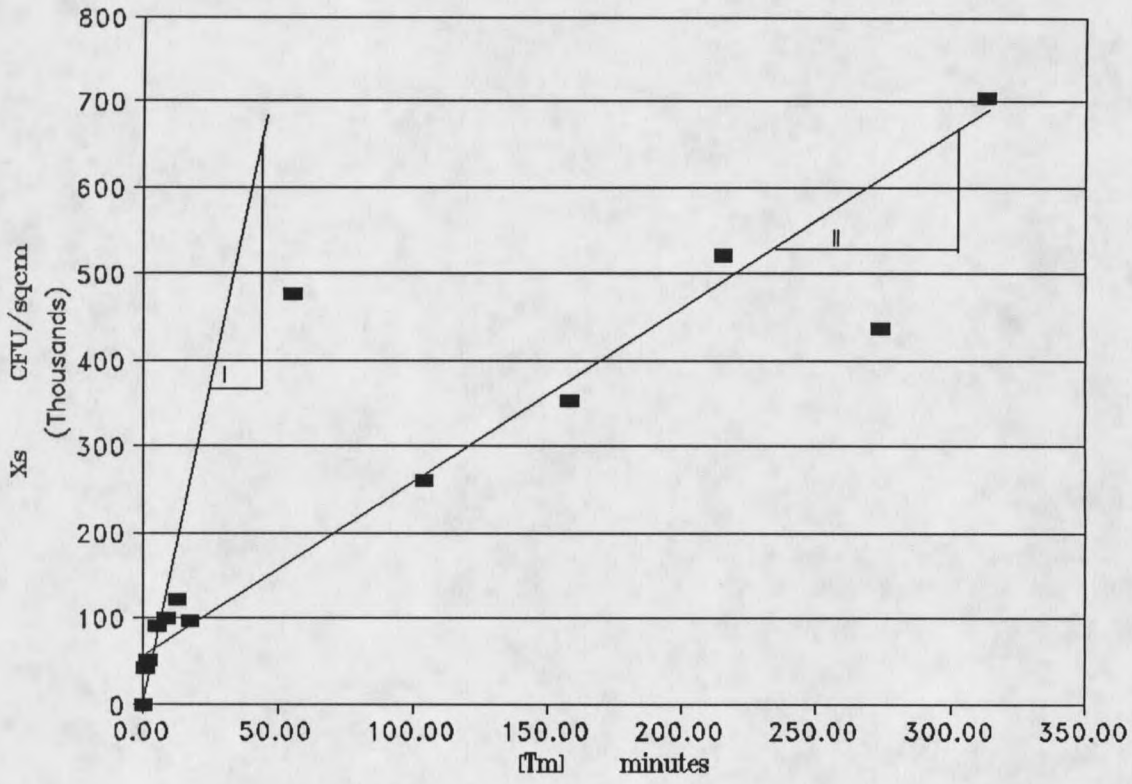

Figure 11. P 2 R 1: Accumulation of C^{14} Viable Cells on The Surface of an Established Biofilm vs. Modified Time [Tm]. Regular RotoTorque, RPM = 289, fluid shear = 20 dyne/cm^2, substrate glucose concentration chemostat influent = 30 mg/l, temperature = 22°C.

The net rate of total cellular attachment per unit area to an established biofilm, R_{An}^{total}, is correlated to R_{An}^{14}, the net rate of C^{14} cellular attachment per unit area by equation (36).

The modified time, [Tm], is correlated to time, t, as given by equation (41).

$$R_{An}^{14} = (1 - e^{-t/\tau})\, R_{An}^{total} \qquad t \geq t_L \tag{36}$$

$$[Tm] = t - \tau\,(1 - e^{-t/\tau}) \tag{41}$$

By using equation (36) to calculate R_{An}^{total}, it is said that the value of R_{An}^{total} is estimated based on the R_{An}^{14} calculated from an experimental data set when the C^{12} and C^{14} cells on the surface of biofilm are behaving identically. That is, the C^{14} detachment rate has stabilized and now assumed steady. Based on this procedure, R_{Ag}^{total} of 16,000 CFU/(cm^2 minute) and R_{An}^{total} of 1,800 CFU/(cm^2 minute) for P 2 R 1 are obtained.

The rate of total cellular detachment per unit area can be computed as the difference between the gross rate of total cellular attachment per unit area, R_{Ag}^{total}, and the net rate of total cellular attachment per unit area, R_{An}^{total}. This method to calculate the rate of total cellular detachment per unit area will be called the first method of calculating R_d^{total}. R_d^{total} of 14,000 CFU/(cm^2 minute) is obtained using the first method.

The net rate of C^{14} cellular attachment per unit area to an established biofilm, R_{An}^{14}, is the slope (dX_s^{14}/dt) of the

graph of C^{14}-cell accumulation vs. time. R_{An}^{14} is a function of time.

The gross rate of C^{14} cellular attachment area, R_{Ag}^{14}, equals the gross rate of total cellular attachment per unit area, R_{Ag}^{total}, multiplied by $(1 - e^{-t/\tau})$ as shown by equation (35).

$$R_{Ag}^{14} = (1 - e^{-t/\tau})\, R_{Ag}^{total} \qquad t \geq 0 \qquad \textbf{(35)}$$

The rate of C^{14} cellular detachment per unit area, R_d^{14}, which is a function of time, is the difference between the gross rate of C^{14} cellular attachment per unit area to an established biofilm, R_{Ag}^{14}, and the net rate of C^{14} cellular attachment per unit area, R_{An}^{14}.

A saturation-type equation can be used to fit the rate of R_d^{14} as a function of time. The maximum rate of C^{14} cellular detachment per unit area, R_{dmax}^{14}, should be the same as the rate of total cellular detachment per unit area, R_d^{total}. This provides a second method for computing R_d^{total}. R_{dmax}^{14} obtained (see Figure 12) is 16,000 CFU/(cm^2 minute). R_d^{total} obtained using the first method is 14,000. See summary of results below for the results of the other experimental conditions.

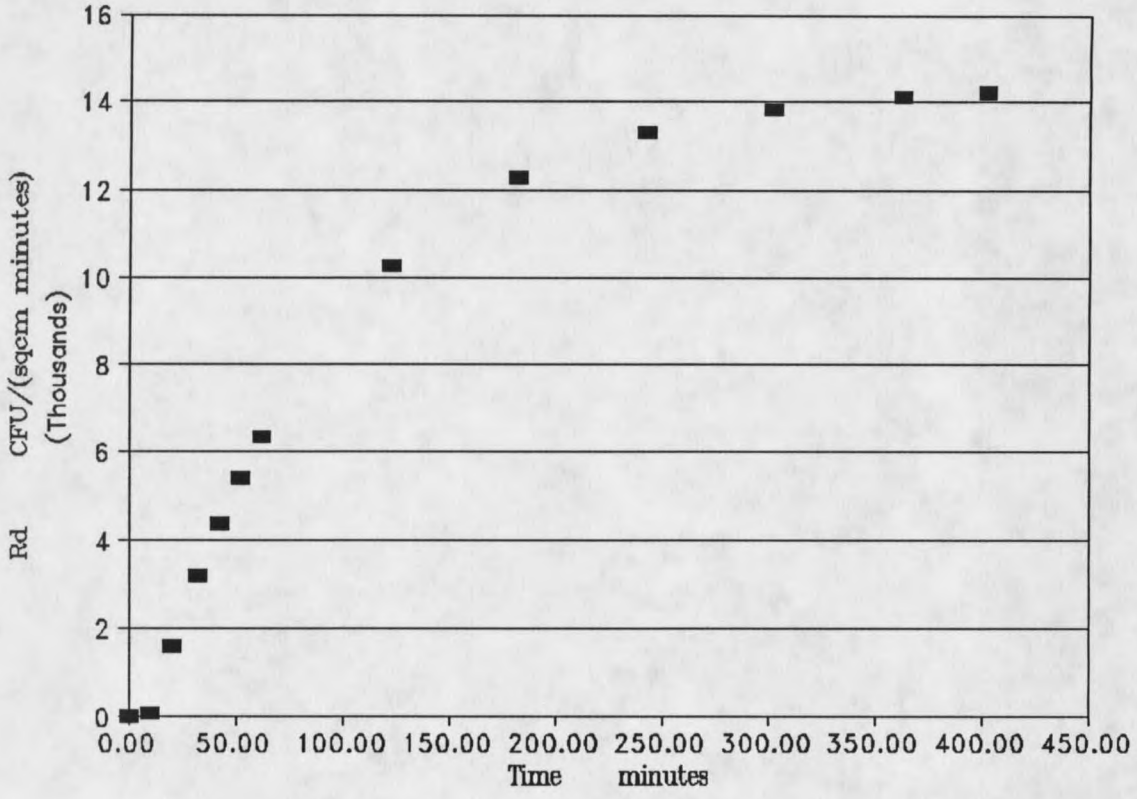

Figure 12. P 2 R 1: Rate of C^{14} Cellular Detachment vs. Time. Regular RotoTorque, RPM = 289, fluid shear = 20 dyne/cm^2, temperature = 22°C, substrate glucose concentration chemostat influent = 30 mg/l.

Summary of Results

Based on the experimental procedures and the theoretical background described in this work, it is possible to measure the rate of total cellular detachment per unit area, and the gross and net rates of total cellular attachment per unit area to an established biofilm.

Table 8. Summary of Results. X_b = the cell concentration of the bulk liquid in the RotoTorque (CFU/ml), T = temperature in °C, FS = fluid shear (dyne/cm^2), the units of R_{Ag}^{total}, R_{An}^{total}, and R_d^{total} are CFU/(cm^2 minute) (computed by the first method).

	X_b (10^6) CFU/ml	T °C	FS dyne/cm^2	R_{Ag}^{total} (10^{-4})	R_{An}^{total} (10^{-4})	R_d^{total} (10^{-4})
				CFU/(cm^2 minute)		
P 1 R 1	4.5	22	20	0.16	-	-
P 2 R 1	45	22	20	1.6	0.18	1.4
P 2 R 2	51	22	0.2	-	-	-
P 2 R 3	12	22	20	0.18	0.018	0.16
P 2 R 4	58	28	20	11	0.89	10.1
P 2 R 5	55	28	2	5.1	2.6	2.5
P 2 R 6	52.5	22	20	-	0.12	-
P 2 R 7	43.3	22	20	2.1	0.14	1.5

Effect of Suspended Cell Concentration on Attachment Rate

Both gross and net rates of total cellular attachment per unit area, R_{Ag}^{total} and R_{An}^{total}, are functions of the cell concentration in the bulk liquid of the RotoTorque as shown by the results of P 1 R 1, P 2 R 1 and P 2 R 3 (see Figure 13 and Table 9).

P 1 R 1, P 2 R 1, and P 2 R 3 have the same experimental conditions except for the cell concentration in the bulk liquid of the RotoTorques, X_b. The P 1 R 1 run was performed using the small RotoTorques.

Table 9. Net Rate of Total Cellular Attachment per Unit Area as a function of bulk suspended cell concentration, X_b.

EXPERIMENT	X_b CFU/ml	R_{An} CFU/(cm^2 minute)
P 2 R 3	12. 10^6	180
P 2 R 1	45. 10^6	1800

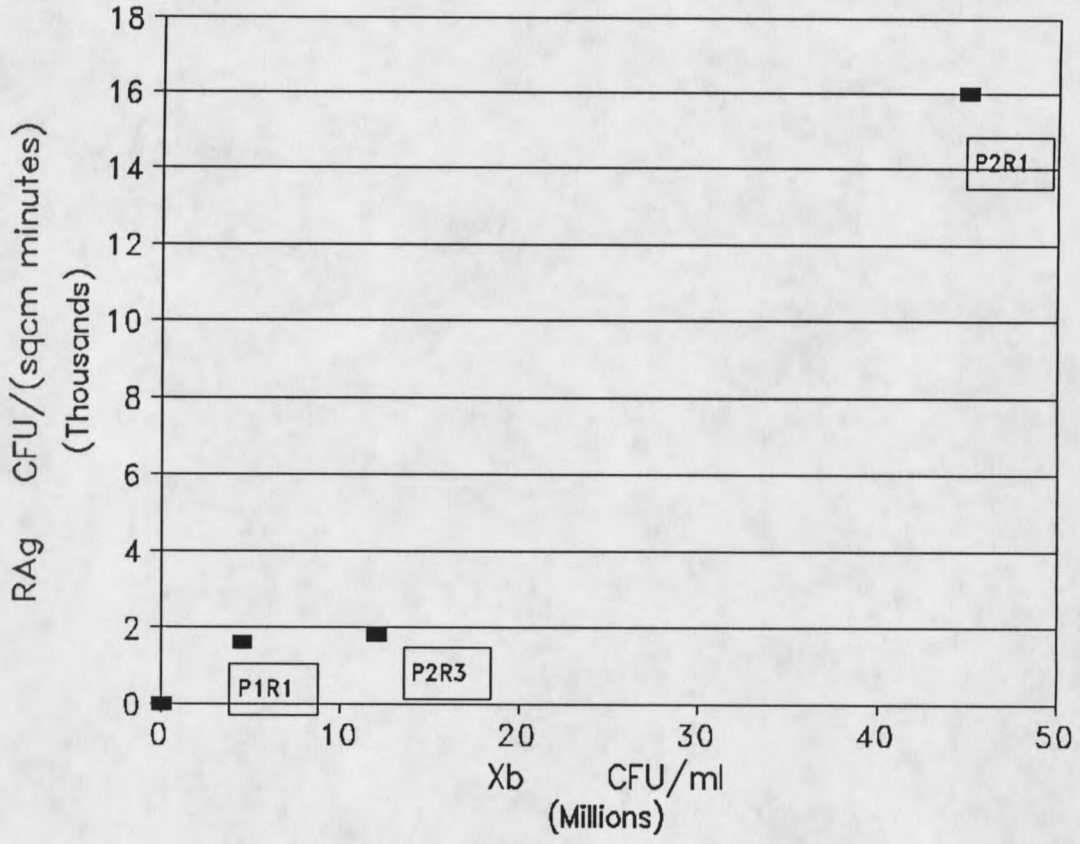

Figure 13. R_{Ag} vs. X_b. R_{Ag} = the gross rate of total cellular attachment to an established biofilm, X_b = cell concentration in the bulk liquid of the RotoTorques.

At this point, however, no correlation can be made between the rate (both gross and net) of total cellular attachment pee unit area and the cell concentration in the bulk liquid RotoTorque, X_b. More experimental data are needed.

Effect of Temperature

Both gross and net rates of total cellular attachment per unit area seem also to increase with temperature as shown by the result of P 2 R 1, and P 2 R 4 (see Table 10).

Table 10. Net and Gross Rates of Cellular Attachment per unit area as a Function of Temperature, T.

EXPERIMENT	T °C	R_{An} CFU/(cm^2 minute)	R_{Ag_2} CFU/(cm^2 minute)
P 2 R 1	22	1,800	16,000
P 2 R 4	28	8,900	110,000

The rate of total cellular detachment per unit area also appears to increase with temperature. Table 8 was obtained using data from P 2 R 1, and P 2 R 4. The P 2 R 4 run was performed at a temperature of 28°C. The net accumulation of C^{14} cells is higher in P 2 R 4 than the net accumulation of C^{14} cells in P 2 R 1 (see Figures B.18 and B.21). It seems likely that the higher accumulation of C^{14} cells in P 2 R 4 causes a higher rate of detachment.

Table 11. Rate of Cellular Detachment per Unit Area (first method) as a function of Temperature, T.

EXPERIMENT	T °C	R_d CFU/(cm^2 minute)
P 2 R 1	22	14,000
P 2 R 4	28	101,000

Effect of Fluid Shear on The Rate of Cellular Detachment

In agreement with Characklis [11], increasing the fluid shear increases the rate of total cellular detachment per unit area (see Table 12). Table 12 is obtained from P 2 R 4, and P 2 R 5.

Table 12. Rate of Cellular Detachment per Unit Area (first method) as a Function of Fluid Shear, FS.

EXPERIMENT	FS dyne/cm^2	R_d CFU/(cm^2 minute)
P 2 R 5	20	101,000
P 2 R 4	2	25,000

Detachment

Independent Measurement of Detachment

The rate of total cellular detachment per unit area can be calculated using equation (43) and the graph of the concentration of viable cells in the bulk liquid RotoTorque vs. time during flushing with mineral solution. Refer to Figures 14 and 15 for X_b vs. time graphs.

$$R_{dexp}^{total} = \frac{X_b^{st} F_i}{A_{rot}} \qquad (43)$$

where,

R_{dexp}^{total} = the rate of total cellular detachment per unit area, CFU/(min $cm^{2)}$.

X_b^{st} = steady-state value of the viable cells in effluent during flushing, (CFU/ml).

F_i = flow rate of mineral solution into the RotoTorque, (ml/min).

A_{rot} = Surface area for detachment, (cm^2).

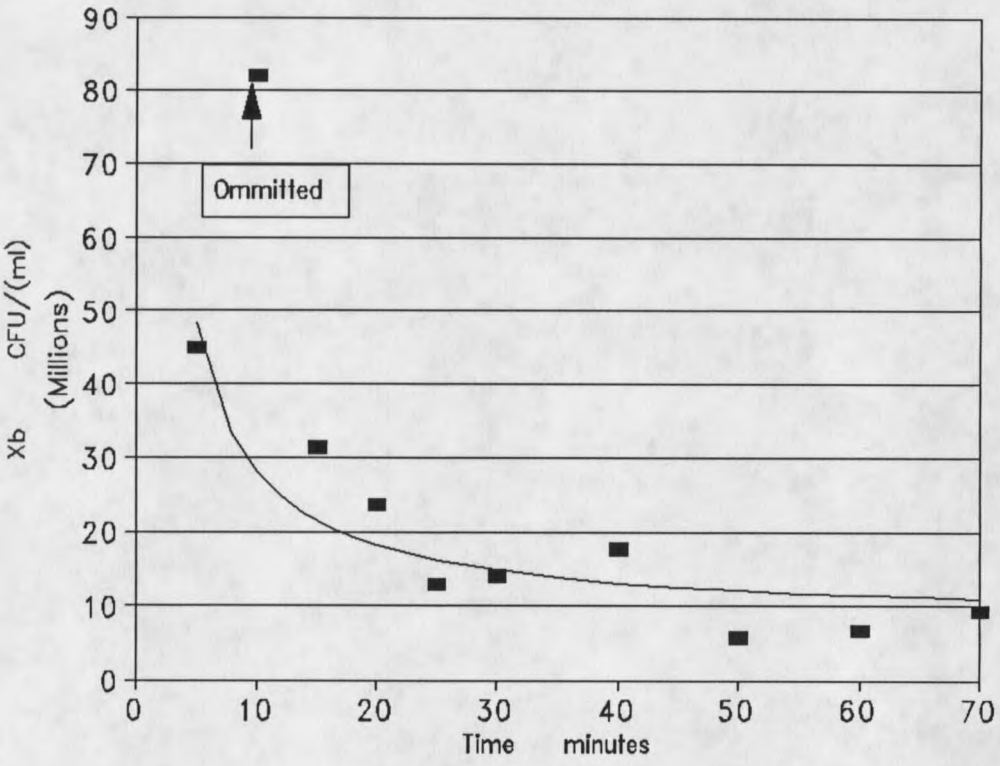

Figure 14. Detachment: P 2 R 4. Plot of the cell concentration in the bulk liquid of RotoTorque, X_b (CFU/ml) vs. time (minutes), inlet and outlet volumetric rate of fresh substrate to the RotoTorque = 94 ml/min, no cells flow in, the line is a curve fit (X_b = 8080938 + 2.0 10^8 t^{-1}, r^2 = 0.82, t = time).

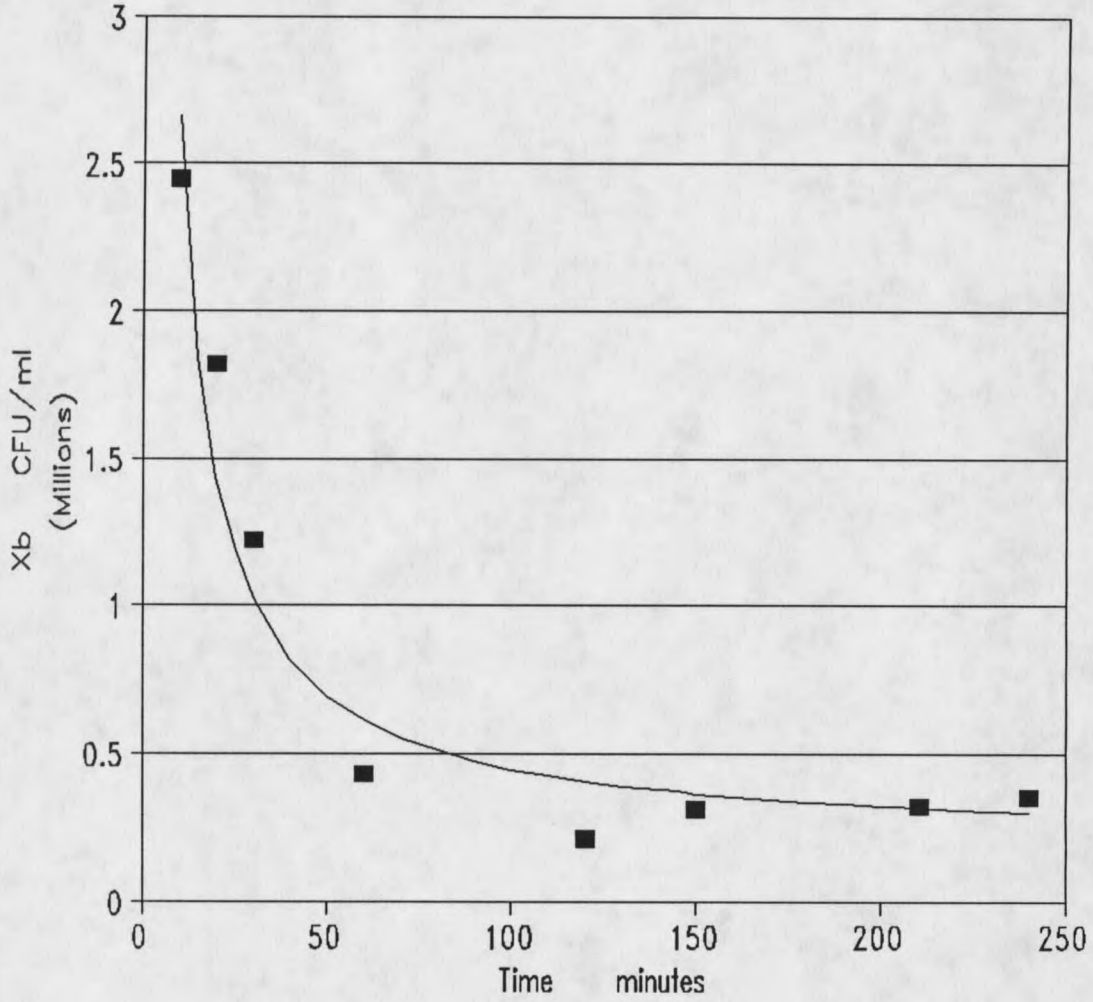

Figure 15. Detachment: P 2 R 6. Plot of the cell concentration in the bulk liquid of RotoTorque, X_b (CFU/ml) vs. time (minutes), inlet/outlet volumetric rate of fresh substrate to the RotoTorque = 67 ml/min, no cells flow in, the line is a curve fit (X_b = 198891 + 24645686 t^{-1}, r^2 = 0.94, t = time).

Comparing The Rates of Total Cellular Detachment Computed by First and Second Method

By fitting the rate of C^{14} cellular detachment per unit area data with equation (44), the maximum value of the curve of equation (44), R_{dmax}^{14}, (see Figures 16 - 21) should be the same as the rate of total cellular detachment per unit area.

$$R_d^{14} = \frac{R_{dmax}^{14}\, t}{k_d + t} \qquad (44)$$

Table 13. Rate of Total Cellular Detachment I. R_d^{total} is the rate of total cellular detachment per unit area using the first method (CFU/cm^2 minute), R_{dmax}^{14} is the maximum rate of C^{14} cellular detachment per unit area (CFU/cm^2 minute), R_{dexp}^{total} is the rate of total cellular detachment per unit area measured independently.

	R_d^{total} (10^{-4})	R_{dmax}^{14} (10^{-4})	R_{dexp}^{total} (10^{-4})
Units		CFU/(cm^2 minute)	
P 2 R 1	1.4	1.6	-
P 2 R 3	0.16	0.23	-
P 2 R 4	10.1	11.6	45
P 2 R 5	2.5	5.6	-
P 2 R 6	-	1.9	1.7
P 2 R 7	1.95	2.1	-

The results of these calculations are compared in Table 13 with the rate of total cellular detachment per unit area, R_d^{total}, calculated by substracting the net rate of total cellular detachment per unit area to an established biofilm, R_{An}^{total}, from the gross rate of total cellular attachment per

unit area to an established biofilm, R_{Ag}^{total}. R_d^{total} has been called the first method used to calculate the rate of total cellular detachment per unit area.

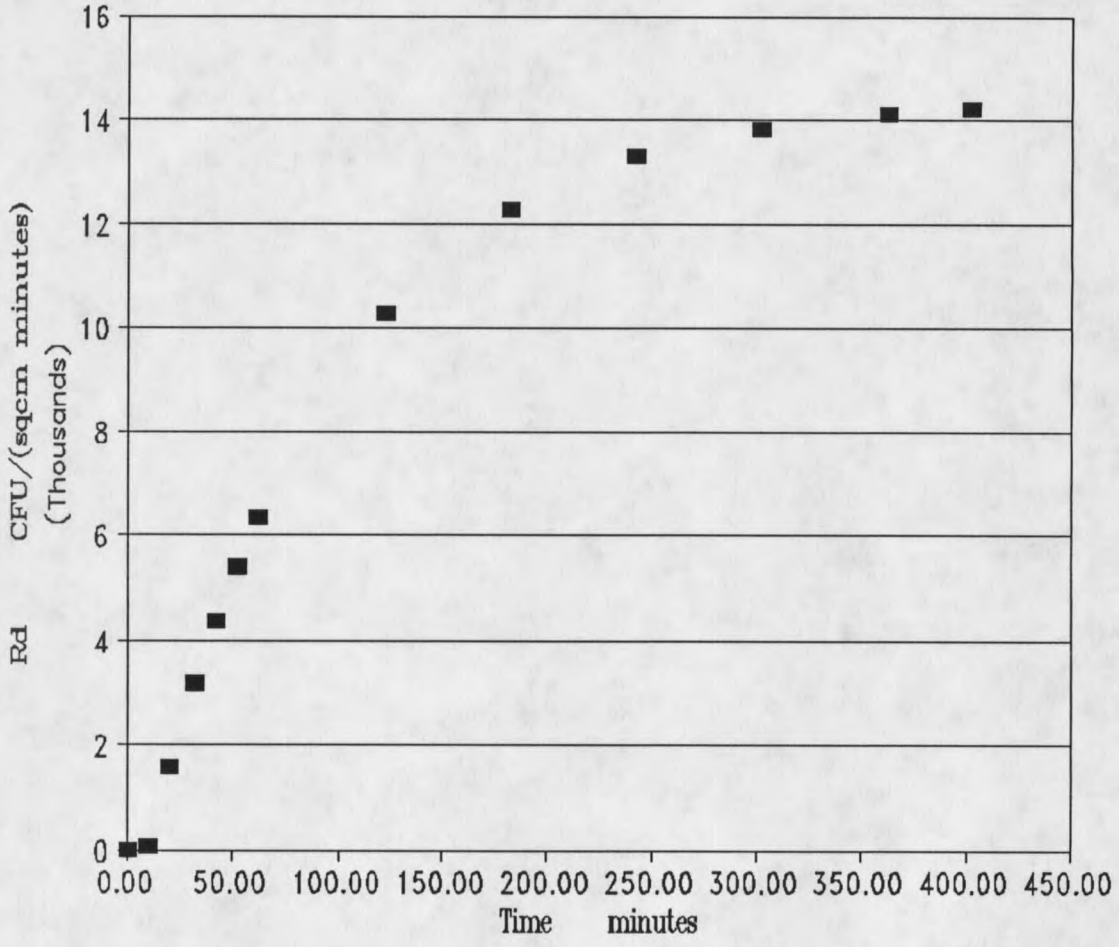

Figure 16. P 2 R 1: Rate of C^{14} Cellular Detachment per Unit Area vs. Time. Regular RotoTorque, RPM = 289, fluid shear = 20 dyne/cm^2, temperature = 22°C, substrate glucose concentration chemostat influent = 30 mg/l.

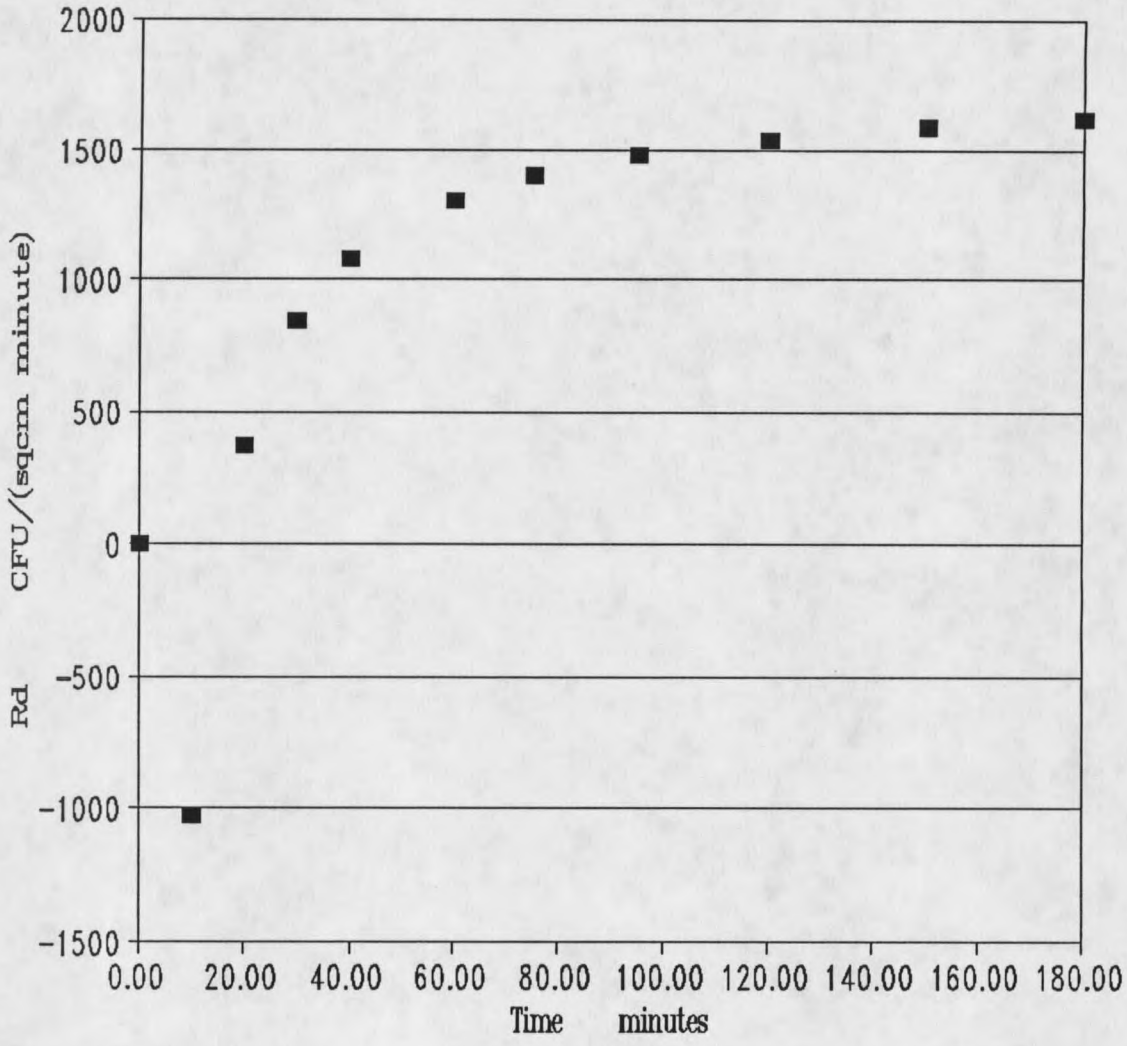

Figure 17. P 2 R 3: Rate of C^{14} Cellular Detachment per Unit Area vs. Time. Regular RotoTorque, RPM = 289, fluid shear = 20 dyne/cm^2, temperature = 22°C, substrate glucose concentration chemostat influent = 3 mg/l.

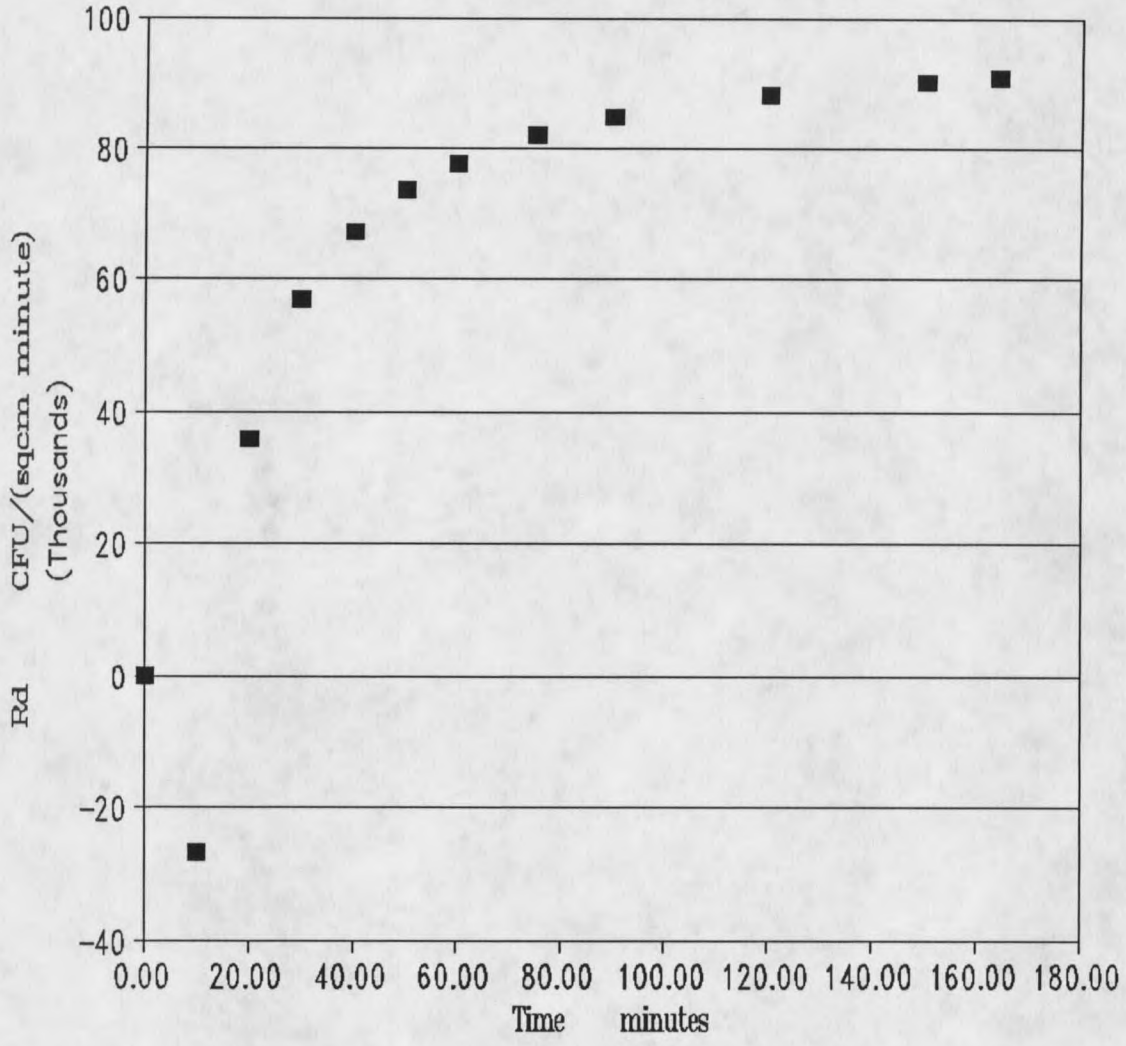

Figure 18. P 2 R 4: Rate of C^{14} Cellular Detachment per Unit Area vs. Time. Regular RotoTorque, RPM = 289, fluid shear = 20 dyne/cm^2, temperature = 28°C, substrate glucose concentration chemostat influent = 30 mg/l.

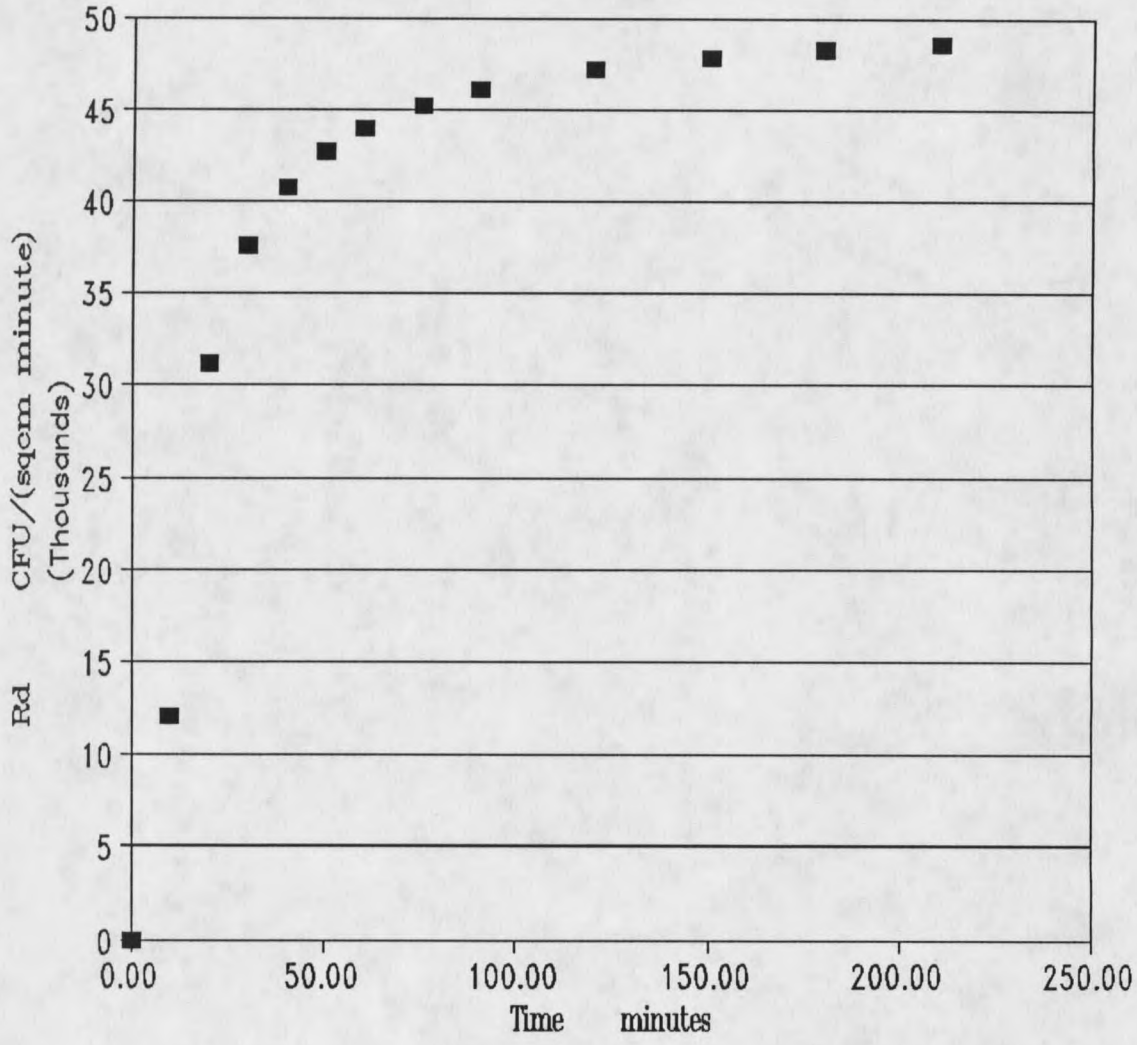

Figure 19. P 2 R 5: Rate of C^{14} Cellular Detachment per Unit Area vs. Time. Regular RotoTorque, RPM =70, fluid shear = 2 dyne/cm^2, temperature = 28°C, substrate glucose concentration chemostat influent = 30 mg/l.

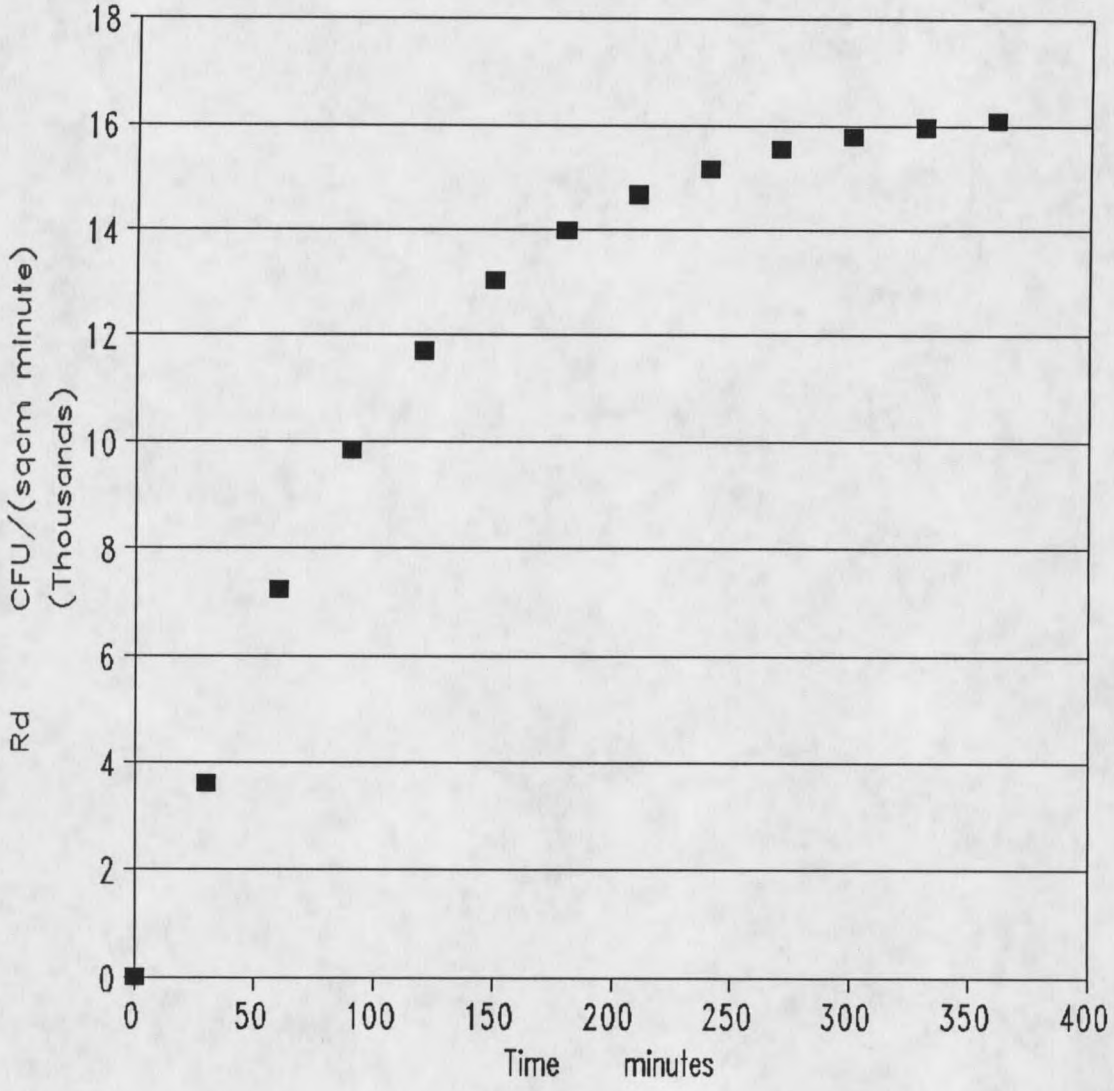

Figure 20. P 2 R 6: Rate of C^{14} Cellular Detachment per Unit Area vs. Time. Regular RotoTorque, RPM = 289, fluid shear = 20 dyne/cm^2, temperature = 22°C, substrate glucose concentration chemostat influent = 30 mg/l.

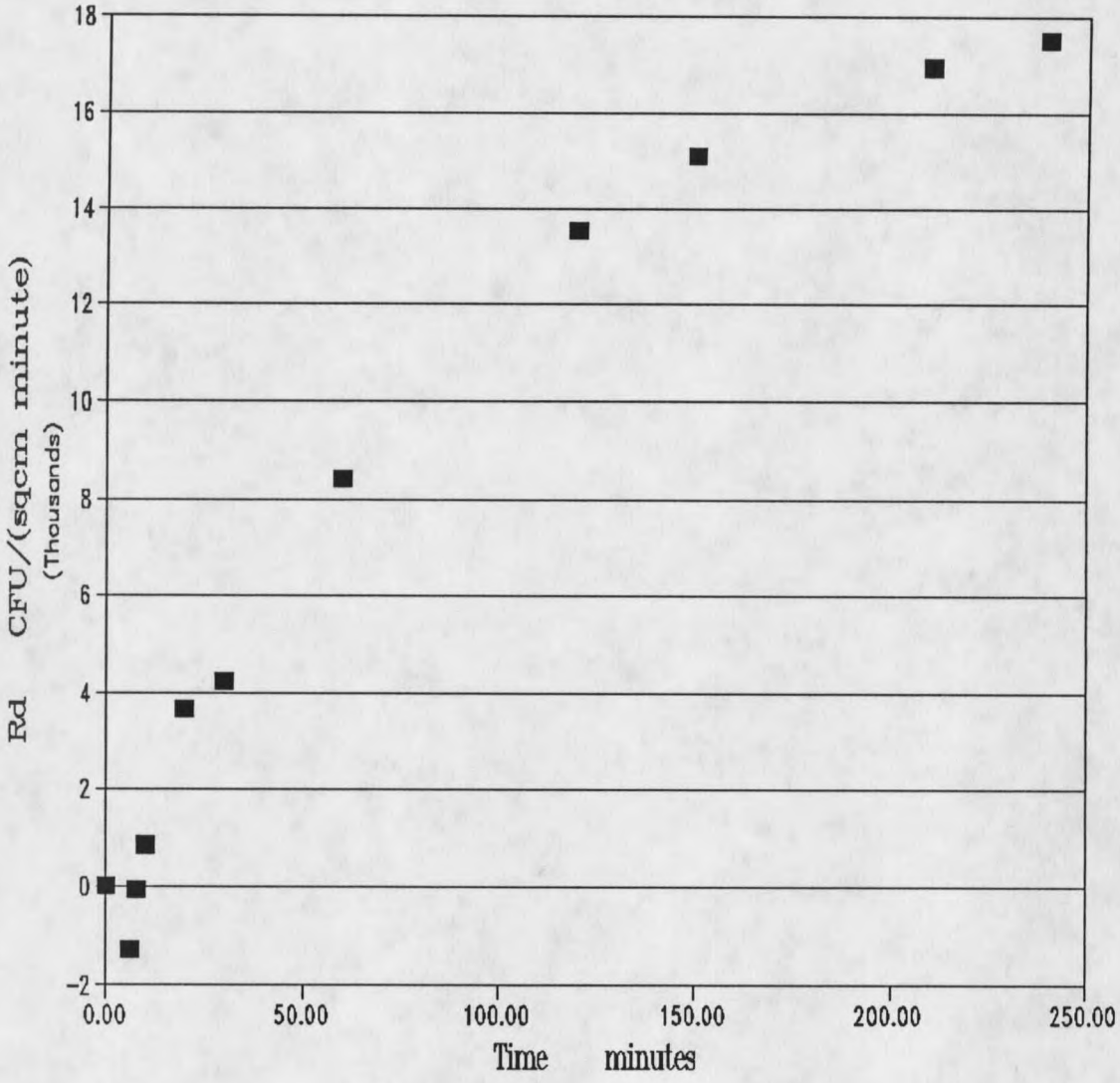

Figure 21. P 2 R 7: Rate of C^{14} Cellular Detachment per Unit Area vs. Time. Regular RotoTorque, RPM = 289, fluid shear = 20 dyne/cm^2, temperature = 22°C, substrate glucose concentration chemostat influent = 30 mg/l, one day C^{12} biofilm.

CONCLUSIONS

The following conclusions are valid within the range of experimental conditions tested, which include a low glucose environment in which P. aeruginosa grown on simple substrate was used for all experiments.

The experimental procedure and method used in this research can be utilized to determine the net or gross rate of celullar attachment per unit area to an established biofilm, while the difference between the gross and net rate attachment per unit area will give the rate of cellular detachment per unit area.

Results obtained by the experimental procedure developed in this work indicate that the rate of cellular attachment per unit area to an established biofilm appears to be a positive function of temperature. The rate of cellular attachment per unit area to an established biofilm also appears to be a positive function of bulk cell concentration. The effect of shear stress upon the rate of cellular attachment per unit area, however, is indeterminate. Reproducibility has been demonstrated at one set of conditions. The rate of cellular detachment per unit area measured by flushing the RotoTorque with mineral solution showed a comparable agreement with the rate of cellular detachment per unit area measured by difference of R_{Ag}^{total} and R_{An}^{total}.

RECOMMENDATIONS

To develop a kinetic expression for a cellular attachment to an established biofilm as a function of bulk cell concentration, more experiments at various bulk cell concentrations are needed.

Although during the attachment experiment (stage 3), good control of experimental temperature was obtained, minimal temperature control throughout all stages of the experiments was available with the current set up. A controlled experimental temperature throughout all stages is required so that more uncertainties in the experimental procedure will be minimized. A water bath with heating and cooling elements and thermostats could be used.

More experiments at various fluid shear are needed to develop a kinetic expression for the rate of cellular attachment as a function of fluid shear.

One of the general conditions of the experiments was an oligothropic (low nutrient) environment. Bacteria would be expected to behave differently in copiotrophic (rich nutrient) environment. By changing the concentration of the glucose in the environment where the bacteria are living, a different behaviour of the rate of cellular attachment may be observed. More experiments in copiothric environment are needed to develop a kinetic expression for the rate of cellular attachment as a function of nutrient concentration.

REFERENCES CITED

REFERENCES CITED

1. Atkinson, Bernard, and Ferda Mavituna, Biochemical Engineering and Biotechnology Handbook, New York: Nature Press, 1983.

2. Baley, James E., and David F. Ollis, Biochemical Engineering Fundamentals, 2d ed., New York: McGraw-Hill,Inc., 1986.

3. Berkeley, R.C.W., et al., eds., Microbial Adhesion to Surfaces, Chicester: Ellis Horwood Limited, 1980.

4. Beyer, William H., C R C Standard Mathematical Tables, 28th ed., Florida: C R C Press, Inc., 1988.

5. Bird, R. Byron, Warren E. Stewart, and Edwin N. Lightfoot, Transport Phenomena, New York: John Wiley & Sons, 1960.

6. Bird, R. B., and C. F. Curtiss, "Tangential Newtonian Flow in Annuli - I," Chemical Engineering Science, 11 (March 1959): 108 -113.

7. Bitton, Gabriel, and Kevin C. Marshall, Adsorption of Microorganisms to Surfaces, New York: Wiley, 1980.

8. Brock, Thomas D., and Michael T. Madigan, Biology of Microorganisms, 5th ed., New Jersey: Prentice Hall, 1988.

9. Bryers, J. D., and W. G. Characklis, "Kinetics of Initial Biofilm Formation Within a Turbulent Flow System," Fouling of Heat Transfer Equipment, Washington, D.C.: Hemisphere Publishing Corp., 1981: 349 - 368.

10. Characklis, W. G., R. Bakke, and M. H. Turakhia, Theoretical and Experimental Analysis of a Pseudomonas Aeruginosa Biofilm, International Conference for Water and Wastewater Microbiology, NewPort, CA., February 1988.

11. Characklis, William G., Kevin C. Marshall, ed., Biofilms, New York: John Wiley & Sons, 1990.

12. Characklis, William G., "Attached Microbial Growth - I, Attachment and Growth," Water Research, 7 (January 1973): 1113 - 1127.

13. Christensen, D. R., and P. L. McCarty, "Multi-process Biological Treatment Model," Journal of the Water Pollution Control Federation, 47 (1975): 2652-2664.

14. Coggle, J. E., Biological Effects of Radiation, 2d ed., New York: International Publications Service, Taylor & Francis, Inc., 1983.

15. Fahien, Ray W., Fundamentals of Transport Phenomena, NewYork: McGraw-Hill, 1983.

16. Grady, C. P. Leslie, Jr., and Henry C. Lim, Biological Waste Water Treatment, New York: Marcel Dekker, 1980.

17. Goodman, B.L., and A.J. Englande, Jr., "A Unified Model of the Activated Sludge Process," Journal of the Water Pollution Control Federation, 46 (1974): 312-332.

18. Hugo, William Barry, and Society of Chemical Industry, Inhibition and Destruction of the Microbial Cell, ed. R.C.W. Berkeley, New York: E. Horwood for the Society of Chemical Industry, London, 1980.

19. Kappesser, R., I. Cornet, and R. Greif, "Mass Transfer to a Rough Rotating Cylinder," J. Electrochem. Soc., 118 (December 1971): 1957 - 1959.

20. Kaye, Joseph, and E. C. Elgar, "Modes of Adiabatic and Diabatic Fluid Flow in an Annulus with an Inner Rotating Cylinder," Transactions of the ASME (April 1958): 753 - 765.

21. Kim, Yeoung-Chul, "Diffusion Coefficients for Klebsiella Pneumoniae and Pseudomonas Aeruginosa," Master's thesis, Montana State University, 1989.

22. LeRoy, Raymond, and Judith Ahrens Powell, Understanding Radioactive Waste, ed. Judith A. Powell, Columbus: Batelle Press, 1989.

23. McCabe, W. L., J. C. Smith, and P. Harriot, Unit Operations of Chemical Engineering, 4th ed., New York: McGraw-Hill, Inc.,1985.

24. McKinney, R. E., "Mathematics of Complete Mixing Activated Sludge," Journal of the Sanitary Engineering Division, ASCE, 88 (1962): 87-113. Quoted in C. P. Leslie Grady, Jr., and Henry C. Lim, Biological Waste Water Treatment, New York: Marcel Dekker, 1980.

25. Matson, J. V., and W. G. Characklis, "Diffusion into Microbial Aggregates," Water Research, 10 (1976): 877 - 885.

26 Mueller, R.F., "Characterization of Initial Events of Bacterial Colonization at Solid-Water Interfaces Using Image Analysis," Master's thesis, Montana State University, 1990.

27. Samson, Philip, Glossary of Bacteriological Terms, London: Butterworth, 1975.

28. Savage, C. Dwayne, and Madilyn Fletcher, Bacterial Adhesion, New York: Academic Press, 1971.

29. Schlichting, Hermann, Boundary Layer Theory, 7th ed., trans. J. Kestin, New York: McGraw-Hill, 1979.

30. Schugerl, Karl, Bioreaction Engineering, trans. Valerie Cottrell, Chichester (West Sussex); New York: Wiley, 1987.

31. Siebel, Maarten Alexander, "Binary Population Biofilms," Ph.D. diss., Montana State University, 1987.

32. Starr, Mortimer P. et al., eds., The Prokaryotes, vol. 1, Introduction to the Family Pseudomonadaceae, by Norberto J. Palleroni. Heidelberg: Springer-Verlag, 1981.

33. Turakhia, M., and W. G. Characklis, "Influence of a Calcium-Specific Chelant on Biofilm Removal," Applied and Environmental Microbiology, 46 (1983): 1236-1238.

34. Wang, A. K., and L. W. Gelhar, "Turbulent Couette Flow," J. of Fluids Engineering, (December 1974).

35. Wanner, O., Personal Communication, 1990.

36. Warwood, Brian, Personal Communication, 1991.

37. Winslow, C. E. A. et al., "The Families and genera of The Bacteria," Preliminary report of the Society of American Bacteriologist on Characterization and Classification of Bacterial Types ," Journal of Bacteriology, 2 (1917): 505-566. Quoted in Mortimer P. Starr et al., eds., The Prokaryotes, vol. 1, 655. Heidelberg: Springer-Verlag, 1981.

APPENDICES

APPENDIX A

RAW DATA

APPENDIX A

PHASE 1 EXPERIMENT

RotoTorque (small)

Surface area for attachment = 258.4 cm^2

Rotor peripheral area = 109.96 cm^2

Inside wall surface area of one RotoTorque = 148.44 cm^2

Liquid volume = 180 ml

RPM = 600

Number of RotoTorques = 6

Units of measurement

Liquid Scintillation (L.S.) = counts per minute (CPM)

plate count = colony forming units (CFU)/ml

Time of measurement of each L.S. sample = 1 minute

Fresh substrate = 1.5 μCi/l as glucose

Bulk liquid of chemostat = 2190 CPM

Table 14. Phase 1, Run 1: Radioactivity Levels. Experimental data on radioactivity levels in the bulk liquid in the RotoTorque (CPM/ml), biofilm on the rotor surface (CPM), and the outer cylinder (CPM).

TIME (min)	BULK LIQUID CPM/ml	ROTOR CPM	WALL CPM
10	404.0	269.0	99.0
20	603.0	555.0	257.0
30	999.0	711.0	237.0
40	494.0	974.0	214.0
50	1023.0	397.0	451.0
60	1437.0	906.0	152.0

Table 15. Phase 1, Run 1: Viable Counts. Experimental data on number of cells (CFU/ml) of the bulk liquid in the chemostat.

TIME (min)	CHEMOSTAT CFU x 10^{-5}/ml
10	42
20	40
30	48
40	44
50	48
60	33

PHASE 2 EXPERIMENT

RotoTorque (standard)

Surface area for attachment = 1289.31 cm^2

Rotor peripheral area = 596.90 cm^2

Number of slides = 12

Area of one slide = 34.2 cm^2.

Time of measurement of each sample = 1 minute

Inside wall surface area = 692.41 sqcm

Liquid volume = 640 ml

Number of RotoTorque(s) = 1

Temperature = 22°C

Unit of measurement

Liquid scintillation = count per minute (CPM)

plate count = colony forming units (CFU)/ml

Run 1

RPM = 289

Fresh substrate = 1.5 μCi/l

Bulk liquid of chemostat = 1591.33 CPM/ml

Temperature = 22°C

Table 16. Phase 2, Run 1: Radioactivity Levels. Experimental data on radioactivity levels in the bulk liquid in the RotoTorque (CPM/ml), and biofilm on the slide surface (CPM).

TIME	BULK LIQUID			SLIDE		
(min)	(CPM/ml)			(CPM)		
10	105	96	97	54	59	53
20	-	-	-	53	85	56
27	226	233	249	-	-	-
32	293	286	298	119	129	103
42	334	338	392	125	115	146
52	426	431	431	152	164	156
62	482	502	463	123	116	133
122	743	819	798	618	618	616
182	890	950	913	328	343	340
242	953	928	906	467	444	459
302	986	1003	1083	663	715	647
362	979	1032	1011	556	560	580
402	1235	1214	1204	906	945	887

Table 17. Phase 2, Run 1: Viable Counts. Experimental data on number of cells (CFU/ml) in the bulk liquid in the RotoTorque.

TIME (min)	BULK LIQUID ROTOTORQUE (CFU x 10^{-6}/ml)	
10	49	52
20	40	39
32	42	42
42	31	37
52	54	50
62	48	49
122	45	45
182	46	42
242	51	50
302	42	44

RUN 2

RPM = 20

Fresh substrate = 2.5 μCi/l as glucose

Bulk liquid of chemostat = 2942 CPM/ml

Temperature = 22°C

Table 18. Phase 2, Run 2: Radioactivity Levels. Experimental data on radioactivity levels in the bulk liquid in the RotoTorque (CPM/ml), and biofilm on the slide surface (CPM).

TIME (min)	BULK LIQUID (CPM/ml)			SLIDE (CPM)		
10	638	549	574	89	85	89
20	715	718	676	132	161	129
30	1001	921	1004	168	182	155
40	1129	1132	1111	432	450	390
50	1164	1140	1156	113	134	128
60	1201	1263	1228	378	363	337
75	1513	1519	1498	204	212	242
90	1545	1568	1546	1049	1021	954
120	1903	1929	1884	253	236	211
225	2369	2417	2380	1123	1058	1075
315	2688	2569	2572	996	987	986
405	2762	2715	2760	778	739	748

Table 19. Phase 2, Run 2: Viable Counts. Experimental data on number of cells (CFU/ml) in the bulk liquid in the RotoTorque and in the chemostat.

TIME (min)	BULK LIQUID ROTOTORQUE (CFU x 10^{-6}/ml)	
10	62	64
20	51	59
30	40	38
40	45	45
50	440	420
60	390	410
75	400	420
	BULK LIQUID CHEMOSTAT (CFU x 10^{-6}/ml)	
	34	50

RUN 3

RPM = 289

Fresh substrate = 2.5 μCi/l as glucose

Bulk liquid of chemostat = 2278.00 CPM/ml

Temperature = 22°C

Table 20. Phase 2, Run 3: Radioactivity Levels. Experimental data on radioactivity levels in the bulk liquid in the RotoTorque (CPM/ml), and biofilm on the slide surface (CPM).

TIME (min)	BULK LIQUID (CPM/ml)			SLIDE (CPM)		
10	259	293	296	78	78	66
20	426	471	515	108	104	107
30	649	612	607	150	150	143
40	715	714	688	175	207	202
50	874	831	884	233	226	231
60	917	929	953	231	222	216
75	1100	984	1051	287	304	365
95	1192	1227	1254	431	460	418
120	1406	1379	1306	500	491	496
150	1417	1423	1443	-	-	-
180	1526	1443	1477	611	614	694

Table 21. Phase 2, Run 3: Viable Counts. Experimental data on number of cells (CFU/ml) in the bulk liquid in the RotoTorque and in the chemostat (CFU/ml).

TIME (min)	BULK LIQUID ROTOTORQUE (CFU x 10^{-6}/ml)	
10	8.3	9
20	5	5.6
30	39	41
40	96	98
50	3.7	4.2
60	3.7	4.0
75	3.4	3.6
95	104	91
120	3	3.6
150	11.2	14
180	11.6	11
	BULK LIQUID CHEMOSTAT (cfu X 10^{-6}/ml)	
	5.1	5.0

RUN 4

RPM = 289

Fresh substrate = 2.5 μCi/l as glucose

Bulk liquid chemostat = 2897 CPM/ml

Temperature = 28°C

Table 22. Phase 2, Run 4: Radioactivity Levels. Experimental data on radioactivity levels in the bulk liquid in the RotoTorque (CPM/ml), and biofilm on the slide surface (CPM).

TIME	BULK LIQUID			SLIDE		
(min)	(CPM/ml)			(CPM)		
10	307	308	301	475	504	469
20	430	438	395	606	590	611
30	551	494	520	1147	1183	1151
40	599	637	619	1000	1029	1000
50	756	692	734	1265	1310	1182
60	774	793	740	1705	1663	1735
75	924	896	868	1743	2032	1910
90	957	964	936	1998	1877	1912
120	1064	1088	1033	3109	3067	3047
150	1461	1519	1425	3538	3633	3711
164	1377	1417	1331	-	-	-

Table 23. Phase 2, Run 4: Viable Counts. Experimental data on number of cells in the bulk liquid in the RotoTorque (CFU/ml) and in the bulk liquid chemostat (CFU/ml).

TIME (min)	BULK LIQUID ROTOTORQUE (CFU x 10^{-6})	
10	47	51
20	54	51
30	98	93
40	56	59
50	65	66
60	59	58
75	60	59
90	62	58
120	40	41
150	41	43

	BULK LIQUID CHEMOSTAT (CFU X 10^{-6}/ml)
31	33

RUN 5

RPM = 75

Fresh substrate = 2.5 μCi/l as glucose

Bulk liquid of chemostat = 2897 μCi/ml

Temperature = 28°C

Table 24. Phase 2, Run 5: Radioactivity levels. Experimental data on radioactivity levels in the bulk liquid in the RotoTorque (CPM/ml), and biofilm on the slide surface (CPM).

TIME (min)	BULK LIQUID (CPM/ml)			SLIDE (CPM)		
10	317	311	306	341	364	353
20	495	505	438	574	587	575
30	614	595	576	947	978	925
40	779	790	798	1223	1234	1173
50	1880	1942	1905	1601	1619	1538
60	-	-	-	1928	1911	1929
75	1180	1173	1189	2266	2254	2301
90	1289	1295	1317	2749	2718	2793
120	1455	1455	1405	4392	4522	4435
150	1553	1636	1639	4164	4160	4168
180	1871	1801	1789	5796	5599	5692
210	1873	1955	1913	7483	7464	7660

Table 25. Phase 2, Run 5: Viable Counts. Experimental data on number of cells (CFU/ml) in the bulk liquid in the RotoTorque and in the chemostat (CFU/ml).

TIME (min)	BULK LIQUID ROTOTORQUE (CFU x 10^{-6})	
10	38	41
20	-	-
30	49	47
40	104	102
50	91	87
60	40	40
75	-	-
90	60	62
120	53	53
150	49	48

BULK LIQUID CHEMOSTAT (CFU x 10^{-6}/ml)	
32	33

RUN 6

RPM = 289

Fresh substrate = 2.5 μCi/l as glucose

Bulk liquid of Chemostat = 1973 CPM/ml

Temperature = 22°C

Table 26. Phase 2, Run 6: Radioactivity Levels. Experimental data on radioactivity levels in the bulk liquid in the RotoTorque (CPM/ml), and biofilm on the slide surface (CPM).

TIME	BULK LIQUID			SLIDE		
(min)	(CPM/ml)			(CPM)		
30	552	552	559	262	226	230
60	827	864	851	265	298	318
90	975	977	1043	332	308	295
120	1113	1086	1152	288	314	323
150	1226	1220	1227	335	373	333
180	1335	1369	1344	476	474	435
210	1392	1374	1371	474	494	490
240	1433	1428	1364	489	502	502
270	1457	1418	1451	537	518	537
300	1505	1479	1505	556	558	571
330	1497	1517	1505	568	613	585
360	1517	1548	1553	595	573	592

Table 27. Phase 2 Run 6: Viable Counts. Experimental data on number of cells (CFU/ml) in the bulk liquid in the RotoTorque and in the chemostat (CFU/ml)

TIME (min)	BULK LIQUID ROTOTORQUE (CFU x 10^{-6}/ml)	
30	49	49
60	62	60
90	43	40
120	27	32
150	50	54
180	42	47
210	51	50
240	44	42
270	48	49
300	82	60
330	31	37

BULK LIQUID CHEMOSTAT (CFU x 10^{-6}/ml)	
81	90

RUN 7

RPM = 289

Fresh substrate = 2.5 μCi/l as glucose

Bulk liquid of chemostat = 2897 CPM/ml

Temperature = 22°C

Table 28. Phase 2, Run 7: Radioactivity Levels. Experimental data on radioactivity levels in the bulk liquid in the RotoTorque (CPM/ml), and biofilm on the slide surface (CPM).

TIME	BULK LIQUID			SLIDE		
(min)	(CPM/ml)			(CPM)		
2	58	56	57	31	33	31
4	114	118	119	32	30	34
6	169	169	162	87	87	90
8	221	223	233	90	96	94
10	275	277	270	97	106	96
20	522	528	528	96	153	101
30	744	756	748	216	210	216
60	1280	1284	1272	225	216	242
120	1930	1976	1945	465	465	570
150	2126	2125	2125	590	600	590
210	2433	2432	2428	740	738	738
240	2483	2484	2680	860	879	860

Table 29. Phase 2, Run 7: Viable Counts. Experimental data on number of cells (CFU/ml) in the bulk liquid in the RotoTorque and in the chemostat (CFU/ml).

TIME (min)	BULK LIQUID ROTOTORQUE (CFU x 10^{-6}/ml)	
10	39	38
20	38	41
30	49	47
60	40	40
120	32	34
150	60	62
210	54	49
240	38	32
	BULK LIQUID CHEMOSTAT (CFU x 10^{-6}/ml)	
	46	50

Detachment Result

Table 30. Phase 2 Run 4: Viable Cell Concentration in the Bulk Liquid in the RotoTorque vs. Time during flushing. Flow rate of mineral solution into the RotoTorque = 94 ml/min, no cells flow in.

TIME (min.)	X_b CFU x 10^{-5}/ml	X_b CFU x 10^{-6}/ml
5	> 400	45
10	> 400	82
15	313	29
20	237	20
25	130	16
30	141	13
40	176	14
50	57	4
60	67	3
70	94	6

Table 31. Phase 2 Run 6: Viable Cell Concentration in the Bulk Liquid in the RotoTorque vs. Time during flushing. Flow rate of mineral solution into the RotoTorque = 67 ml/min, no cells flow in.

Time (min.)	X_b (CFU x 10^{-4}/ml)	X_b (CFU x 10^{-5}/ml)
10	245	24
20	182	18
30	122	16
60	43	4
120	21	2
150	31	3
210	32	3
240	35	2

APPENDIX B

DATA ANALYSIS

APPENDIX B

Units of results presented in this section are CPM/ml (count per minute per milliliter) and CFU/ml (colony forming units per milliliter) for liquid samples. For samples taken from a surface, results are reported on a square centimeter basis.

If more than one measurement was made, the average value will be reported in this section. Individual values are reported in appendix A.

There is one run in the phase one experiment and seven runs in the phase two experiment.

Phase 1

At time zero the RotoTorque influent was switched to the chemostat effluent with C^{14} labelled cells. Intensity of radioactivity at time zero in the RotoTorque was set at zero, it was not obtained experimentallly.

The intensity of radioactivity on the surface of biofilm is obtained by dividing rotor CPM (Table 14) by 109.96 cm^2 which is the rotor peripheral area in square centimeters (not including the top and bottom part of the rotor) since the biofilm accumulated on the rotor peripheral area only were scrapped off.

RUN 1

RPM = 600

Fluid shear = 20 dyne/cm^2

Table 32. Phase 1, Run 1: Result 1. Radioactivity levels of the bulk liquid in the RotoTorque (CPM/ml), and biofilm on the rotor surface (CPM/cm^2) as a function of time.

TIME (min)	BULK LIQUID (CPM/ml)	ROTOR (CPM/cm^2)
0	0	0
10	404.00	2.45
20	603.00	5.05
30	999.00	6.47
40	494.00	8.87
50	1023.00	3.61
60	1437.00	8.24

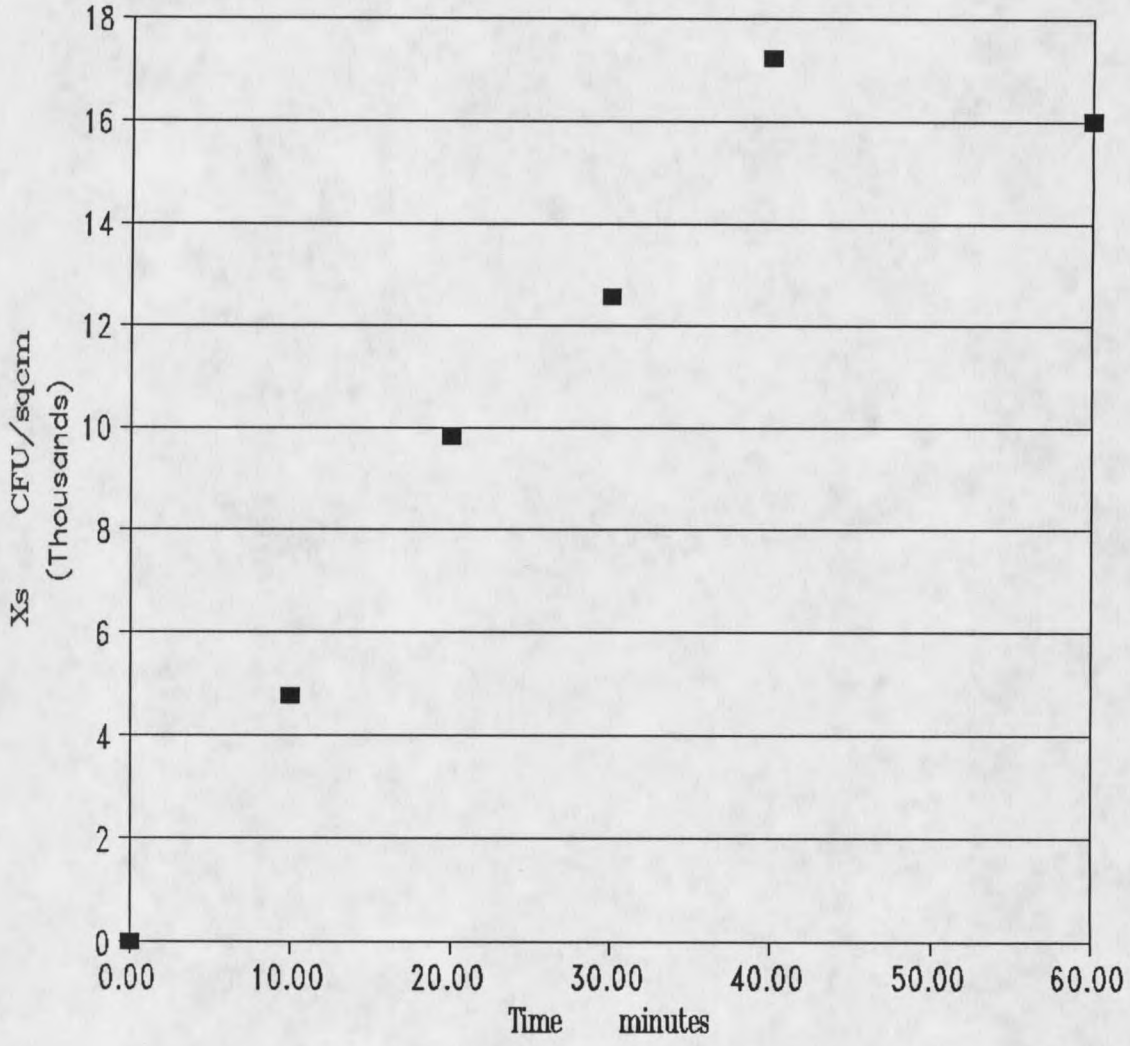

Figure 22. P 1 R 1: Accumulation of C^{14} Viable Cells on the Surface of the Established Biofilm. Small RotoTorque, RPM = 600, fluid shear = 20 dyne/cm^2, substrate glucose concentration chemostat influent = 30 mg/l. temperature = 22°C.

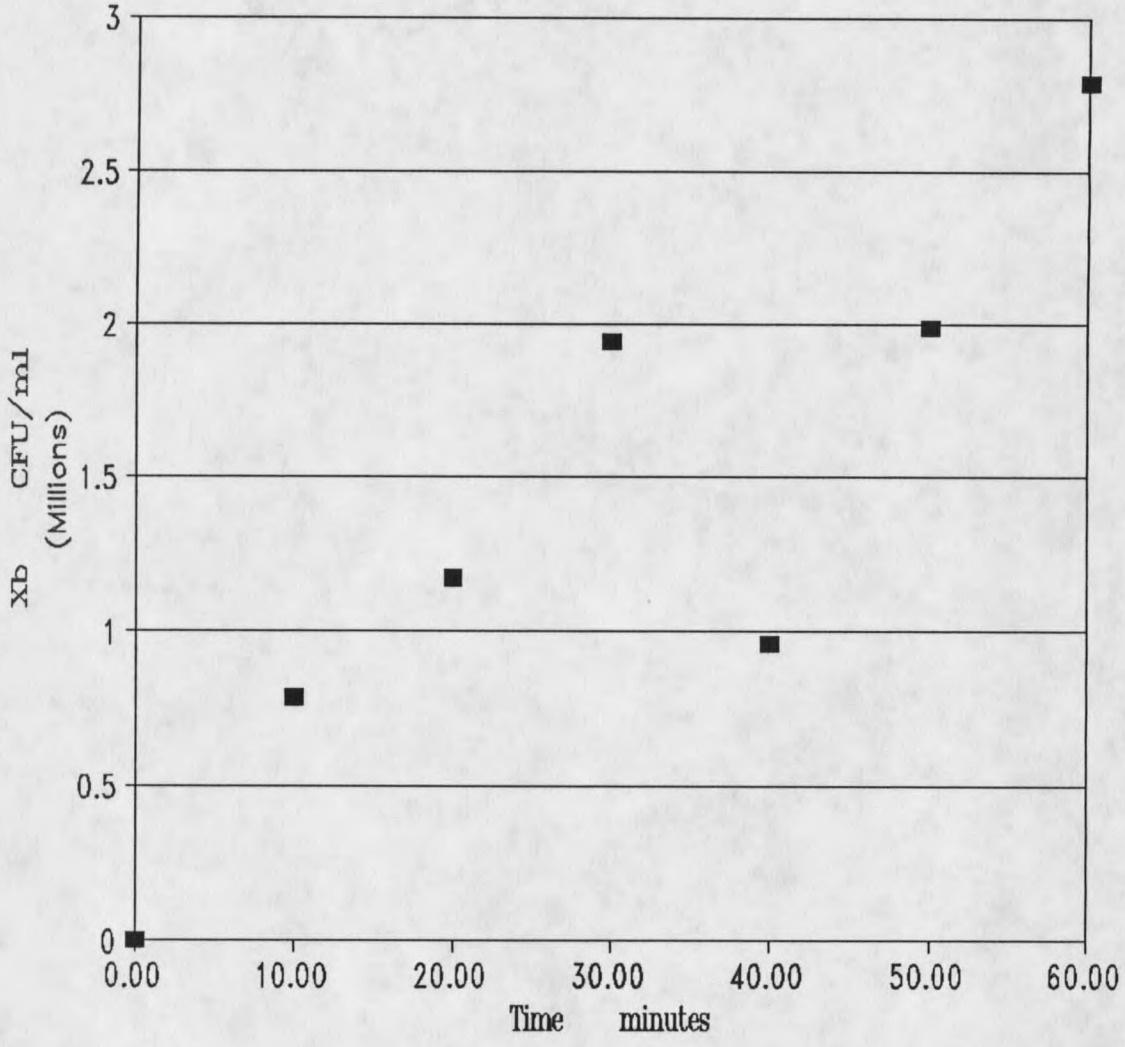

Figure 23. P 1 R 1: C^{14} Viable Cells in the Bulk Liquid in the RotoTorque vs. Time. At the time of data gathering, inlet flow rate = outlet flow rate = 2 ml/min, inlet concentration of viable C^{14} cells = 42.5 x 10^5 CFU/ml, liquid volume in the RotoTorque = 180 ml.

Phase 2

Slide results are obtained by dividing slide CPM by 34.2 cm^2, which is the area of one slide.

Run 1

RPM = 289

Fluid shear = 20 dyne/sqcm.

Table 33. Phase 2, Run 1: Result 2. Radioactivity levels in the bulk liquid in the RotoTorque (CPM/ml), biofilm on the slide surface (CPM/cm^2), and the viable count in the bulk liquid in the RotoTorque as a function of time.

TIME (min)	BULK LIQUID ROTOTORQUE (CPM/ml)	SLIDE (CPM/cm^2)	BULK LIQUID ROTOTORQUE (CFU x 10^{-6}/ml)
0	0	0	-
10	99.33	1.62	50.5
20	-	1.89	39.5
27	236	-	
32	292.33	3.42	42
42	354.67	3.76	34
52	429.33	4.6	52
62	482.33	3.63	48.5
122	786.67	18.05	45
182	917.67	9.85	44
242	929	13.35	50.5
302	1024	19.74	43
362	1007.33	16.53	-
402	1217.67	26.69	-

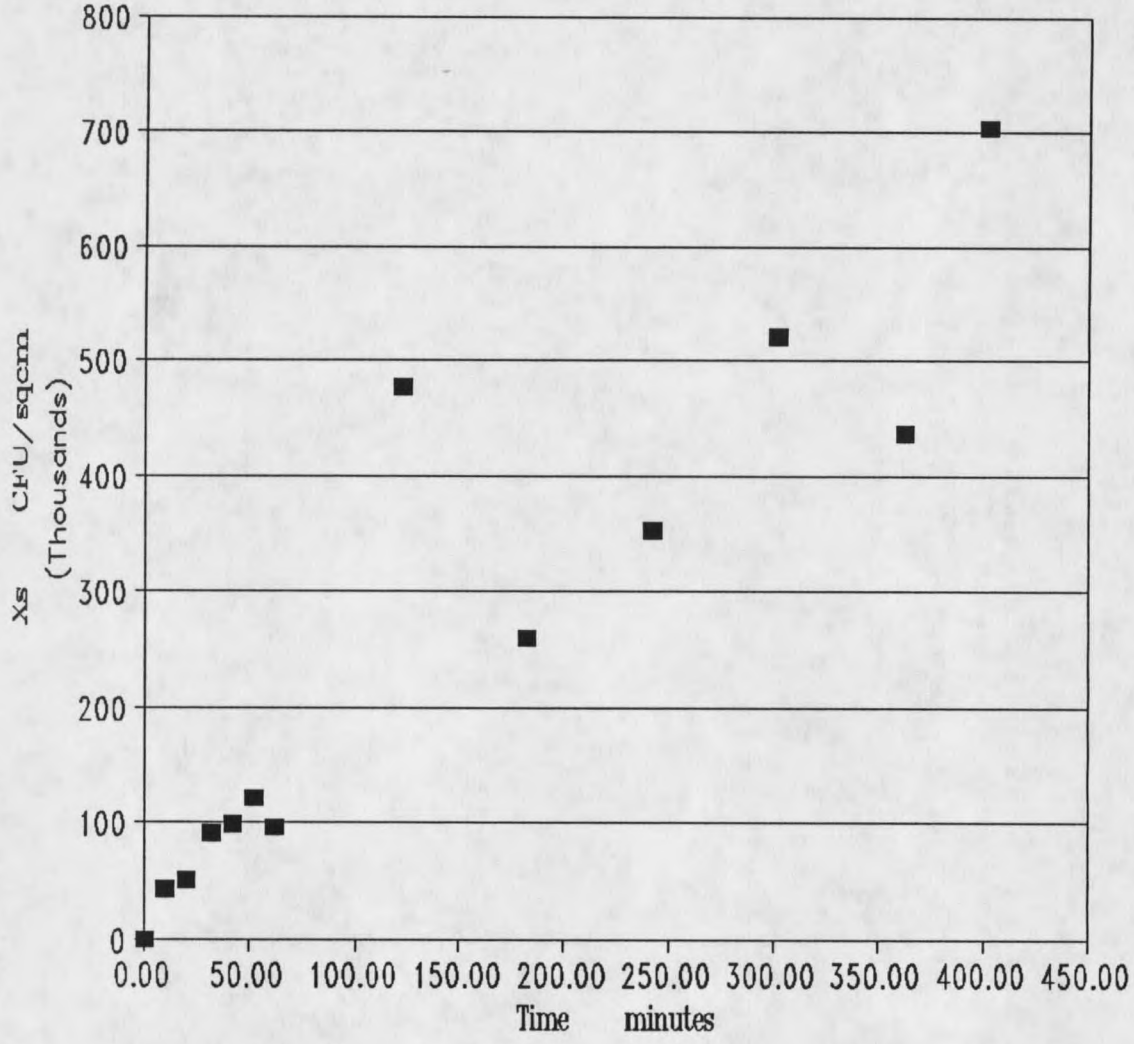

Figure 24. P 2 R 1: Accumulation of C^{14} Viable Cells on the Surface of the Established Biofilm. Regular RotoTorque, RPM = 289, fluid shear = 20 dyne/cm^2, substrate glucose concentration chemostat influent = 30 mg/l. temperature = 22°C.

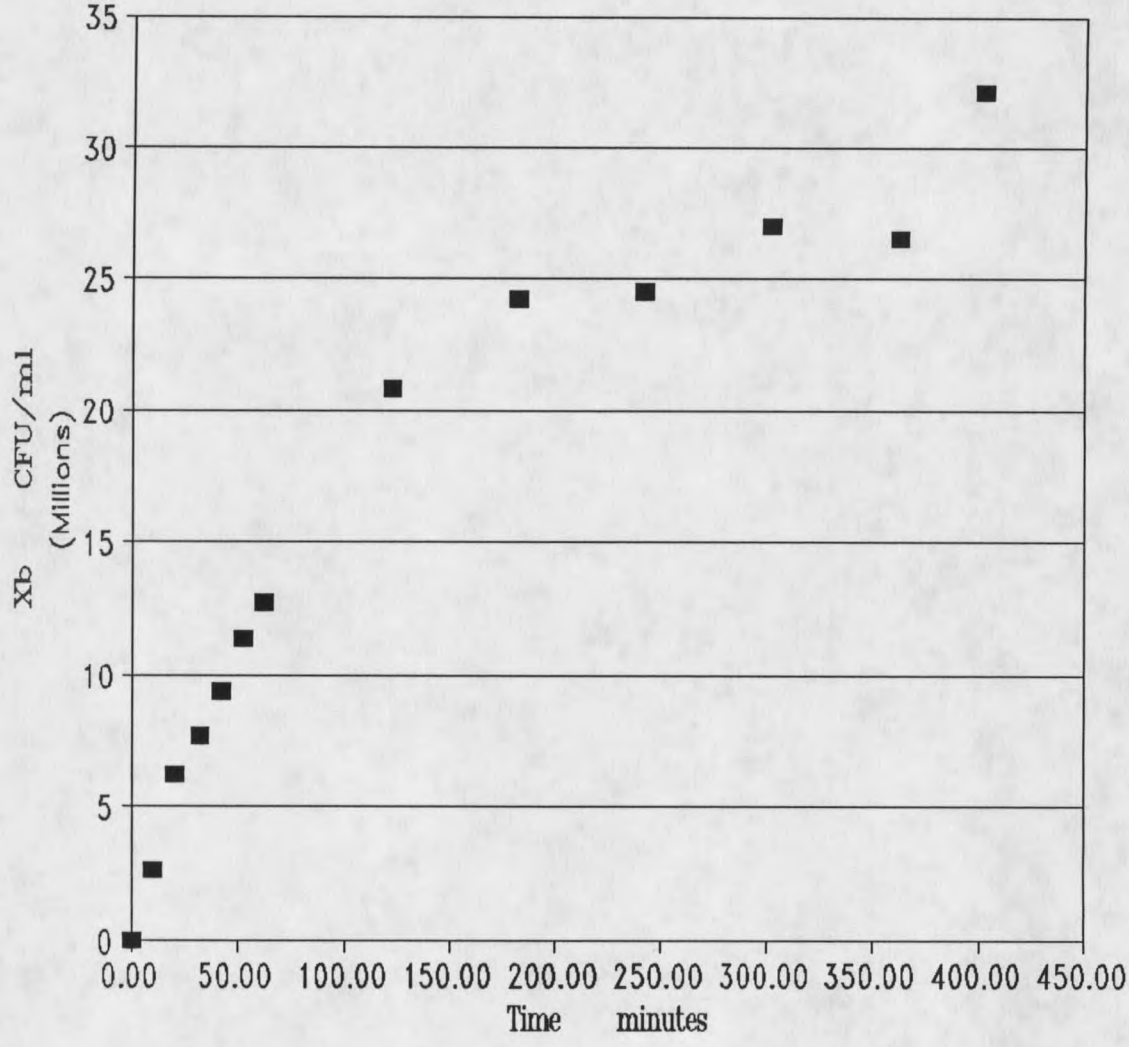

Figure 25. P 2 R 1: C^{14} Viable Cells in the Bulk Liquid in the RotoTorque vs. Time. At the time of data gathering, inlet flow rate = outlet flow rate = 7.1 ml/min, inlet concentration of viable C^{14} cells = 42 x 10^6 CFU/ml, liquid volume in the RotoTorque = 640 ml.

Run 2

RPM = 20

Fluid shear = 0.2 dyne/cm^2

Table 34. Phase 2, Run 2: Result 3. Radioactivity levels in the bulk liquid in the RotoTorque (CPM/ml), biofilm on the slide surface (CPM/cm^2) and, viable count of the bulk liquid in the RotoTorque (CFU/ml).

TIME (min)	BULK LIQUID ROTOTORQUE (CPM/ml)	SLIDE (CPM/cm^2)	BULK LIQUID ROTOTORQUE (CFU x 10^{-6}/ml)
0	0	0	-
10	587	7.69	63
20	703	4.11	54.5
30	975.33	4.92	39
40	1124	12.40	45
50	1153.33	3.65	430
60	1230.67	10.51	400
75	1510	6.41	410
90	1553	29.47	-
120	1905.33	6.82	-
225	2388.67	31.73	-
315	2609.67	28.94	-
405	2745.67	22.08	-

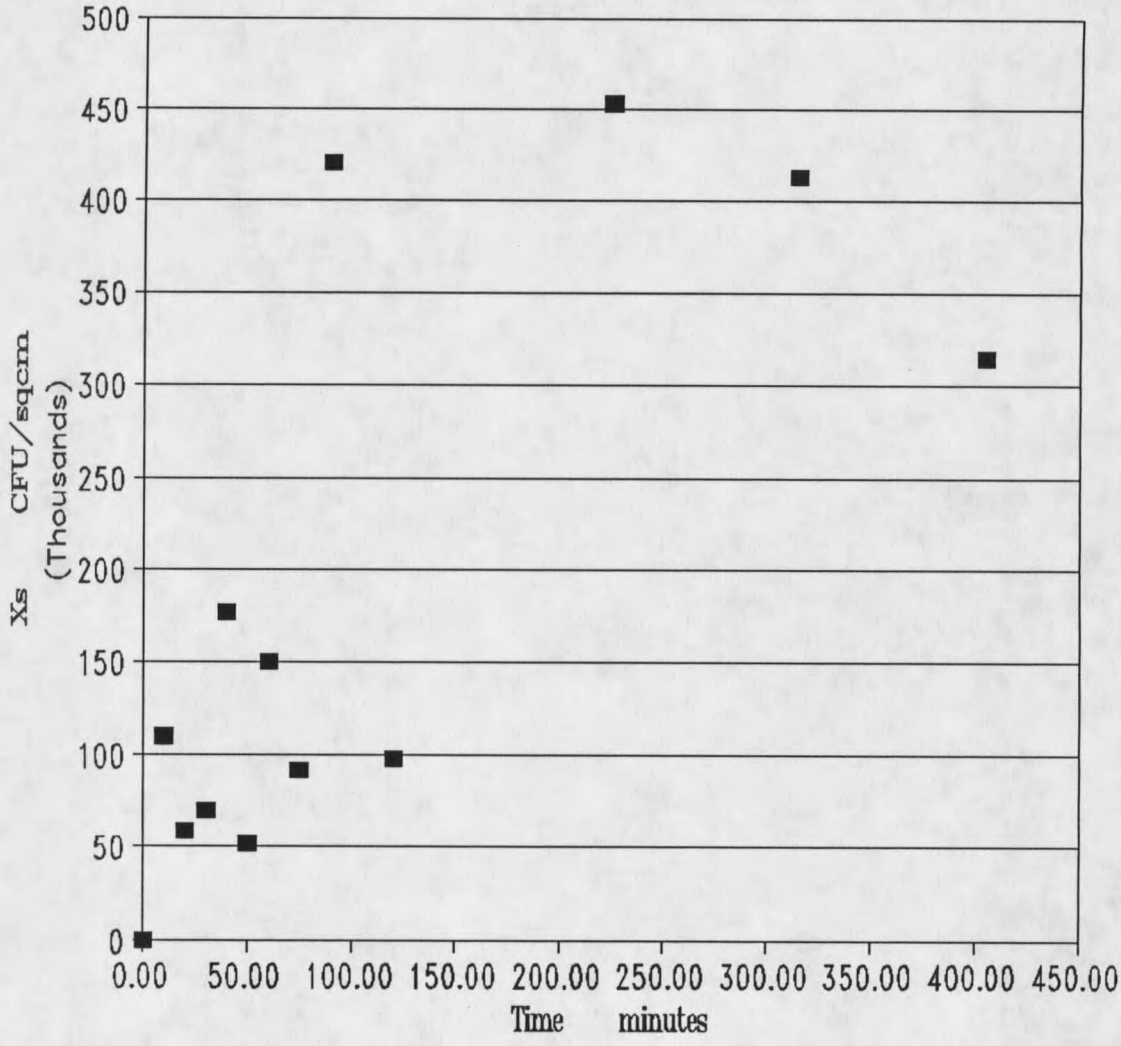

Figure 26. P 2 R 2: Accumulation of C^{14} Viable Cells on the Surface of the Established Biofilm. Regular RotoTorque, RPM = 20, fluid shear = .2 dyne/cm^2, substrate glucose concentration chemostat influent = 30 mg/l. temperature = 22°C.

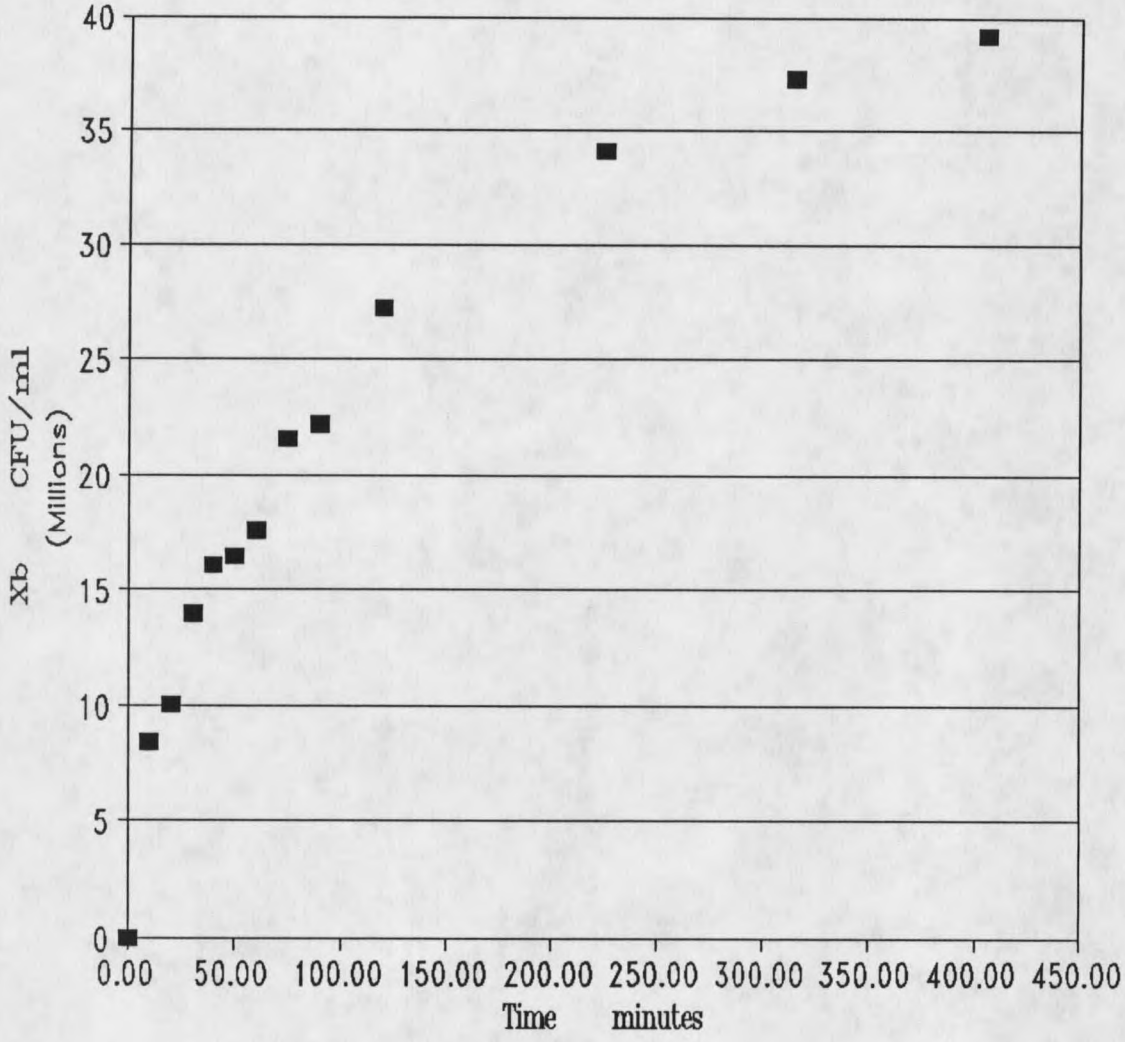

Figure 27. P 2 R 2: C^{14} Viable Cells in the Bulk Liquid in the RotoTorque vs. Time. At the time of data gathering, inlet flow rate = outlet flow rate = 7.1 ml/min, inlet concentration of viable C^{14} cells = 42 x 10^6 CFU/ml, liquid volume in the RotoTorque = 640 ml.

Run 3

RPM = 289

Fluid shear = 20 dyne/cm^2

Glucose concentration chemostat influent = 3 mg/l

Table 35. Phase 2, Run 3: Result 4. Radioactivity levels in the bulk liquid in the RotoTorque (CPM/ml), biofilm on the slide surface (CPM/cm^2), and viable count of the bulk liquid in the RotoTorque (CFU/ml).

TIME (min)	BULK LIQUID ROTOTORQUE (CPM/ml)	SLIDE (CPM/cm^2)	BULK LIQUID ROTOTORQUE (CFU x 10^{-6}/ml)
10	282.67	2.16	8.65
20	470.67	3.1	5.3
30	622.67	4.3	40
40	705.67	5.7	97
50	863	6.7	3.95
60	933	6.5	3.85
75	1045	9.3	3.5
95	1224.33	12.8	97.5
120	1363.67	14.5	3.3
150	1427.67	-	12.6
180	1482	18.7	11.3

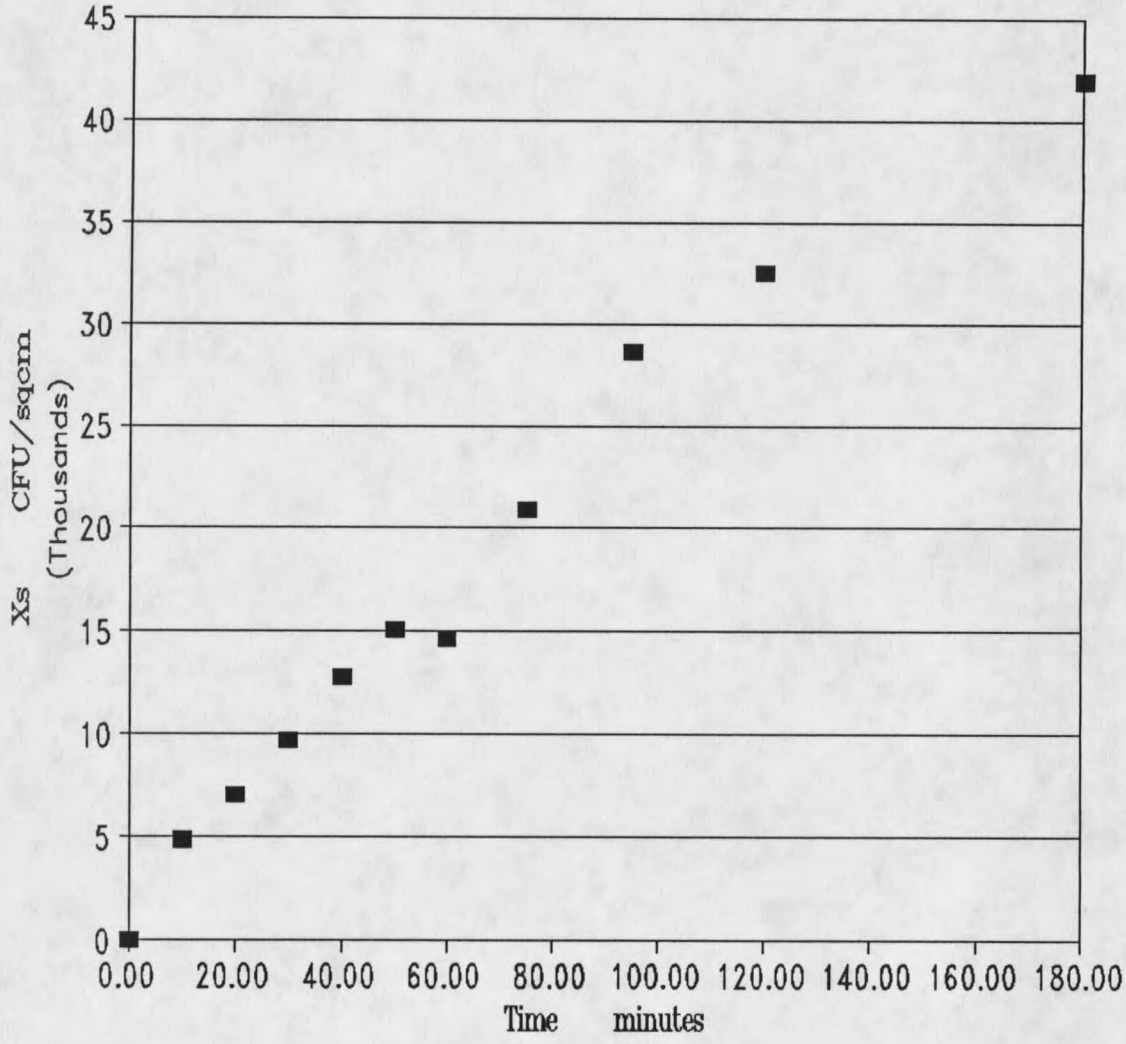

Figure 28. P 2 R 3: Accumulation of C^{14} Viable Cells on the Surface of the Established Biofilm. Regular RotoTorque, RPM = 289, fluid shear = 20 dyne/cm^2, substrate glucose concentration chemostat influent = 3 mg/l. temperature = 22°C.

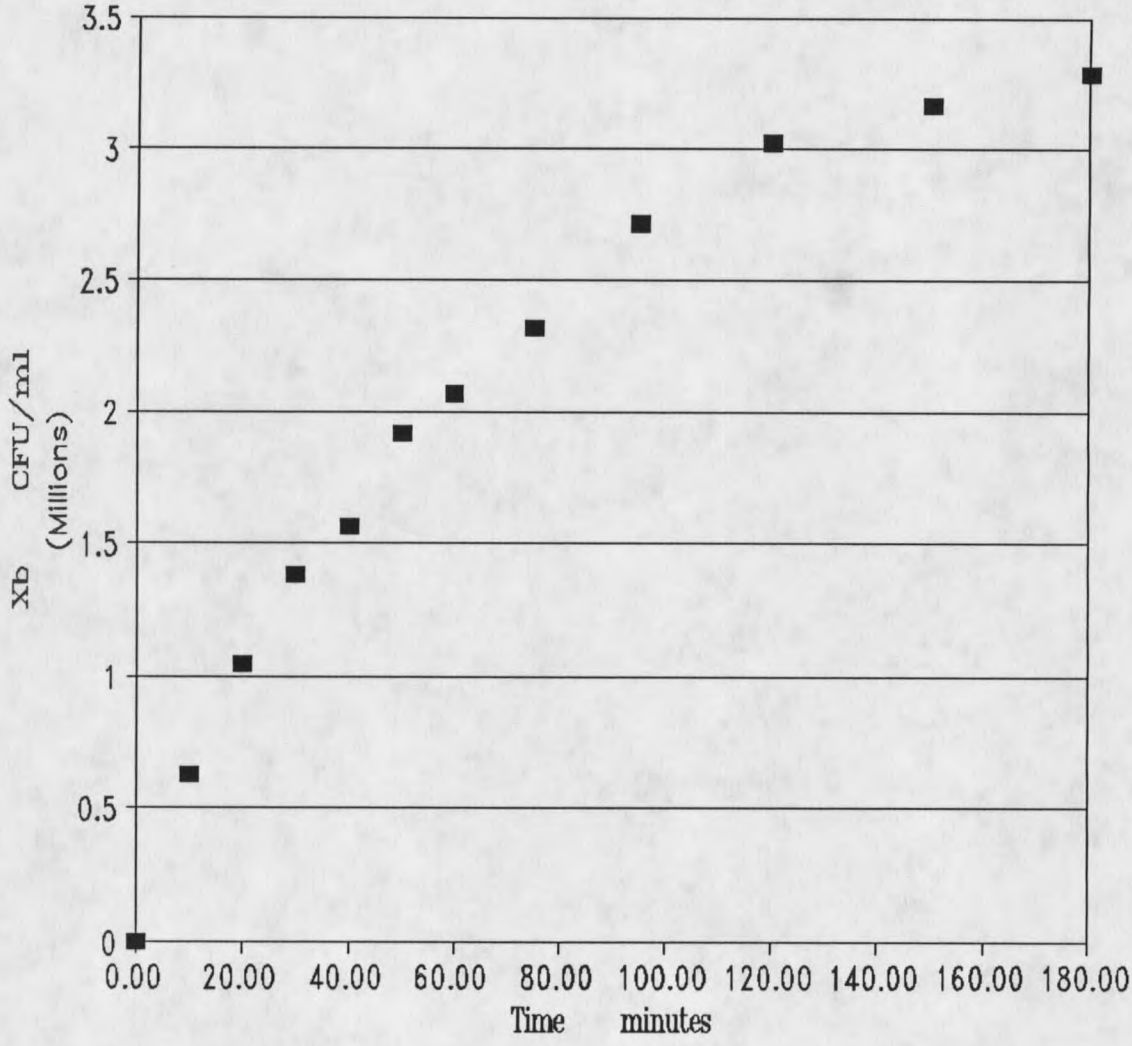

Figure 29. P 2 R 3: C^{14} Viable Cells in the Bulk Liquid in the RotoTorque vs. Time. At the time of data gathering, inlet flow rate = outlet flow rate = 7.1 ml/min, inlet concentration of viable C^{14} cells = 5.05 x 10^6 CFU/ml, liquid volume in the RotoTorque = 640 ml.

Run 4

RPM = 289

Fluid shear = 20 dyne/cm^2

Temperature = 28°C

Table 36. Phase 2, Run 4: Result 5. Radioactivity levels in the bulk liquid in the RotoTorque (CPM/ml), biofilm on the slide surface (CPM/cm^2), and viable count of the bulk liquid in the RotoTorque (CFU/ml).

TIME (min)	BULK LIQUID ROTOTORQUE (CPM/ml)	SLIDE (CPM/cm^2)	BULKLIQUID ROTOTORQUE (CFU x 10^{-6}/ml)
10	305.33	14.7	49
20	421	17.6	52.5
30	461.33	33.9	95.5
40	618.33	29.5	57.5
50	727.33	36.7	58.5
60	769	49.7	59.5
75	896	55.4	60
90	952.33	56.4	40.5
120	1061.67	89.89	42
150	1468.33	106.06	42
164	1375	-	-

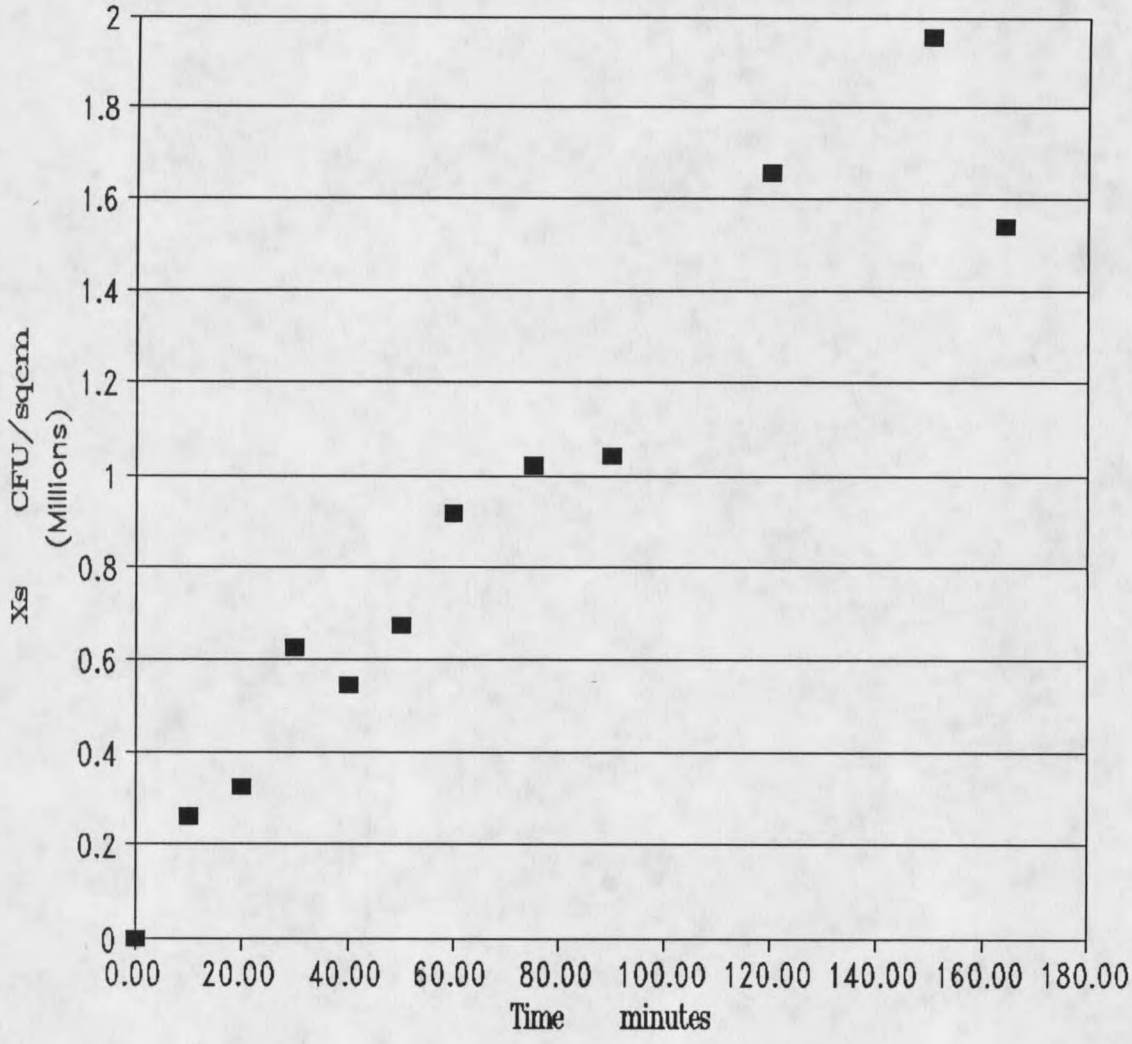

Figure 30. P 2 R 4: Accumulation of C^{14} Viable Cells on the Surface of the Established Biofilm. Regular RotoTorque, RPM = 289, fluid shear = 20 dyne/cm^2, substrate glucose concentration chemostat influent = 30 mg/l. temperature = 28°C.

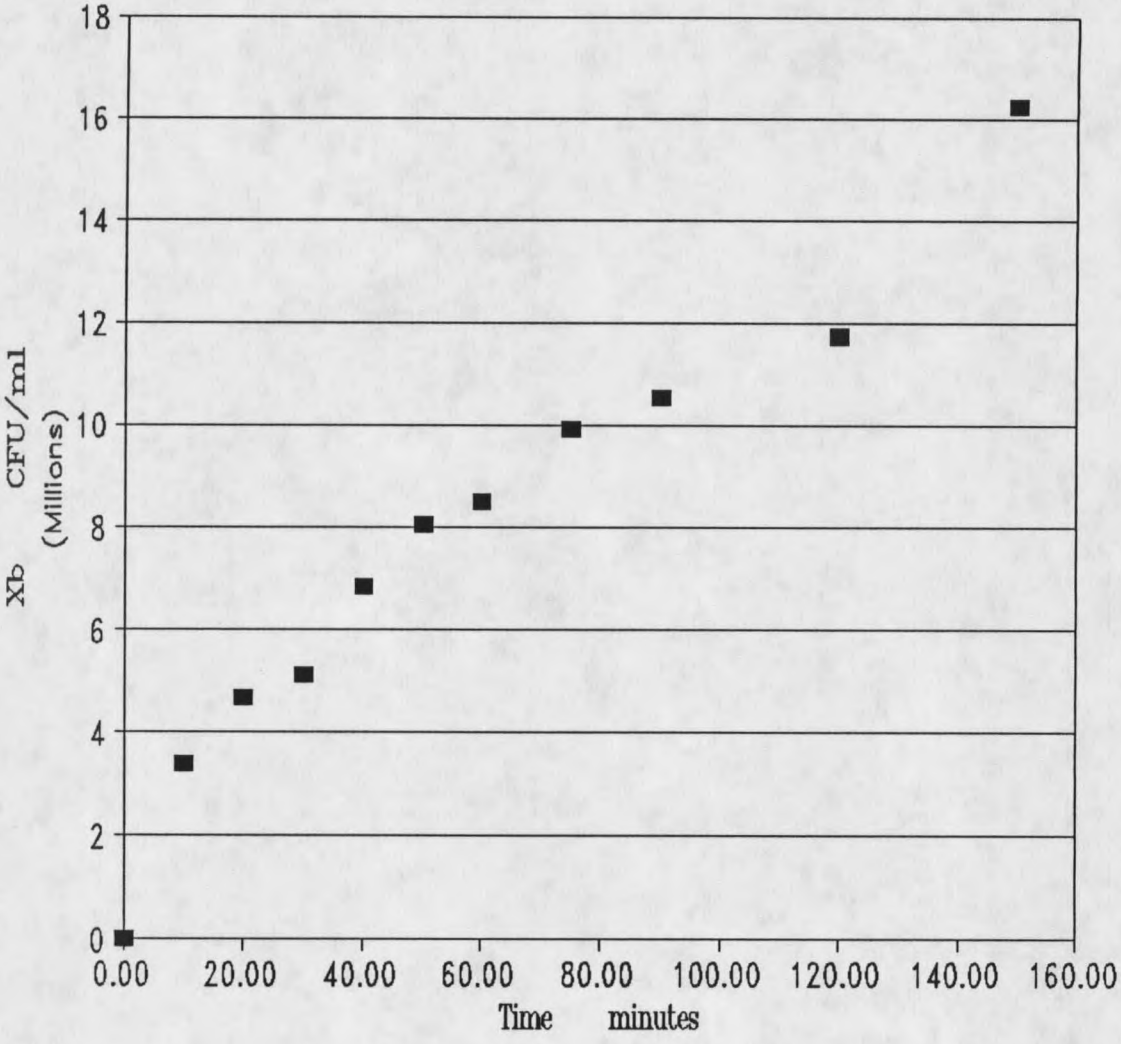

Figure 31. P 2 R 4: C^{14} Viable Cells in the Bulk Liquid in the RotoTorque vs. Time. At the time of data gathering, inlet flow rate = outlet flow rate = 7.1 ml/min, inlet concentration of viable C^{14} cells = 32 x 10^6 CFU/ml, liquid volume in the RotoTorque = 640 ml.

Run 5

RPM = 75

Fluid shear = 2 dyne/cm^2

Temperature = 28°F

Table 37. Phase 2, Run 5: Result 6. Radioactivity levels of the bulk liquid in the RotoTorque (CPM/ml), biofilm on the slide surface (CPM/cm^2), and viable count of the bulk liquid RotoTorque (CFU/ml).

TIME (min)	BULK LIQUID ROTOTORQUE (CPM/ml)	SLIDE (CPM/cm^2)	BULK LIQUID ROTOTORQUE (CFU x 10^{-6}/ml)
10	311.33	10.3	39.5
20	479.33	16.9	-
30	595	27.8	48
40	789	35.4	103
50	1909	46.4	89
60	-	56.2	40
75	1180.67	66.5	40
95	1300.33	80.5	61
120	1438.33	130.1	53
150	1609.33	121.8	48.5
180	1820.33	166.5	-
210	1913.67	20.3	-

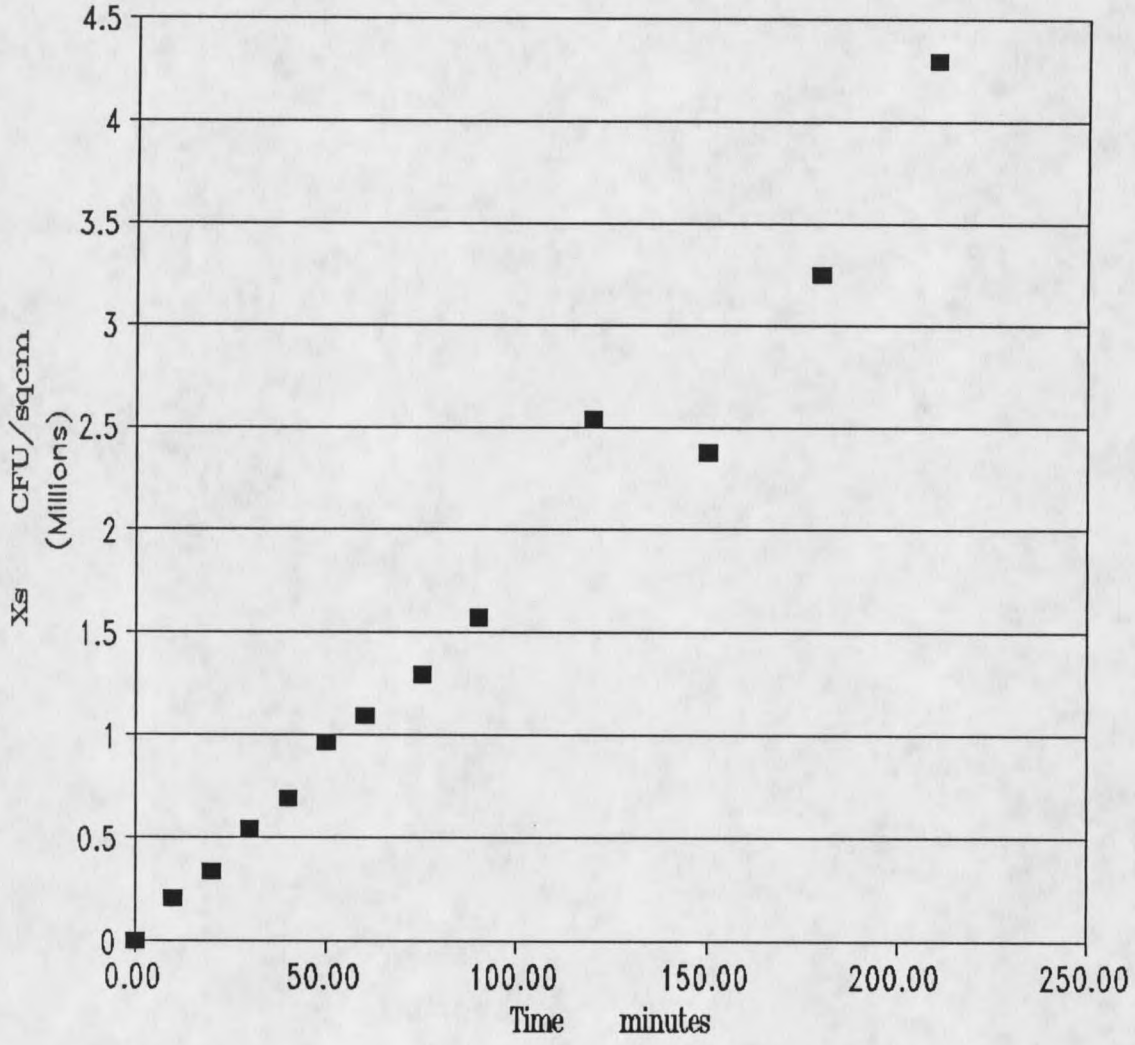

Figure 32. P 2 R 5: Accumulation of C^{14} Viable Cells on the Surface of the Established Biofilm. Regular RotoTorque, RPM = 70, fluid shear = 2 dyne/cm^2, substrate glucose concentration chemostat influent = 30 mg/l. temperature = 28°C.

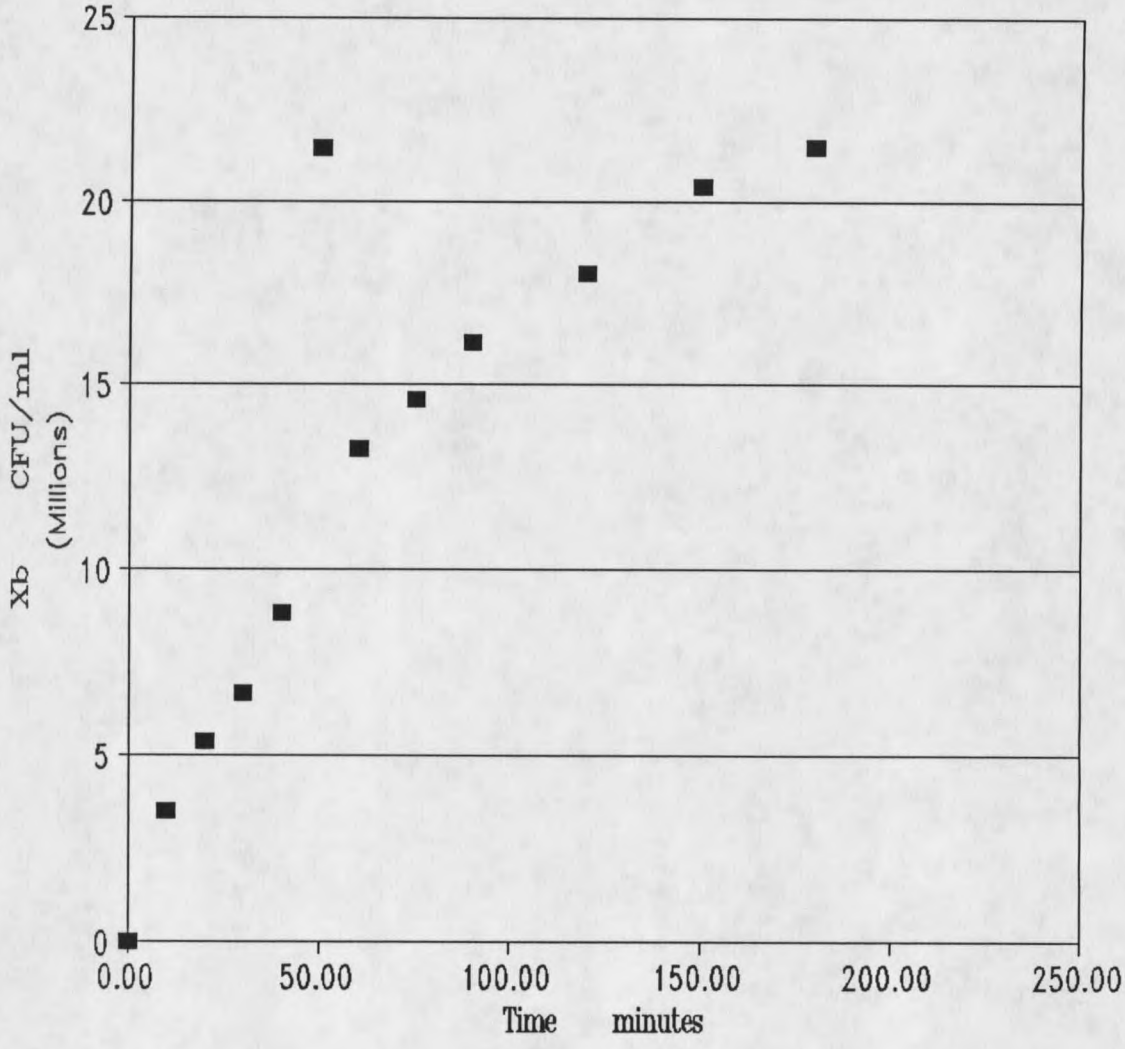

Figure 33. P 2 R 5: C^{14} Viable Cells in the Bulk Liquid in the RotoTorque vs. Time. At the time of data gathering, inlet flow rate = outlet flow rate = 7.1 ml/min, inlet concentration of viable C^{14} cells = 32.5 x 10^6 CFU/ml, liquid volume in the RotoTorque = 640 ml.

Run 6

RPM = 289

Fluid shear = 20 dyne/cm^2

Temperature = 22°C

Duplicate experiment of P 2 R 1.

Table 38. Phase 2, Run 6: Result 7. Radioactivity levels in the bulk liquid in the RotoTorque (CPM/ml), biofilm on the slide surface (CPM/cm^2), and viable count of the bulk liquid RotoTorque (CFU/ml).

TIME	BULK LIQUID ROTOTORQUE	SLIDE	BULK LIQUID ROTOTORQUE
(min)	(CPM/ml)	(CPM/cm^2)	(CFU x 10^{-6}/ml)
30	554.33	7	49
60	847.3	8.6	61
90	998.3	9.1	41.5
120	1117	9.0	29.5
150	1224.3	10.2	52
180	1349.3	13.5	44.5
210	1379	14.2	50.5
240	1408	14.6	43
270	1442	15.5	48.5
300	1496	16.4	72
330	1506	17.21	34
360	1539	17.2	-

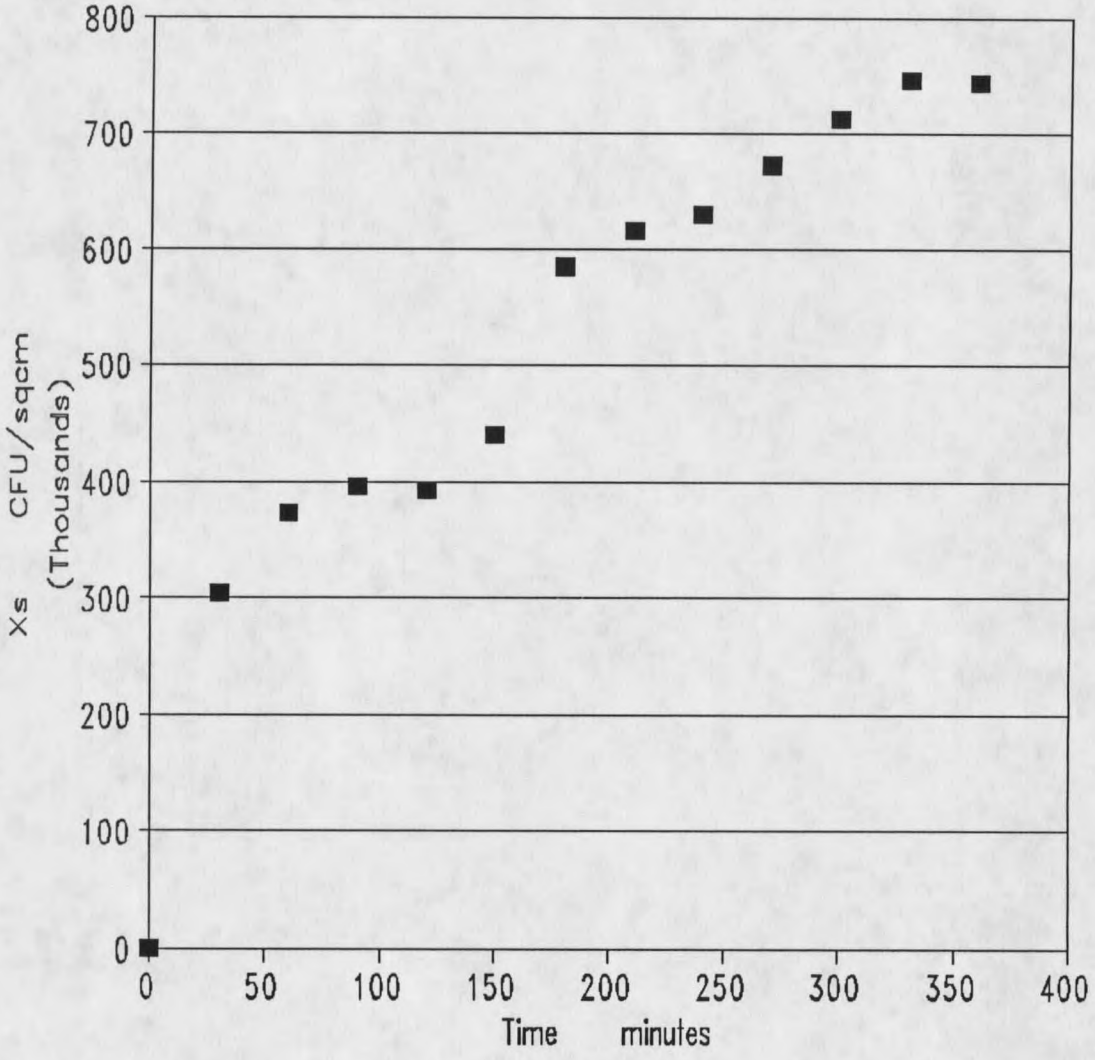

Figure 34. P 2 R 6: Accumulation of C^{14} Viable Cells on the Surface of the Established Biofilm. Regular RotoTorque, RPM = 289, fluid shear = 20 dyne/cm^2, substrate glucose concentration chemostat influent = 30 mg/l, temperature = 22°C.

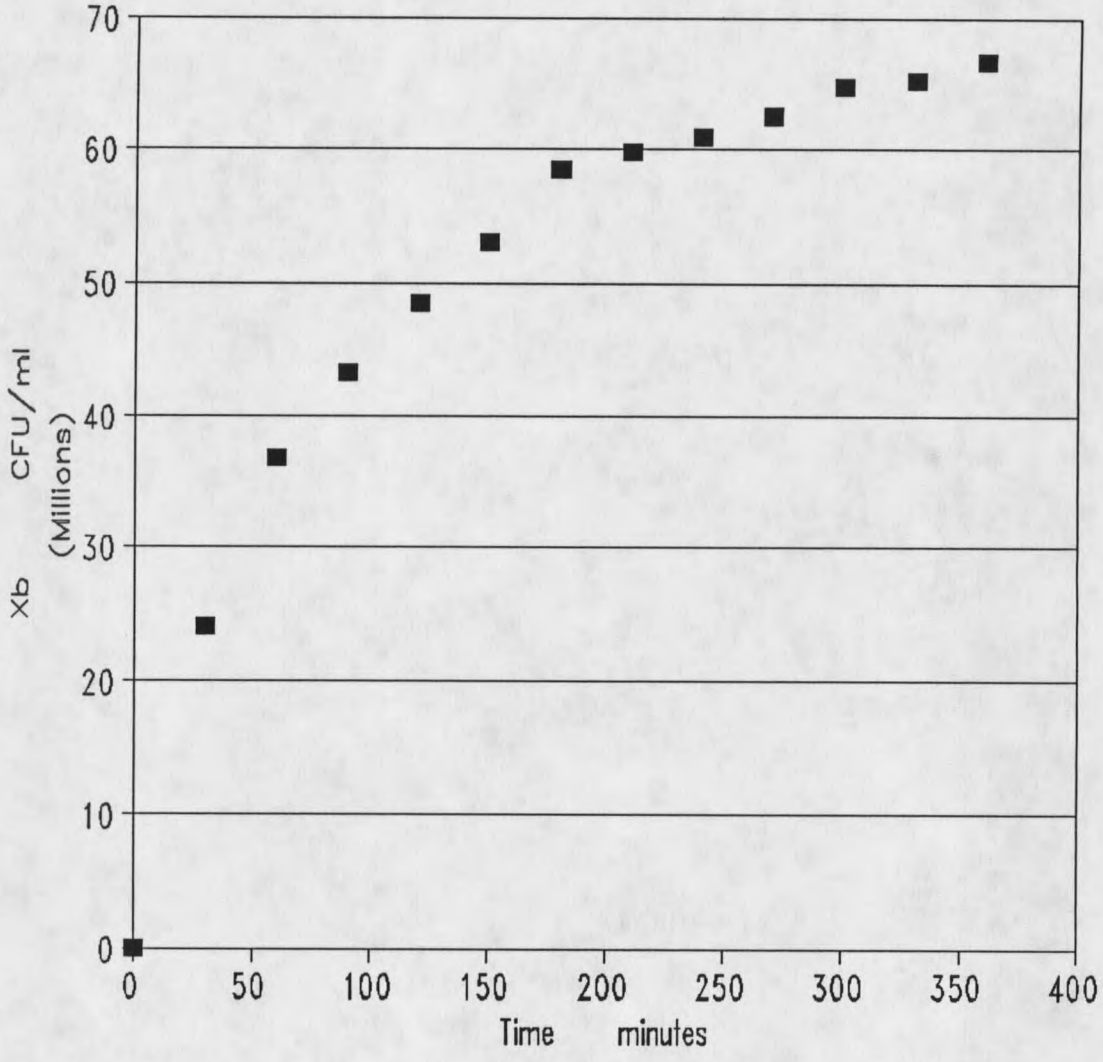

Figure 35. P 2 R 6: C^{14} viable Cells in the Bulk Liquid in The RotoTorque vs. Time. At the time of data gathering, inlet flow rate = outlet flow rate = 7.1 ml/min, inlet concentration of C^{14} viable cells = 85.5 x 10^6 CFU/ml, liquid volume in the RotoTorque = 640 ml.

Run 7

RPM = 289

Fluid shear = 20 dyne/cm^2

Temperature = 22°C

Experimental condition is the same as P 2 R 6 except, the C^{12} biofilm was grown for only 24 hours instead of 7 days.

Table 39. Phase 2, Run 7: Result 8. Radioactivity levels of the bulk liquid in the RotoTorque (CPM/ml), biofilm on the slide surface (CPM/ml), and viable count of the bulk liquid RotoTorque (CFU/ml).

TIME (min)	BULK LIQUID ROTOTORQUE (CPM/ml)	SLIDE (CPM/cm^2)	BULK LIQUID ROTOTORQUE (CFU x 10^{-6}/ml)
2	57	0.9	-
4	117	0.9	-
6	166.7	2.6	-
8	225.7	2.7	
10	274	2.9	38.5
20	526	3.4	39.5
30	749.3	6.3	48
60	1278.7	6.7	40
120	1950.3	14.6	33
150	2125.3	17.3	61
210	2431	21.6	51.5
240	2549	25.3	35

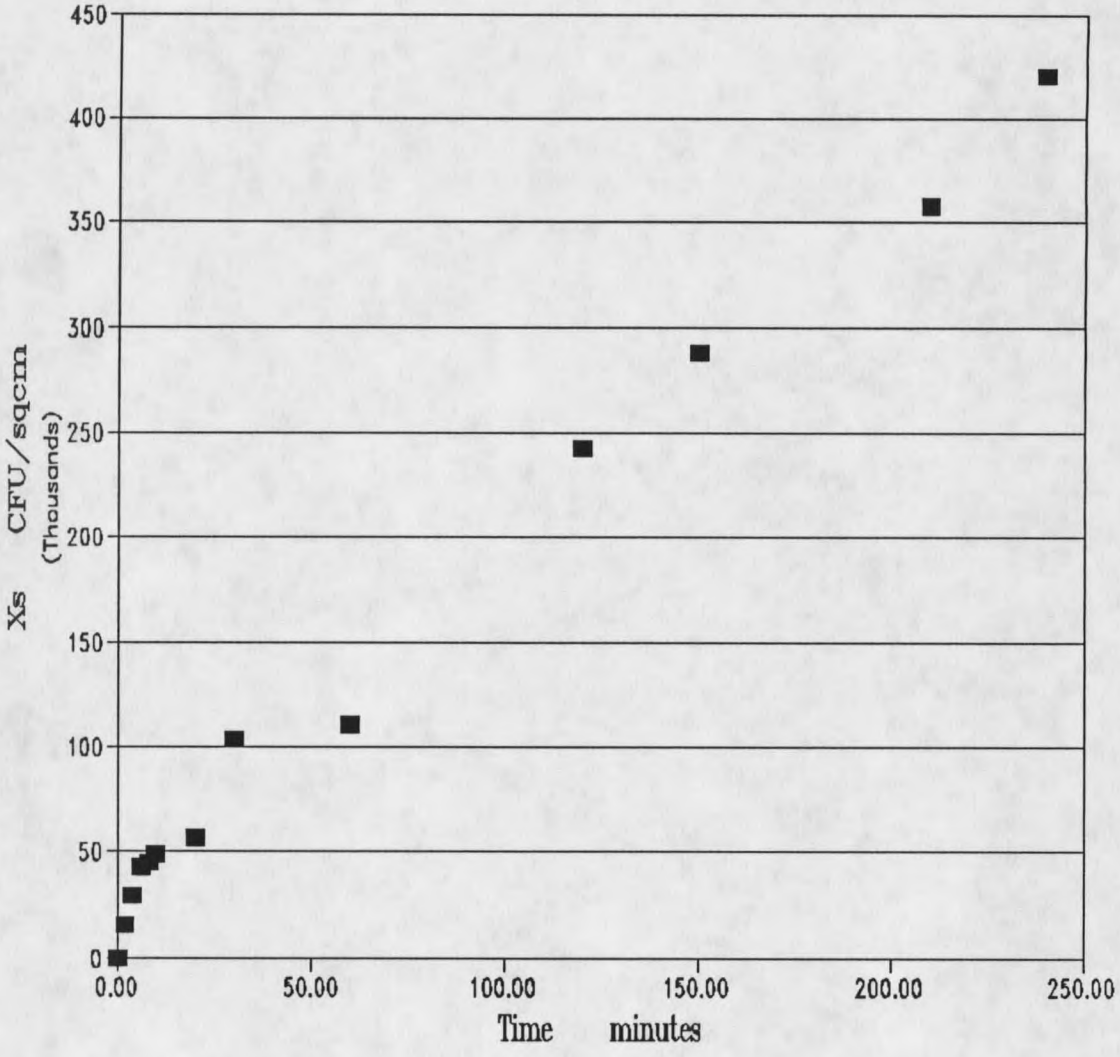

Figure 36. P 2 R 7: Accumulation of C^{14} Viable Cells on the Surface of the Established Biofilm. Regular RotoTorque, RPM = 289, fluid shear = 20 dyne/cm^2, substrate glucose concentration chemostat influent = 30 mg/l, temperature = 22°C.

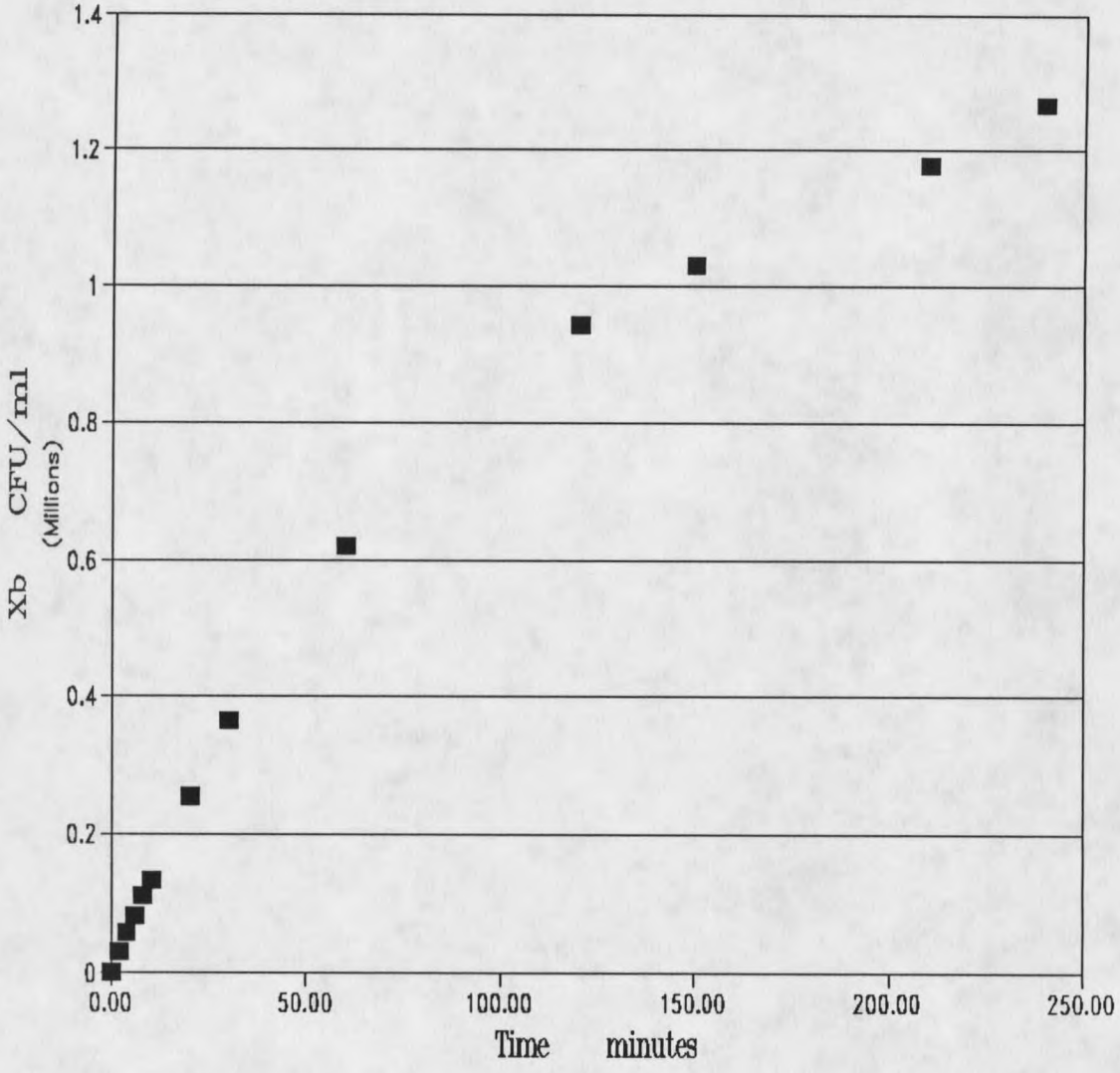

Figure 37. P 2 R 7: C^{14} Viable Cells in the Bulk Liquid in the RotoTorque vs. Time. At the time of data gathering, inlet flow rate = outlet flow rate = 7.1 ml/min, inlet concentration of C^{14} viable cells = 48 x 10^6 CFU/ml, liquid volume in the RotoTorque = 640 ml.

At large times, the net rate of C^{14} cellular attachment per unit area to an established biofilm is correlated to the net rate of total cell attachment per unit area to an established biofilm as given by equation (36).

$$R_{An}^{14} = (1 - e^{-t/\tau})\, R_{An}^{total} \qquad (47)$$

The net rate of total cellular attachment per unit area to an established biofilm, R_{An}^{total}, is constant throughout each experimental run. It also means that R_{An}^{total} is constant for a fixed bulk cell concentration (within a specific experimental run). At time $t \longrightarrow \infty$, R_{An}^{14} will equal to R_{An}^{total} for the same specific condition. This means that each experimental run will give one value of R_{An}^{14}.

The method described in the Model Development section and the experimental data enable us to calculate the gross rate of total cellular attachment per unit area, R_{Ag}^{total}, the net rate of total cellular attachment per unit area, R_{An}^{total}, the rate of total cellular detachment per unit area, R_{d}^{total}, and the rate of C^{14} cellular detachment per unit area, R_{d}^{14}.

Equations (35), (40), (41), and (42) as derived previously in the Model Development section will be used to calculate R_{An}^{total}, and R_{Ag}^{total}.

$$R_{Ag}^{14} = (1 - e^{-t/\tau})\, R_{Ag}^{total} \qquad t \geq 0 \qquad (35)$$

$$accumulation\ of\ C^{14}\ per\ unit\ area = R_{An}^{total}\,[T] \qquad (42)$$

which is true for time $t \geq t_L$.

$$accumulation\ of\ C^{14}\ per\ unit\ area = R_{Ag}^{total}\,[T] \qquad (40)$$

which is true for time $t = 0$.

$$[T] = t - \tau\,(1 - e^{-t/\tau}) \qquad (41)$$

The graphs of the accumulation C^{14} per unit area, X_s^{14}, as a function of modified time, [Tm], are given on the following pages.

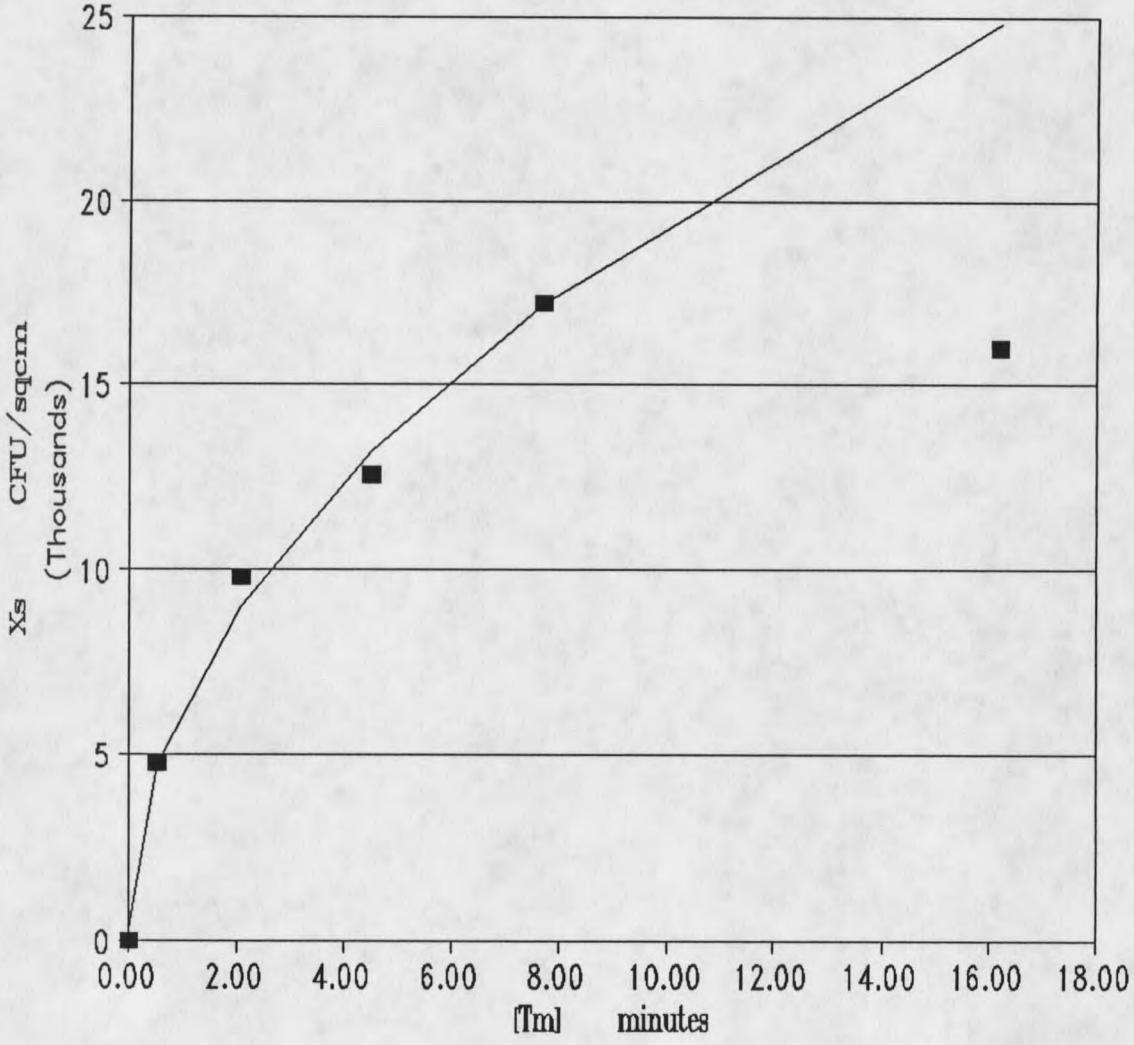

Figure 38. P 1 R 1: Accumulation of C^{14} Viable Cells on the Surface of an Established Biofilm vs. Modified Time, [Tm]. Small RotoTorque, RPM = 600, fluid shear = 20 dyne/cm^2, substrate glucose concentration chemostat influent = 30 mg/l, temperature = 22°C, ■ experimental data, - curve fit (X_s^{14} = 261.63 + 6089.97 $[Tm]^{.5}$, r^2 = 0.99, the last point was omitted).

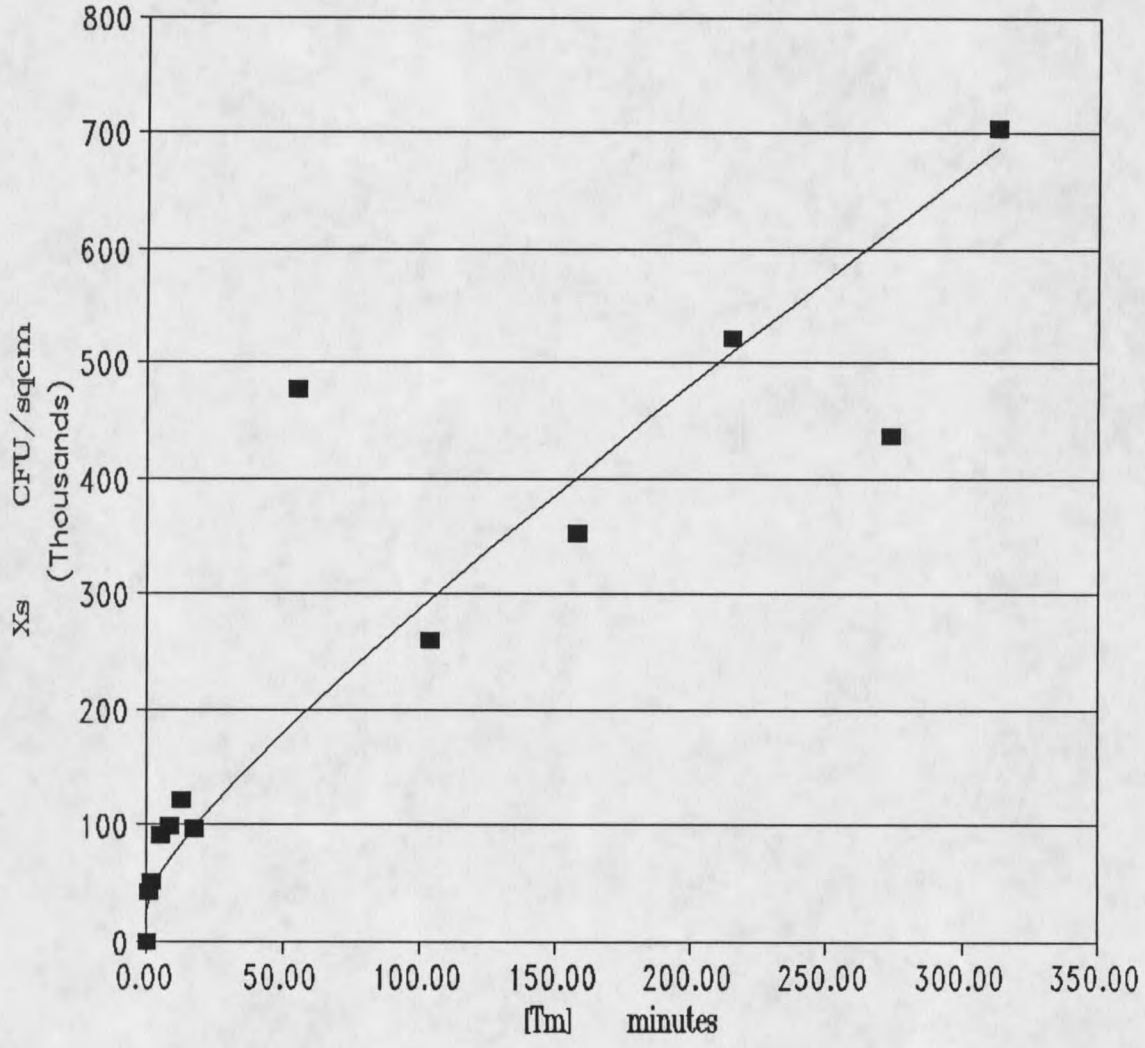

Figure 39. P 2 R 1: Accumulation of C^{14} Viable Cells on the Surface of an Established Biofilm vs. Modified Time, [Tm]. Regular RotoTorque, RPM = 289, fluid shear = 20 dyne/cm^2, substrate glucose concentration chemostat influent = 30 mg/l, temperature = 22°C, ■ experimental data, - curve fit (X_s^{14} = 153.97 + 38.13 $[Tm]^{.5}$, r^2 = 0.99, the two most divergant points were omitted).

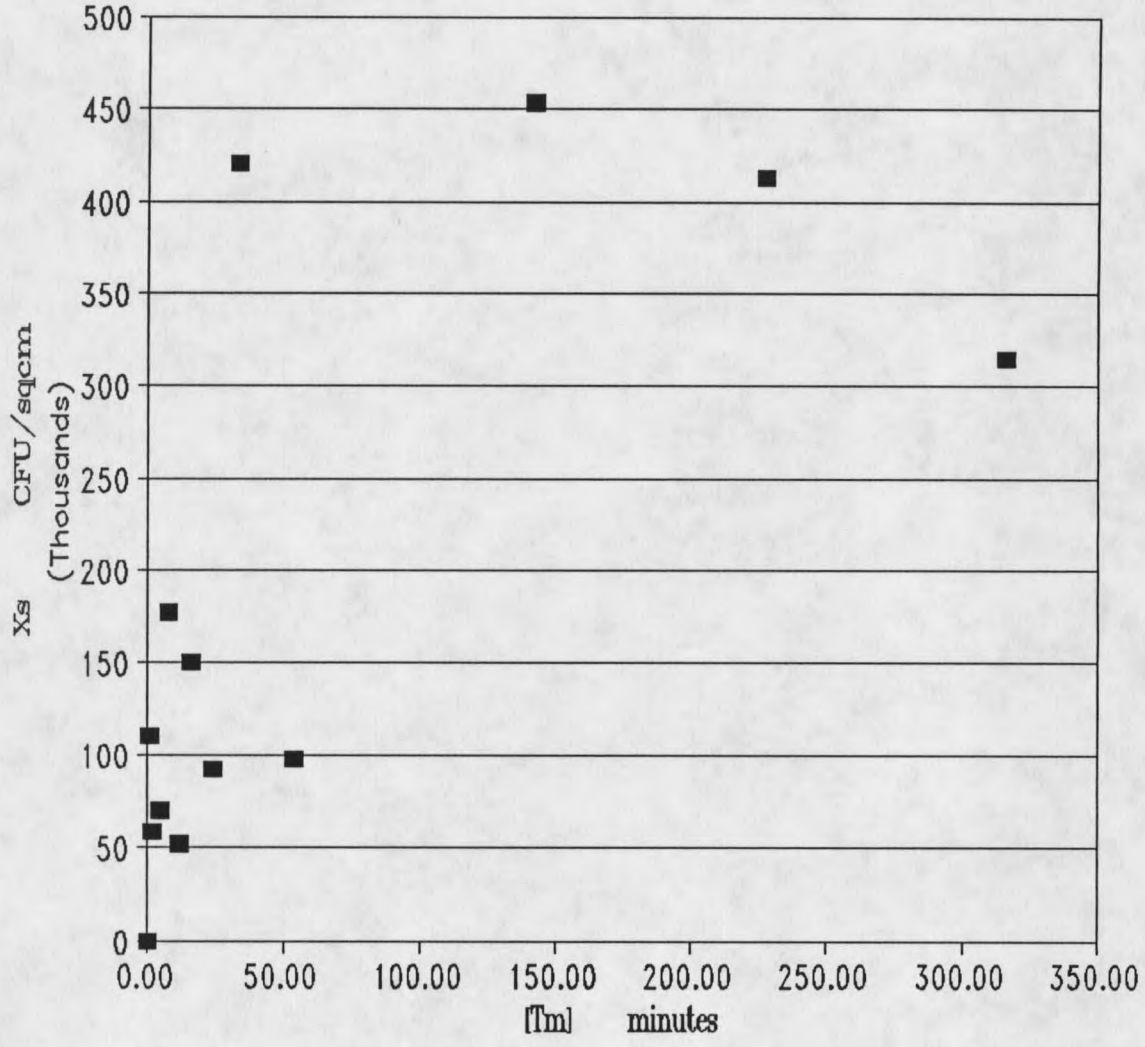

Figure 40. P 2 R 2: Accumulation of C^{14} Viable Cells on the Surface of an Established Biofilm vs. Modified Time, [Tm]. Regular RotoTorque, RPM = 20, fluid shear = 0.2 dyne/cm^2, substrate glucose concentration chemostat influent = 30 mg/l, temperature = 22°C, ■ experimental data.

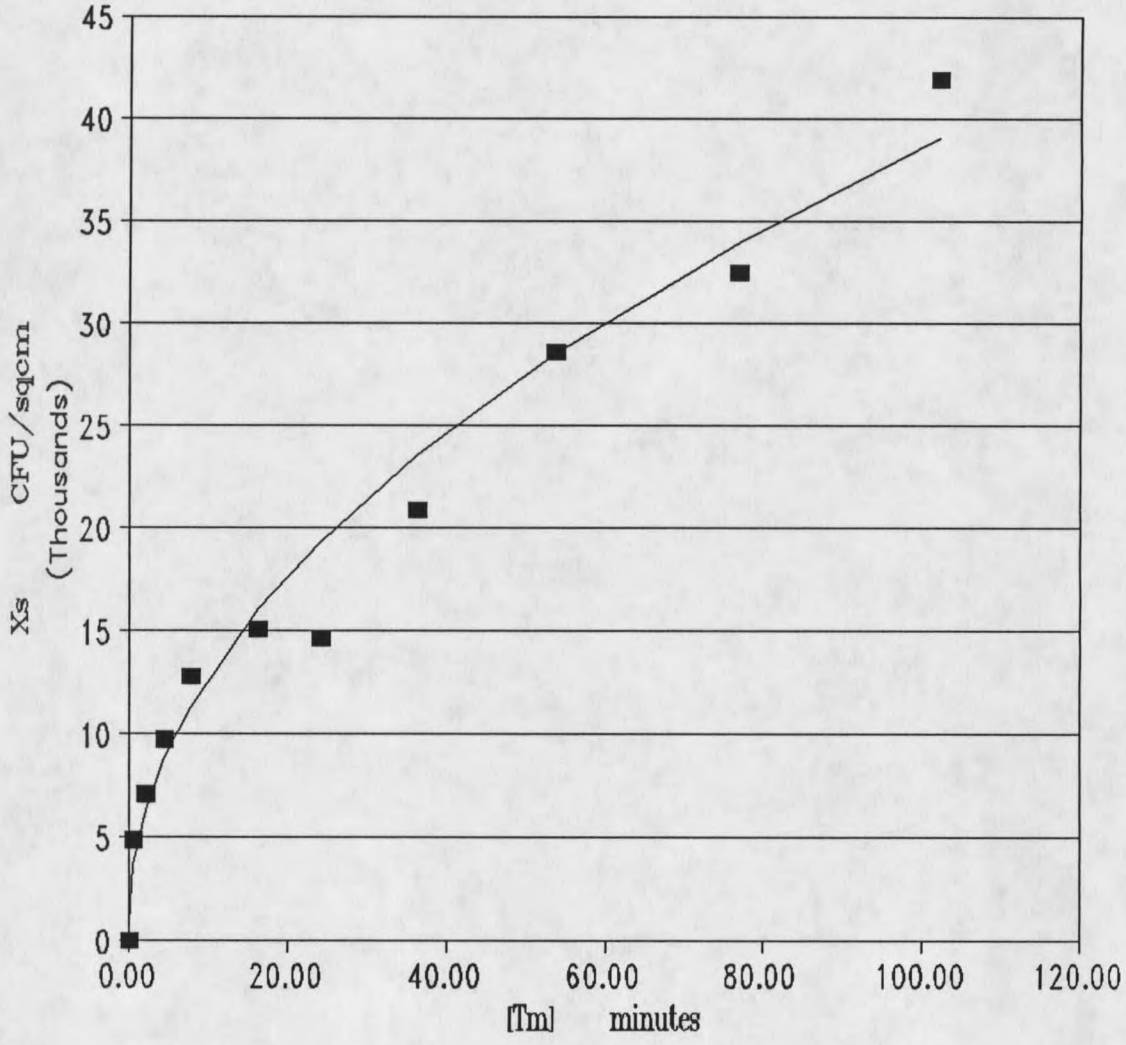

Figure 41. P 2 R 3: Accumulation of C^{14} Viable Cells on the Surface of an Established Biofilm vs. Modified Time, [Tm]. Regular RotoTorque, RPM = 289, fluid shear = 20 dyne/cm^2, substrate glucose concentration chemostat influent = 3 mg/l, temperature = 22°C, ■ experimental data, - curve fit (X_s^{14} = 772.4 + 4179.1 $[Tm]^{.5}$, r^2 = 0.99).

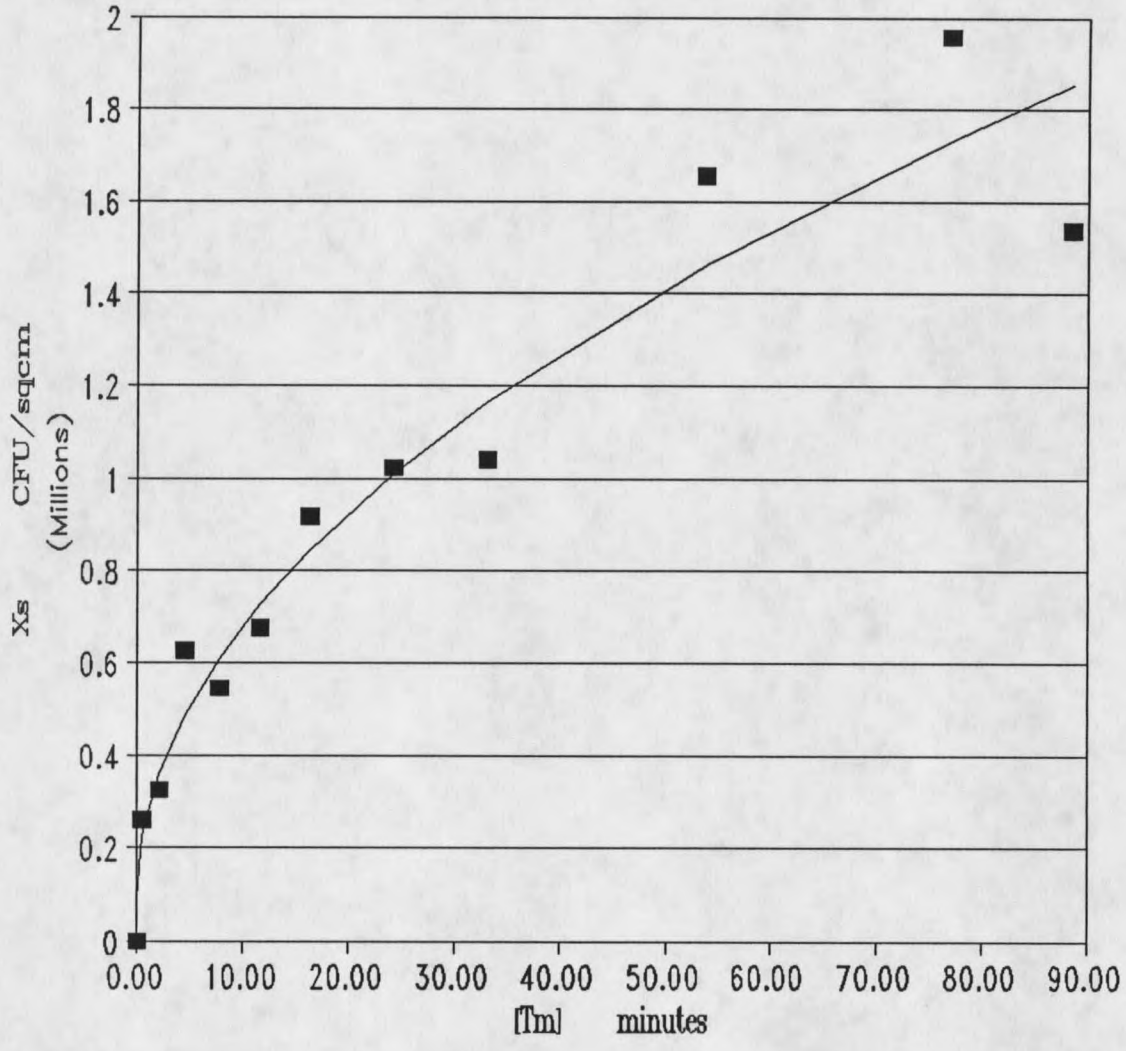

Figure 42. P 2 R 4: Accumulation of C^{14} Viable Cells on the Surface of an Established Biofilm vs. Modified Time, [Tm]. Regular RotoTorque, RPM = 289, fluid shear = 20 dyne/cm^2, substrate glucose concentration chemostat influent = 30 mg/l, temperature = 28°C, ■ experimental data, - curve fit (X_s^{14} = 89209.7 + 187194.4 $[Tm]^{.5}$, r^2 = 0.94).

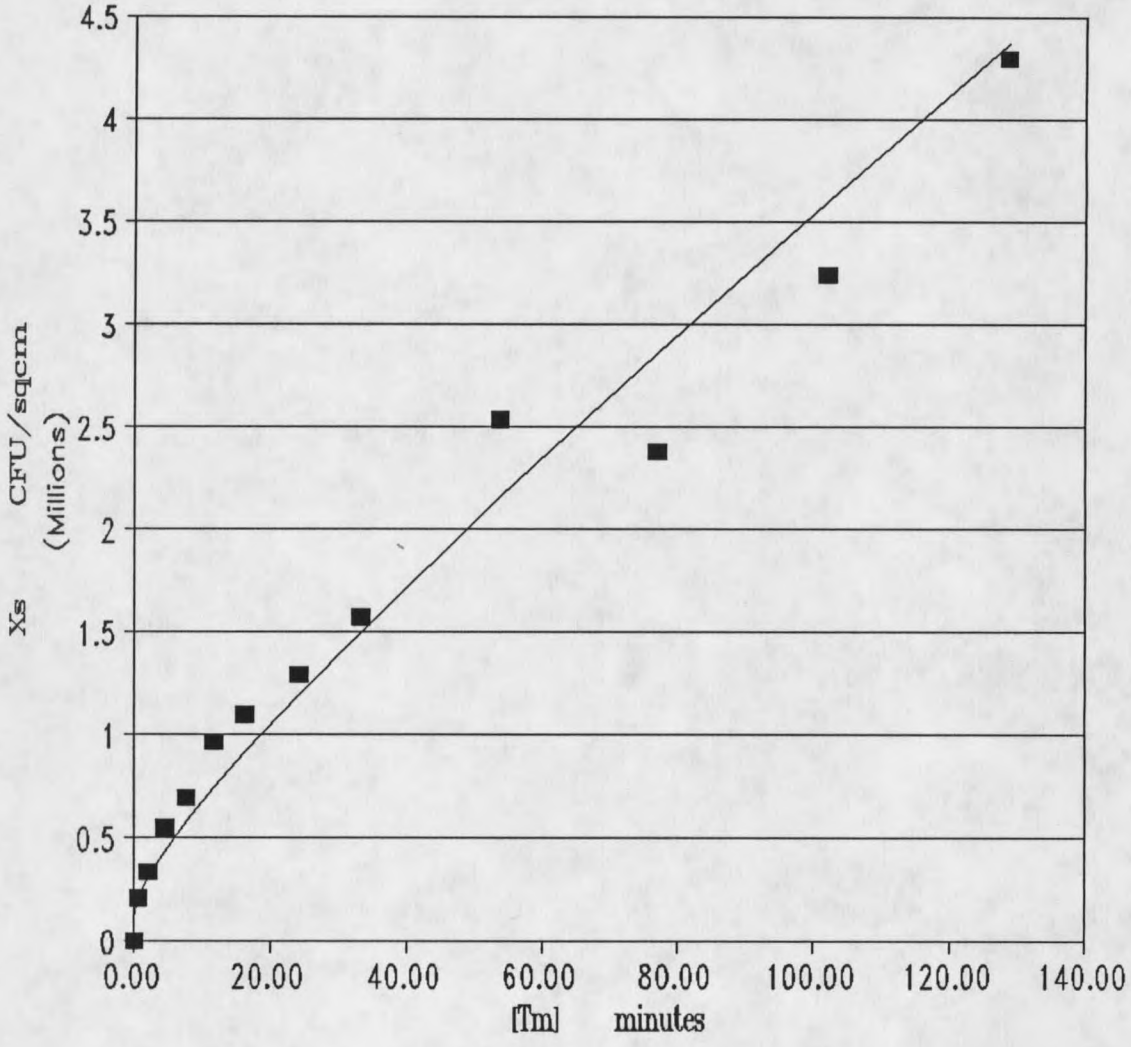

Figure 43. P 2 R 5: Accumulation of C^{14} Viable Cells on the Surface of an Established Biofilm vs. Modified Time, [Tm]. Regular RotoTorque, RPM = 70, fluid shear = 2 dyne/cm^2, substrate glucose concentration chemostat influent = 30 mg/l, temperature = 28°C, ■ experimental data, - curve fit (X_s^{14} = 328.3 + 155.2 $[Tm]^{.5}$, r^2 = 0.97).

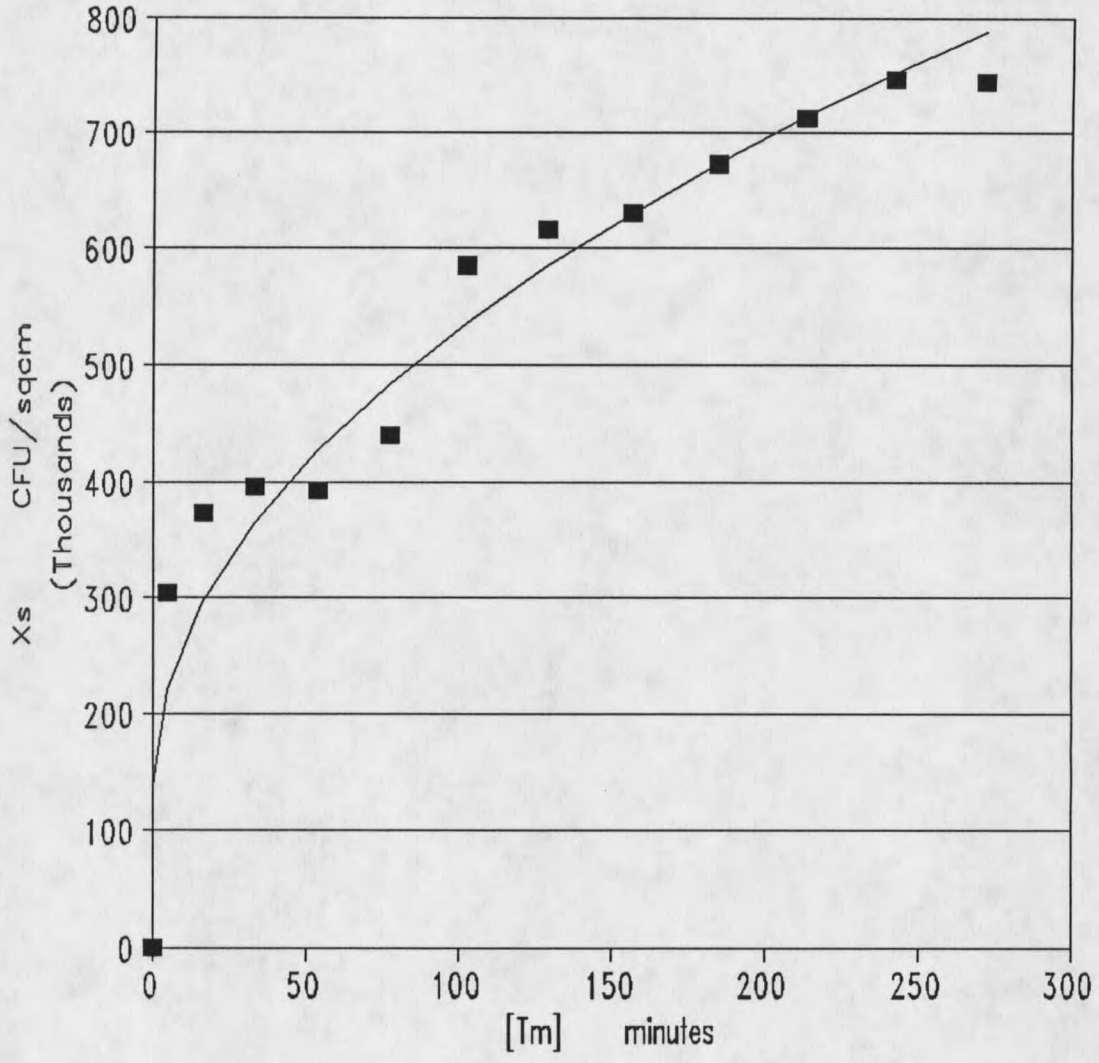

Figure 44. P 2 R 6: Accumulation of C^{14} Viable Cells on the Surface of an Established Biofilm vs. Modified Time, Time [Tm]. Regular RotoTorque, RPM = 289, fluid shear = 20 dyne/cm^2, substrate glucose concentration chemostat influent = 30 mg/l, temperature = 22°C, ■ experimental data, - curve fit (Xs^{14} = 137043.6 + 39478.5 $[T]^{.5}$, r^2 = 0.93)

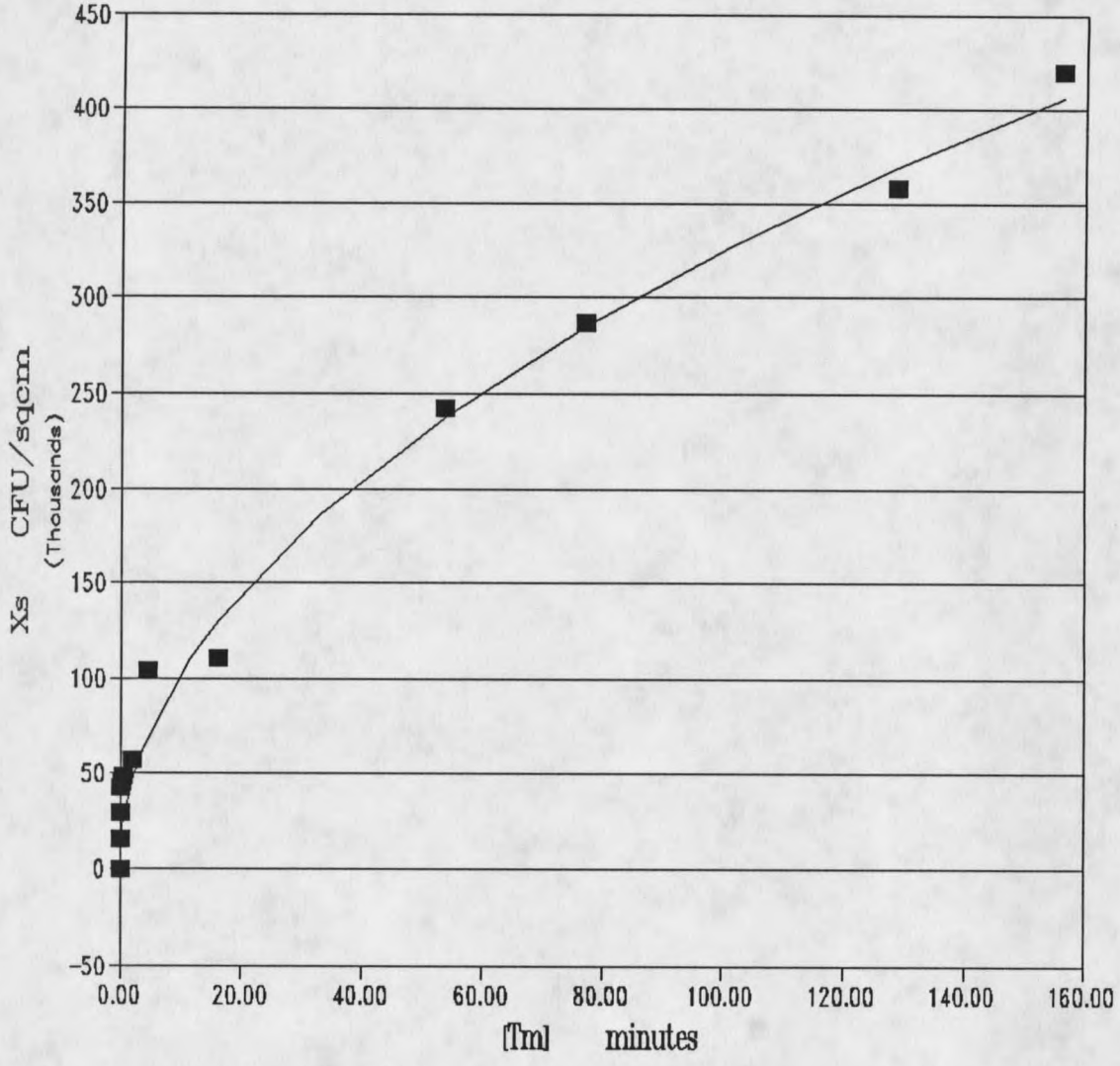

Figure 45. P 2 R 7:Accumulation of C^{14} Viable Cells on the Surface of an Established Biofilm vs. Modified Time, [Tm]. Regular RotoTorque, RPM = 289, fluid shear = 20 dyne/cm^2, substrate glucose concentration chemostat influent = 30 mg/l temperature = 22°C, one day C^{12} biofilm, ■ experimental data, - curve fit (Xs^{14} = -664.6 +32542.2 $[T]^{.5}$, r^2 = 0.97).

The slope of each graph at time t = 0, and at time $t \geq t_L$ yields the values of R_{Ag}^{14}, and R_{An}^{14} respectively for each

experimental run (Figures 38 through 45). Given R_{Ag}^{14}, and R_{An}^{14}; R_{Ag}^{total}, and R_{An}^{total} are then calculated using equations (35) and equation (36). Ideally, t_L would be chosen where the rate of C^{14} cellular detachment per unit area is reaching steady-state at $t_L \longrightarrow \infty$. In this work, however, t_L was chosen as large the data allowed.

Equation (36) was used to correlate R_{An}^{total} to R_{An}^{14} by $(1 - e^{-t/\tau})$ as given in equation (36) at times $t \geq t_L$. Basically, by using equation (36), it is said that R_{An}^{total} will be estimated based on the R_{An}^{14} calculated from an experimental data set when the C^{14} labelled cells on the surface of biofilm are behaving as the C^{12} cells on the surface of biofilm.

The solid line on each graph is a curve fit. The slope of each graph at t_L was calculated using one of the curve fit equations given in Table 40. However, because of the inability of the equations to predict the slope at time t = 0, the slope of each graph at time t = 0 was determined by calculating the slope of another curve fit to the lower portion of each data set (the first 5 points).

Table 40. Numerical Values of Coefficients for Regression Equations.

Equation	Form
$X^{14}_s = A + B\ [Tm]^{.5}$	i
$X^{14}_s = (A + B\ [Tm]^{.5})^2$	ii
$X^{14}_s = (A - B\ e^{-[Tm]/\tau})^2$	iii
$X^{14}_s = A + B\ [Tm]$	iv

Run	All Data Points				First 5 Points			
	Form	A	B	r^2	Form	A	B	r^2
P 1 R 1	i	261.6	6090	0.99	iii	123	116.1	0.94
P 2 R 1	ii	154*	38.1*	0.98	iii	314.3	286.2	0.82
P 2 R 3	i	772.4	4179.1	0.99	iii	110.3	101.3	0.83
P 2 R 4	i	89209.7	187194.4	0.94	iii	773.0	701	0.86
P 2 R 5	ii	328.3*	155.2*	0.97	iii	820.8	788.4	0.77
P 2 R 6	i	137043.6	39478.5	0.93		-	-	-
P 2 R 7	i	-664.6	32542.2	0.97	iv	0	20549.9	0.98

Calculated slopes from each graph are listed in Table 41. Slope I is the slope at time t = 0. Slope II is the slope as time approaches t_L. "Time" is the time at which the slope II is calculated

Table 41. $dX_s^{14}/d[Tm]$. dX_s^{14}/dTm is the slope of the accumulation curve, C^{14} labelled cell concentration on the surface of an established biofilm, X_s^{14}, vs. modified time, [Tm], slope I is the slope at time $t = 0$, slope II is the slope as time approaches t_L.

Run	Slope I	Slope II	t_L	R_{An}^{total}
	CFU/(cm^2 minute)		(min)	(CFU/cm^2 min)
P 1 R 1	$1.6\ 10^3$	-	-	-
P 2 R 1	$1.6\ 10^4$	$1.8\ 10^3$	402	$1.76\ 10^3$
P 2 R 3	$1.8\ 10^3$	$2.1\ 10^2$	180	$1.8\ 10^2$
P 2 R 4	$1.1\ 10^5$	$1.1\ 10^4$	150	$8.9\ 10^3$
P 2 R 5	$5.1\ 10^4$	$2.9\ 10^4$	210	$2.6\ 10^4$
P 2 R 6	-	$1.2\ 10^3$	360	$1.22\ 10^3$
P 2 R 7	$2.1\ 10^4$	$1.4\ 10^3$	240	$1.5\ 10^3$

The rate of total cellular detachment per unit area is the difference between the gross rate of total cellular attachment per unit area, R_{Ag}^{total}, and the net rate of total cellular attachment per unit area, R_{An}^{total}. This method to calculate the rate of total cellular detachment per unit area has been called the first method to calculate R_d^{total}.

$$R_d^{total} = R_{Ag}^{total} - R_{An}^{total} \qquad \textbf{(B.4)}$$

The net rate of C^{14} cellular attachment per unit area to an established biofilm, R_{An}^{14}, is the slope (dX_s^{14}/dt) of the

graph of net C^{14} cellular accumulation vs. time. It is a function of time.

The rate of C^{14} cellular detachment per unit area, R_d^{14} which is a function of time, is the difference between the gross rate of C^{14} cellular attachment per unit area to an established biofilm, R_{Ag}^{14}, and the net rate of C^{14} cellular attachment per unit area, R_{An}^{14}.

Table 42. The Rate of Total Cellular Detachment II. R_d^{total} is calculated using the first method.

Run	Fluid Shear (dyne/cm^2)	Temperature (°C)	R_d^{total} (CFU/cm^2 min)
P 2 R 1	20	22	14240
P 2 R 3*	20	22	1620
P 2 R 4	20	28	101100
P 2 R 5	2	28	25000
P 2 R 7**	20	22	19500

*) Low glucose substrate concentration in chemostat feed therefore low bulk cell concentration in the RotoTorque.
**) One day C^{12} biofilm.

A saturation-type equation (B.5) can be used to fit the rate of C^{14} cellular detachment per unit area, R_d^{14}, as a function of time.

$$R_d^{14} = \frac{R_{dmax}^{14}\, t}{k_d + t} \qquad \text{(B.5)}$$

The maximum rate of C^{14} cellular detachment per unit area, R_{dmax}^{14}, is supposed to be the same as the rate of total cellular detachment per unit area, R_d^{total}. The values of k_d and R^{14}_{max} in equation (B.5) for each experimental run are given in Table 43.

Table 43. Values for Saturation-Type Equation. The units of R_{dmax}^{14} is (CFU of C^{14} labelled cells/ cm^2 minute), while k_d has units of minutes.

Run	R_{dmax}^{14} (CFU/cm^2 min)	k_d (min)	r^2
P 2 R 1	16117	70	0.99
P 2 R 3	2328.55	56.1	0.95
P 2 R 4	116307.	33.61	0.98
P 2 R 5	56270.	19.94	0.96
P 2 R 6	18920	70	0.99
P 2 R 7	21376	70	0.99

APPENDIX C

FLUID SHEAR PREDICTION IN THE ROTOTORQUE

APPENDIX C

Fluid shear on the surface of the biofilm, induced by the rotational speed of the rotor, can be predicted using Figure 46. Two methods of predicted the fluid shear as a function of RPM of the inner rotating cylinder are shown in the graph.

The lower line, marked "predicted", was calculated using Figure 3. Details of the computational procedure are given in the Model Development Section. The upper line, marked "measured", weas obtained by measuring the torque experimentally using a torque monitor (Torque Monitor TDS-DN-TM1, General Thermodynamics Corporation, Plymouth, Massachusetts). The fluid inside the RotoTorque during the torque measurement was water. No biofilm was present on the inside surface of the RotoTorque. No significant torque difference can be measured using this equipment with a RotoTorque with or without biofilm [36].

In this work, fluid shear was reported using the "predicted" line (the lower line on Figure 46)

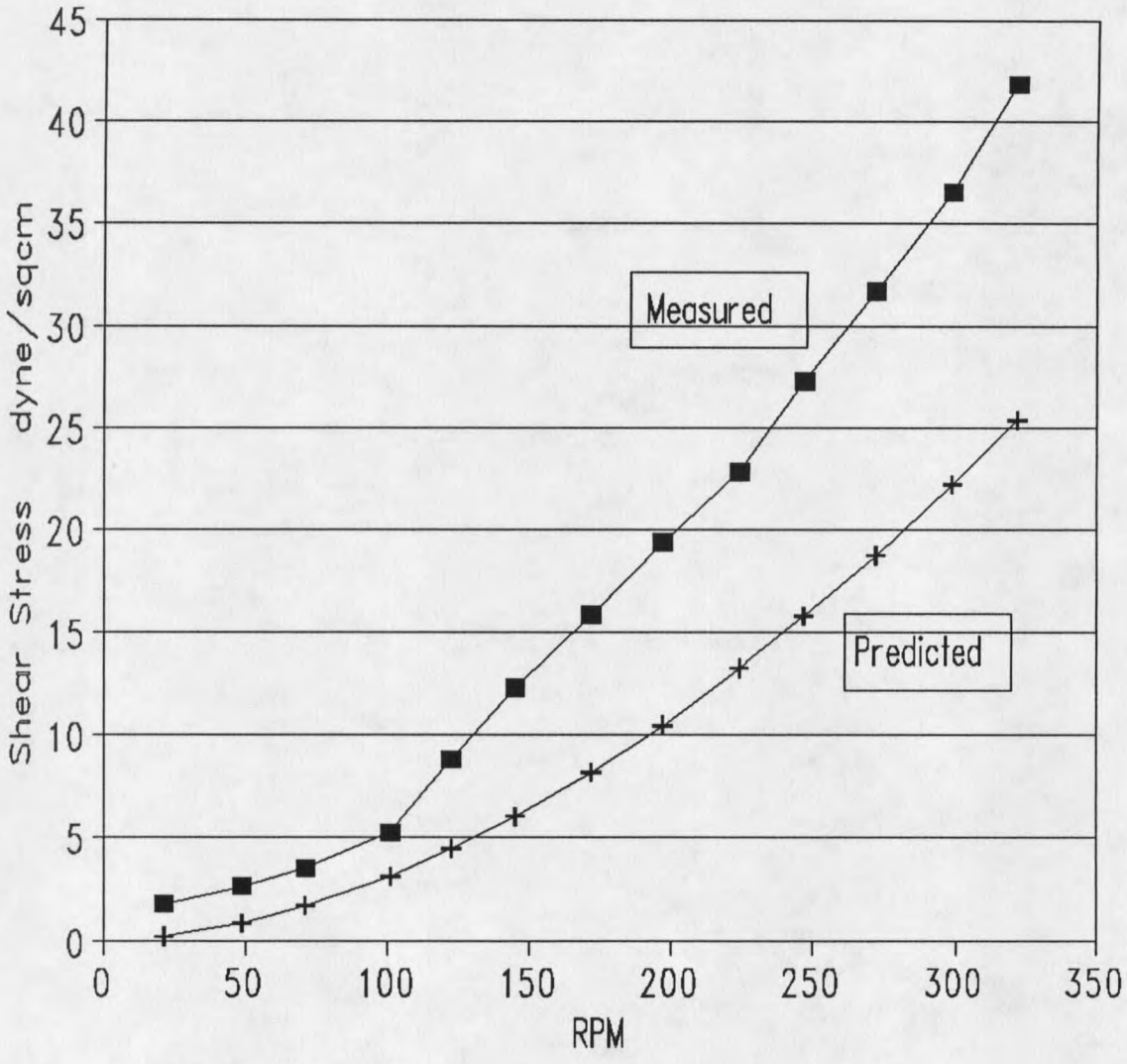

Figure 46. Fluid Shear on The Inner Surface of RotoTorque